5-2017

Secondary Land to Water Transitions: Turtles as Models for Understanding Morphological Evolution

Vanessa K. Hilliard Young
Clemson University, vanessakhyoung@gmail.com

SECONDARY LAND TO WATER TRANSITIONS: TURTLES AS MODELS FOR UNDERSTANDING MORPHOLOGICAL EVOLUTION

A Dissertation
Presented to
the Graduate School of
Clemson University

In Partial Fulfillment
of the Requirements for the Degree
Doctor of Philosophy
Biological Sciences

---

by
Vanessa K Hilliard Young
May 2017

Accepted by:
Dr. Richard W. Blob, Committee Chair
Dr. Margaret B. Ptacek
Dr. Michael W. Sears
Dr. Miriam A. Ashley-Ross

ABSTRACT

Transitions between water and land have occurred multiple times in vertebrate evolutionary history. Secondary land-to-water transitions are often accompanied by characteristic evolutionary changes in morphology, including a shift from tubular limbs to flattened flippers. Differences in limb structure across taxa are often attributed to differences in skeletal loading. However, empirical data on loading differences between land and water are lacking, making it difficult to evaluate which mechanistic changes accompany morphological adaptations in lineages that shift from terrestrial to aquatic habitats.

I used turtles as a model lineage for examining structural and functional implications of differences in limb bone loading between water and land. My examination is comprised of four studies. First, I compared loading regimes for the femur of semi-aquatic sliders (*Trachemys scripta*) during walking and swimming. These trials generated empirical data to test assumed loading differences between water and land. As the extent of limb flattening in many secondarily aquatic tetrapods is especially pronounced in the forelimb, compared to the hindlimb, I next compared loading of the humerus during walking and swimming in the semi-aquatic river cooter (*Pseudemys concinna*). Turtles have transitioned between land and water several times throughout evolutionary history, and such historical transitions may have influenced morphological adaptations of extant taxa. To examine this potential, I compared the swimming kinematics of four turtle species that included two semi-aquatic taxa (*Chrysemys picta* and *T. scripta*) and two independently evolved terrestrial specialists (*Testudo horsfieldii*

and *Terrapene carolina*). This work evaluated the retention of ancestral swimming ability among taxa that have shifted to terrestrial habitats. Finally, it is difficult to assess how differences in loading between land and water may have influenced the morphological diversity of turtle limbs without considering data from taxa that span a complete range of locomotor habits. I collected morphological data from four functionally divergent clades, and calculated allometric comparisons of humerus and femur shape using phylogenetic comparative methods to test for divergence in limb bone morphology among taxa that use different habitats. Together, these studies provide biomechanical, kinematic, and phylogenetic insight to the mechanisms influencing the evolution of limb morphology associated with secondary aquatic invasions.

DEDICATION

This body of work is dedicated to my family. First, to my grandmother, Gail Hilliard for instilling in her children and grandchildren the great value of education, and for teaching me about the peace that can be found in quiet moment and a good cup of tea. To my parents, Scott and Joelle Hilliard, for showing me how to live well, the delight that comes with loving life in all its ups and downs, and that there are few ills that a little time outdoors can't remedy. To my in-laws, Kenneth and Lorie Young and Sera and Danny Rogers, for always lifting me up, both with prayer and conversation. To my husband, Trevis Young, for his incredible support along this long journey, sacrificing opportunities to grow his own career in order to support mine, and for his unfailing faith in my ability to succeed. You have been a solid foundation, a source of quiet strength, and a wonderful sounding board when I have been overwhelmed and unable to sort out my thoughts on my own. Finally, to my children, Samuel and Benjamin Young. You bring me incredible joy each day, and I am beyond blessed to have you. You continuously remind me to look at the world with a sense of wonder and curiosity, and my wish for you is to maintain that perspective all your days. All of you have been a perpetual source of strength and encouragement to me, and I could not have completed this dissertation without you.

ACKNOWLEDGMENTS

There are a great many people who have influenced my scientific career and contributed to the improvement and completion of this body of work in particular.

First, I would like to recognize the many scientists who inspired me as a student and who helped to mold me into the professional I am now. Drs. Mary Lang Edwards and David Ritland introduced me to field biology and a career I didn't know existed. Dr. Nora Espinoza quelled my fear of snakes and sowed the seeds for my love of everything herp. Dr. Matt Gifford took a chance on me as a Master's student and trained me in how to be a real scientist. It was his encouragement that spurred me into pursuing a Ph.D., an endeavor that I had never thought I was smart enough to pursue.

I owe special acknowledgement to my mentor, Dr. Rick Blob. Rick was instrumental in helping me to hone my interests and develop a line of inquiry for my dissertation and career. He has been incredibly supportive of both my professional and personal growth during my five years in his lab, and I could not have hoped for a better person to help guide me in so many ways. I would also like to recognize the members of my committee: Drs. Margaret Ptacek, Miriam Ashley-Ross, and Mike Sears for their advisement. Finally, I am grateful to the many dear friends I have made along my journey: Eric Riddell, Kylie Smith, Christopher Mayerl, Kelly Diamond, and Drs. Tammy McNutt-Scott, Kristine Moody, Sandy Kawano, Gabe Rivera, Angie Rivera, Jeremy Chamberlain, Tim Clay, and Robin Verble. They have been sources of advice, reassurance, hope, and, most importantly, laughter.

TABLE OF CONTENTS

Table of Contents (Continued)

LIST OF TABLES

LIST OF FIGURES

CHAPTER ONE

INTRODUCTION

During the evolutionary history of tetrapod vertebrates, numerous lineages have undergone transitions between drastically different habitats, shifting between water, land, and air as the primary medium of their locomotion. The differing physical properties of these habitats expose animals to different functional demands (Ashley-Ross et al. 2013; Vogel 2013). In turn, these demands may impose selection pressures that contribute to evolutionary divergence in the morphology or performance of taxa (Lanyon et al. 1982; Gillis and Blob 2001; Botton-Divet et al. 2016).

Among major habitat transitions in tetrapod history, the invasion of land by early aquatic tetrapods has been the subject of many studies, particularly with regard to changes in the appendicular skeleton (i.e., the fin-to-limb transition: Shubin et al. 1997, Coates and Cohn 1998, Kawano and Blob 2013). However, secondary invasions of aquatic habitats by terrestrial tetrapods also represent landmark events that, despite multiple occurrences (e.g., sea turtles, mosasaurs, manatees, cetaceans), have received comparatively less study (Caldwell 2002). These land-to-water transitions frequently entail the evolution of flattening of the limbs into flippers (Zimmer 1999; Wyneken 2001; Renous et al. 2008). In many taxa, these flippers may be used to perform "aquatic flight", a specialized mode of swimming in which the forelimbs are flapped dorsally and ventrally to generate lift-based thrust (Fish 1996; Walker and Westneat 2000; Renous et al. 2008; Rivera et al. 2011a, 2011b). However, the mechanisms driving the evolution of flattened limbs from the tubular-shaped limbs of terrestrial ancestors remain unclear.

How do the physical and mechanical properties of the different environments, land versus water, influence the evolution of limb shape in each habitat?

Bones can respond to changes in loads through changes in shape over the course of an individual's lifetime. For example, Lanyon and colleagues (1982) found that, in adult sheep, increases in strain magnitudes on the radius following removal of the ulna resulted in compensatory remodeling and thickening of the cortex of the radius. By extension, changes in bone shape through evolutionary time may reflect differences in the loading environments that taxa experience (Bertram and Biewener 1990, Carter and Beaupré 2001). However, the extent to which loading changes might have contributed to changes in limb shape during invasions of aquatic habitats is unclear, due to a lack of data on both aquatic limb bone loading, and the stages of morphological change in lineages between walking and aquatic flapping.

The contrasting environmental demands to which organisms must respond on land versus in water are well known (Gillis and Blob 2001, Vogel 2013, Gingerich 2015). However, the impact of these factors on the mechanical environment to which bones are exposed is less clear. For example, strains on skeletal elements are assumed to be reduced in water due to a reduction in body support demands placed on the skeleton (Zug 1971, Gillis and Blob 2001), but the magnitude of strain reduction in water has not been evaluated previously (Young and Blob 2015). Furthermore, on land, tetrapods contact the substrate at a specific point on the body (i.e. the foot) to produce forward propulsion, but in water they contact the propulsive medium with the entire body (Vogel 2013). Such contrasts could result in different loading regimes (e.g., twisting versus bending) for locomotor structures on land versus in water. Together, differences in strain magnitudes

and loading regimes between land and water may influence limb bone morphology in tetrapods that have made a transition between these habitats. In terrestrial environments, tubular limb bones are advantageous for resisting bending and torsional (i.e. twisting) loads associated with body support and terrestrial walking (Buckwalter et al. 1995, Carter and Beaupré 2001, Butcher et al. 2008, Vogel 2013). However, reduction of loads in water would release aquatic tetrapods from the demands imposed by high load magnitudes on land. Such a release could facilitate the evolution of novel, limb bone shapes, such as a flattened flipper, that would enable specialized swimming modes and confer hydrodynamic advantages that are unavailable to species with tubular limbs (Walker and Westneat 2000).

Turtles have particularly advantageous features for understanding morphological changes in the appendicular skeleton associated with habitat transitions. Unlike other tetrapods, turtles possess vertebrae that are fused to a bony shell. This unique anatomy requires that all locomotion must be powered exclusively by the limbs (Pace et al. 2001). As a result, comparisons of limb bone loads during locomotion in turtles are not confounded by shifts from limb-powered movement on land to body-axis-powered movement in water, as in other secondarily aquatic tetrapod taxa (Fish 1996, Lindgren et al. 2011). In addition, living turtle species include taxa that employ terrestrial walking, freshwater aquatic rowing (i.e. asynchronous, anteroposterior limb cycles), and freshwater and marine flapping (i.e. synchronous, dorsoventral limb cycles; Rivera et al., 2013). This range of locomotor modes provides functional analogues to the stages of locomotor transitions during aquatic invasions. Taxa that have recently invaded aquatic habitats tend to swim using rowing, which is considered to be an intermediate locomotor

form between walking and flapping; in contrast, taxa that have become more fully specialized for aquatic life tend to swim using flapping (Davenport et al. 1984, Fish 1996, Lindgren et al. 2011, Smith and Clarke 2014, Blob et al. 2016).

Previous work has shown that kinematics differ between the forelimb and hindlimb in reptiles, despite the limbs sharing many features (Russell and Bels 2001). Forelimbs and hindlimbs are also often functionally divergent in turtle taxa. For instance, in many semi-aquatic turtle species (e.g. *Chrysemys picta, Trachemys scripta*), propulsion is primarily driven by the hindlimb (Walker 1971, Pace et al. 2001, Rivera and Blob 2010). However, in sea turtles the hindlimbs assume a reduced propulsive role, as forward thrust is generated predominantly by the forelimbs (Wyneken 2001). Such functional differences between the forelimb and hindlimb might produce different loading patterns on these structures. However, limb loading in the forelimb has been largely unexplored in reptiles, as previous studies have concentrated on femoral loading (Blob and Biewener 1999, Butcher et al. 2008, Sheffield et al. 2011).

In addition to loading regime, phylogenetic history also influences the limb bone shapes of tetrapods (Botton-Divet et al. 2016). Turtles have a history of multiple land-to-water and water-to-land transitions. The oldest fully-shelled turtle was likely terrestrial, but all extant species of turtle can be traced to an aquatic common ancestor (Joyce and Gauthier 2004, Scheyer and Sander 2007, Gosnell et al. 2009, Schoch and Sues 2015). Nonetheless, several turtle lineages have specialized for terrestriality and rarely encounter ancestral aquatic habitats (Blob et al. 2016). Such specialization has resulted in distinct morphologies associated with terrestriality, such as highly domed shells and, in tortoises, reduced wrist and ankle structures (Walker 1973, Young et al. 2017).

To investigate the implications of mechanical differences between aquatic and terrestrial environments for the evolution of skeletal morphology in secondarily aquatic vertebrates, I conducted a series of comparative studies of limb function and structure in turtles. Chapter 2 compares loading regimes of the femur during aquatic swimming versus terrestrial walking in the semi-aquatic red-eared slider turtle (*Trachemys scripta*). This work was published in 2015 in the journal *Biology Letters* (Young and Blob 2015). Chapter 3 builds upon Chapter 2 by comparing aquatic and terrestrial loading regimes of the forelimb of the river cooter turtle (*Pseudemys concinna*), a semi-aquatic turtle species with a similar ecology and evolutionary history to *T. scripta*. These data provide empirical evidence of differences in appendicular loading regimes during locomotion between aquatic and terrestrial habitats. Furthermore, they provide a framework for evaluating forelimb and hindlimb function during locomotion in differing habitat types. Chapter 4 evaluates the retention of swimming capability by species that have undergone specialization for terrestrial habitats by comparing forelimb and hindlimb kinematics of two terrestrially specialized turtle species (*Testudo horsfieldii* and *Terrapene carolina*) to two semi-aquatic species (*Chrysemys picta* and *T. scripta*). This study was published in *Biology Letters* in early 2017 (Young et al. 2017). The final chapter investigates humeral and femoral morphology across four functionally diverse groups of turtles to test if functionally intermediate taxa also show intermediate limb shapes between aquatic and terrestrial specialists. Using phylogenetic comparative analyses, this chapter draws upon molecular phylogenetic data to account for shared evolutionary history of the taxa represented, and provides insight into the potential stages in morphological change of the limb bones across functional analogs of stages in secondary aquatic invasions by

tetrapods.

REFERENCES

Ashley-Ross, M.A., S. T. Hsieh, A. C. Gibb, and R. W. Blob. 2013. Vertebrate land invasions—past, present, and future: an introduction to the symposium. *Integrative and Comparative Biology* 53: 192-196.

Bertram, J. E. A. and A. A. Biewener. 1990. Differential scaling of the long bones in the terrestrial Carnivora and other mammals. *Journal of Morphology* 204: 157-169.

Blob, R. W. and A. A. Biewener. 1999. *In vivo* locomotor strain in the hindlimb bones of *Alligator mississippiensis* and *Iguana iguana*: implications for the evolution of limb bone safety factor and non-sprawling limb posture. *Journal of Experimental Biology* 202: 1023-1046.

Blob, R. W., C. J. Mayerl, A. R. V. Rivera, G. Rivera, and V. K H. Young. 2016. "One the fence" versus "all in": insights from turtles for the evolution of aquatic locomotor specialization and habitat transitions in tetrapod vertebrates. *Integrative and Comparative Biology* 56: 1310-1322.

Botton-Divet, L., R. Cornette, A-C. Fabre, A. Herrel, and A. Houssaye. 2016. Morphological analysis of long bones in semi-aquatic mustelids and their terrestrial relatives. *Integrative and Comparative Biology* 56: 1298-1309.

Buckwalter, J. A., M. J. Glimcher, R. R. Cooper, and R. Recker. 1995. Bone biology. Part I: structure, blood supply, cells, matrix, and mineralization. *Journal of Bone and Joint Surgery* 77: 1256-1275.

Butcher, M. B., N. R. Espinoza, S. R. Cirilo, and R. W. Blob. 2008. *In vivo* strains in the femur of river cooter turtles (*Pseudemys concinna*) during terrestrial locomotion: tests of force-platform models of loading mechanics. *Journal of Experimental Biology* 211: 2397-2407.

Caldwell, M. W. 2002. From fins to limbs to fins: limb evolution in fossil marine reptiles. *American Journal of Medical Genetics* 112: 236-249.

Carter D.R. and G. S. Beaupré. 2001. *Skeletal function and form*. Cambridge: Cambridge University Press.

Coates M. and M. Cohn. 1998. Fins, limbs, and tails: outgrowths and axial patterning in vertebrate evolution. *Bioessays* 20: 371-381.

Davenport, J., S. A. Munks, and P. J. Oxford. 1984. A comparison of the swimming of marine and freshwater turtles. *Proceedings of the Royal Society B* 220: 447-475.

Fish F. E. 1996. Transitions from drag-based to lift-based propulsion in mammalian swimming. *American Zoologist* 36: 628-641.

Gillis, G. B. and R. W. Blob. 2001. How muscles accommodate movement in different physical environments: aquatic versus terrestrial locomotion in vertebrates. *Comparative Biochemistry and Physiology Part A* 131: 61-75.

Gingerich, P. D. 2015. Evolution of whales from land to sea. In *Great transformations in vertebrate evolution* (ed. K. P. Dial, N. Shubin, and E. L. Brainerd), pp. 239-256. Chicago, IL: University of Chicago Press.

Gosnell, J. S., G. Rivera, and R. W. Blob. 2009. A phylogenetic analysis of sexual size dimorphism in turtles. *Herpetologica* 65: 70-81.

Joyce, W. G. and J. A. Gauthier. 2004. Paleoecology of Triassic stem turtles sheds new light on turtle origins. *Proceedings of the Royal Society B* 271: 1-5.

Kawano, S. M. and R. W. Blob. 2013. Propulsive forces of mudskipper fins and salamander limbs during terrestrial locomotion: implications for the invasion of land. *Integrative and Comparative Biology* 53:283-294.

Lanyon, L. E., A. E. Goodship, C. Pye, and H. McFie. 1982. Mechanically adaptive bone remodeling: a quantitative study on functional adaptation in the radius following ulna osteotomy in sheep. *Journal of Biomechanics* 12:141-154.

Lindgren, J., M. J. Polcyn, and B. A. Young. 2011. Landlubbers to leviathans: evolution of swimming in mosasaurine mosasaurs. *Paleobiology* 37: 445-469.

Pace, C. M., R. W. Blob, and M. W. Westneat. 2001. Comparative kinematics of the forelimb during swimming in red-eared slider (*Trachemys scripta*) and spiny softshell (*Apalone spinifera*) turtles. *Journal of Experimental Biology* 204: 3261-3271.

Renous, S., F. de Lapparent de Broin, M. Depecker, J. Davenport, and V. Bels. 2008. Evolution of locomotion in aquatic turtles. In *Biology of turtles* (ed. J. Wyneken, M. H. Godfrey, and V. Bels), pp. 139-162. Boca Raton, FL: CRC Press.

Rivera, A. R. V. and R. W. Blob. 2010. Forelimb kinematics and motor patterns of the slider turtle (*Trachemys scripta*) during swimming and walking: shared and novel strategies for meeting locomotor demands of water and land. *Journal of Experimental Biology* 213: 3515-3526.

Rivera, A. R. V., J. Wyneken, and R. W. Blob. 2011a. Forelimb kinematics and motor patterns of swimming loggerhead sea turtles (*Caretta caretta*): are motor patterns conserved in the evolution of new locomotor strategies? *Journal of Experimental Biology* 214: 3314-3323.

Rivera, G., A. R. V. Rivera, and R. W. Blob. 2011b. Hydrodynamic stability of the painted turtle (*Chrysemys picta*): effects of four-limbed rowing versus forelimb flapping in rigid-bodied tetrapods. *Journal of Experimental Biology* 214: 1153-1162.

Rivera, A. R. V., G. Rivera, and R. W. Blob. 2013. Forelimb kinematics during swimming in the pig-nosed turtle, *Carettochelys insculpta*, compared with other turtle taxa: rowing versus flapping, convergence versus intermediacy. *Journal of Experimental Biology* 216: 668-680

Russell, A. P. and V. Bels. 2001. Biomechanics and kinematics of limb-based locomotion in lizards: review, synthesis, and prospectus. *Comparative Biochemistry and Physiology Part A* 131: 89-112.

Scheyer, T. M. and P. M. Sander. 2007. Shell bone histology indicates terrestrial paleoecology of basal turtles. *Proceedings of the Royal Society B* 274: 1885-1893.

Schoch, R. R. and H-D. Sues. 2015. A Middle-Triassic stem-turtle and the evolution of the turtle body plan. *Nature* 523: 584-587.

Sheffield, K. M., M. T. Butcher, S. K. Shugart, J. C. Gander, and R. W. Blob. 2011. Locomotor loading mechanics in the hindlimbs of tegu lizards (*Tupinambis merianae*): comparative and evolutionary implications. *Journal of Experimental Biology* 214: 2616-2630.

Shubin, N., C. Tabin, and S. Carroll. 1997. Fossils, genes, and the evolution of animal limbs. *Science* 388: 639-648.

Smith, N. A. and J. A. Clarke. 2014. Osteological histology of the Pan-Alcidae (Aves, Charadriiformes): correlates of wing-propelled diving and flightlessness. *The Anatomical Record* 297: 188-199.

Vogel, S. 2013. *Comparative biomechanics: life's physical world*. Princeton, NJ: Princeton University Press.

Walker, J. A. and M. W. Westneat. 2000. Mechanical performance of aquatic rowing and flying. *Proceedings of the Royal Society B* 267: 1875-1881.

Walker, W. F. Jr. 1971. A structural and functional analysis of walking in the turtle, *Chrysemys picta marginata*. *Journal of Morphology* 134: 195-214.

Walker, W. F. 1973. The locomotor apparatus of Testudines. In *Biology of the reptilia*, vol. 4 Morphology D (eds. C. Gans and P. Parsons), pp. 1-100. London, UK: Academic Press.

Wyneken J. 2001. *The anatomy of sea turtles.* U.S. Department of Commerce NOAA Technical Memorandum NMFS-SEFSC-470, p. 172.

Young, V. K H. and R. W. Blob. 2015. Limb bone loading in swimming turtles: changes in loading facilitate transitions from tubular to flipper-shaped limbs during aquatic invasions. *Biology Letters* 11: 1-5.

Young, V. K H., K. G. Vest, A. R. V. Rivera, N. R. Espinoza, and R. W. Blob. 2017. One foot out the door: limb function during swimming in terrestrial versus aquatic turtles. *Biology Letters* 13: 1-5.

Zimmer, C. 1999. *At the water's edge: fish with fingers, whales with legs, and how life came ashore but then went back to sea.* New York, NY: Touchstone.

Zug, G. R. 1971. Buoyancy, locomotion, morphology of the pelvic girdle and hind limb, and systematics of cryptodiran turtles. *Miscellaneous Publications of the Museum of Zoology, University of Michigan* 142: 1-98.

CHAPTER TWO

LIMB-BONE LOADING IN SWIMMING TURTLES: CHANGES IN LOADING FACILITATE TRANSITIONS FROM TUBULAR TO FLIPPER-SHAPED LIMBS DURING AQUATIC INVASIONS

This is a pre-copy-editing, author-produced copy of an article accepted for publication in *Biology Letters* following peer-review. The definitive publisher-authenticated version:

Vanessa K Hilliard Young and Richard W. Blob. Limb-bone loading in swimming turtles: changes in loading facilitate transitions from tubular to flipper-shaped limbs during aquatic invasions. *Biology Letters* 11: 20150110. 1 – 5. *doi:10.1098/rsbl.2015.0110*

is available online at: http://rsbl.royalsocietypublishing.org/content/11/6/20150110.

ABSTRACT

Members of several terrestrial vertebrate lineages have returned to nearly exclusive use of aquatic habitats. These transitions were often accompanied by changes in skeletal morphology, such as flattening of limb bone shafts. Such morphological changes might be correlated with the exposure of limb bones to altered loading. Though the environmental forces acting on the skeleton differ substantially between water and land, no empirical data exist to quantify the impact of such differences on the skeleton, either in terms of load magnitude or regime. To test how locomotor loads change between water and land, we compared *in vivo* strains from femora of turtles (*Trachemys scripta*) during swimming and terrestrial walking. As expected, strain magnitudes were much lower (by 67.9%) during swimming than during walking. However, the loading regime of the femur

also changed between environments: torsional strains are high during walking, but torsion is largely eliminated during swimming. Changes in loading regime between environments may have enabled evolutionary shifts to hydrodynamically advantageous flattened limb bones in highly aquatic species. Although circular cross sections are optimal for resisting torsional loads, the removal of torsion would reduce the advantage of tubular shapes, facilitating the evolution of flattened limbs.

INTRODUCTION

Transitions between aquatic and terrestrial habitats represent milestone events in vertebrate history [1-3]. The initial invasion of land by tetrapods was among the most profound of such events [1,3]; however, members of many terrestrial vertebrate lineages have since developed or returned to nearly exclusive use of aquatic habitats (e.g. sea turtles, mosasaurs, penguins, whales). These transitions have often been accompanied by characteristic changes in skeletal morphology, such as shifts from tubular to flattened shafts in the long bones of the limbs [3-5]. Such flattening conveys hydrodynamic advantages to appendages, making them effective propulsors for generating drag- or lift-based thrust during swimming [6]. However, the mechanical environment underlying the structural changes that provide such hydrodynamic advantages is unclear. The shapes of bones can respond to changes in their loading environment, both within generations and over evolutionary time [7-9]. Differences in the forces to which animals are exposed between water and land are also well known [10,11]. Could changes in skeletal loading have facilitated changes in limb bone shape among tetrapod lineages that became primarily aquatic?

For tetrapods that shifted from terrestrial to aquatic habitats, loads imposed on the limbs by both internal (muscular) and external (environmental) propulsive forces are retained; however the demands of bodily support on the limbs are reduced [11]. Thus, a decrease in overall load magnitudes is expected in aquatic habitats, but the size of this reduction is difficult to predict. Moreover, overall loading decreases do not clearly correlate with the directional (i.e. flattening) shape change observed in the limbs of primarily aquatic taxa. Such shape changes might, instead, correlate with a change in loading regime. Many terrestrial tetrapods experience significant torsional (twisting) loads on their limb bones [12,13], a regime that tubular bone cross-sections are well suited to resist [10]. If such torsion were reduced more than bending loads during aquatic locomotion, the mechanical environment favoring tubular bones might have been released, facilitating the evolution of flattened, asymmetric cross-sections.

To test how limb bone loading changes between water and land, we compared *in vivo* strains from the femur of the semi-aquatic slider turtle (*Trachemys scripta*) between swimming and terrestrial walking. Extreme terrestriality is a derived condition among turtles (e.g. tortoises), and sliders are not descended from more terrestrial ancestors [14,15]. However, turtles are particularly appropriate models in the context of understanding changes in limb loading through evolutionary transitions because, with the fusion of the backbone to the shell, they generate all propulsion by the limbs [16]. Thus, comparisons between environments are not confounded by shifts to propulsive structures of the body axis [2]. Moreover, semi-aquatic turtles swim with rowing motions of the limbs [16], which were likely used in the initial stages of evolutionary transitions to highly aquatic lifestyles [2]. Our focus on the femur reflects evidence that the hind limb

is the dominant propulsive structure among semi-aquatic turtles [16]. Thus, by quantifying femoral loading differences in turtles between water and land, we could test for the reduction of long bone torsion during limb-propelled swimming compared to walking, potentially facilitating changes in limb bone shape during secondary aquatic invasions.

MATERIALS AND METHODS

Five adult *T. scripta* (2 males, 3 females; plastron length 19.4 ± 2.5 cm; mass: 1.4 ± 0.6 kg) were collected from Lake Hartwell, Pickens County, SC (USA). Housing and husbandry followed published standards [13].

One rosette (FLK-1-11) and two single element (FRA-1-11) strain gauges (Tokyo Sokki Kenkyujo Co., Ltd., Japan) were surgically implanted onto the midshaft of each turtle's right femur following published methods [13]. After 24h recovery, individuals were prompted to swim in a flowtank [16] and walk on a motorized treadmill [13] while *in vivo* strains were collected (see [13] for details). Trials were conducted at the highest speed individuals could maintain for several seconds (flowtank, 0.44-0.86m/s; treadmill 0.04-0.20m/s). Such speeds may not be strictly dynamically equivalent, but do provide comparable ecological relevance for understanding selection pressures on skeletal design. During aquatic trials, microconnectors between the animal's strain gauge wires and the shielded amplifier cable were sealed with plumber's epoxy to prevent water leakage into contacts. Strain trials were simultaneously filmed from lateral and dorsal (walking) or ventral (swimming) views (100 Hz; Phantom V5.1, Vision Research Inc., Wayne, NJ, USA). Turtles were euthanized following recordings (Euthasol® pentobarbital sodium

solution; Delmarva Laboratories Inc., Midlothian, VA, USA; 200 mg/kg intraperitoneal injection). For each gauge location in each turtle, strains were compared between the thrust and recovery phases of swimming (determined from video records), and between walking and swimming, using Mann-Whitney *U*-tests which were conducted in SAS® (SAS 9.3, SAS Institute Inc. 2010, Cary, NC, USA).

RESULTS

During swimming, longitudinal strains at each gauge location typically maintained the same orientation (i.e. tensile or compressive) during both thrust and recovery (figure 2.1, table 2.1). Thus, the direction of femoral bending did not change as the direction of limb oscillation reversed between retraction and protraction. However, absolute magnitudes of peak strain (longitudinal, principal, and shear) were greater during thrust (retraction) than during recovery (protraction) for 18 of 19 comparisons, and significantly greater for 15 of 19 comparisons (table 2.1). The orientation of peak principal tensile strain to the long axis of the femur (φ_T) showed small differences between thrust and recovery (averaging 3.7° across animals); however, φ_T averaged under 10° throughout the limb cycle (table 2.1), showing close alignment of strains with the femoral long axis (i.e. limited torsion).

Longitudinal strains at each gauge location typically maintained the same orientation between swimming and walking (figure 2.1, table 2.1). Peak strain magnitudes during swimming were significantly lower than during walking (figures 2.1-2.2, table 2.1) except at the ventral gauge location due to its proximity to the femoral neutral axis [13]. Focusing on the phases of the limb cycle when strains are highest in each behavior (thrust and stance), peak swimming strains from non-ventral gauges are

roughly 33.1% of peak walking strains. This difference was particularly prominent for shear, for which swimming magnitudes were only ~10% of those during walking (table 2.1, figure 2.2). Though due partly to an overall reduction in femoral loading while in water, the difference in shear between swimming and walking also appears to reflect a difference in load orientation. Whereas φ_T for swimming shows a nearly longitudinal average orientation of -6.1°, during walking φ_T averages -19.8°, nearer to an absolute value of 45° that signifies maximal torsion [8,12,13].

DISCUSSION

We found single peaks of loading during the thrust phase of swimming that were consistently higher than the variable strains experienced during limb recovery. This difference in femoral strain magnitudes between limb cycle phases parallels that found in walking turtles [13], and highlights the impacts of external (environmental) versus internal (muscular) forces acting on the limb. During thrust, the paddle of the foot is oriented perpendicular to the flow of water [16], maximizing drag for the production of thrust [2,6]. Such external forces compound the internal forces applied to the femur by active limb muscles [17], elevating strains. In contrast, the paddle is parallel to oncoming flow during recovery [16], minimizing drag that could impede forward swimming [2,6]. Such drag reduction appears to greatly decrease environmental forces on the femur, significantly reducing peak strains during recovery.

Femoral loads of rowing turtles also differ substantially between water and land. Peak longitudinal strains are reduced by 2/3 during swimming, and torsional (shear) strains decreased by a factor of 19. Some reduction in femoral shear strains during

swimming reflects the lower overall magnitudes of loading in water. However, reorientation of femoral loading also plays a considerable role in reducing shear strains, as φ_T shifts from values on land that indicate considerable twisting, to values in water that indicate close alignment of strains with the femoral long axis (table 2.1, figure 2.2). Given the prominence of foot rotation during the aquatic limb cycle of swimming turtles [16], the limitation of longitudinal twisting of the femur is puzzling. However, just as humans can pronate and supinate the hand at the wrist independent of oscillations at the shoulder, rotation of the foot in rowing turtles may be achieved largely through the action of distal limb components that have limited impact on femoral loading during fore-aft oscillations.

That femoral torsion is reduced during swimming in rowing turtles suggests a mechanism that may have facilitated the evolution of hydrodynamically advantageous limb bone flattening among tetrapods that shifted to primarily aquatic habitats. Although tubular shapes are advantageous for resisting torsional loads [8,10], the reduction of torsional loads during rowing could have released aquatic tetrapods from a mechanical environment favoring tubular limb bones, opening opportunities for diversification into hydrodynamically specialized limb morphologies. How broadly such patterns might apply across the multiple secondary invasions of water by tetrapods [2,3,5,11] is uncertain, particularly for lineages in which limb bone torsion was already limited [9]. However, at least for amphibian, reptilian [12,13], and, potentially, avian [18] lineages in which torsion during non-aquatic locomotion is high, the combination of changes in both the magnitude and regime of limb bone loads during aquatic propulsion may have

provided conditions for the eventual morphological specialization of these taxa as swimmers.

ACKNOWLEDGEMENTS

We thank H. Barnett, J. Sutton, and C. Wienands for assistance with experiments, and C. Mayerl, K. Diamond, M. Sears and two anonymous reviewers for feedback on the manuscript.

FUNDING

Work was supported by Clemson University (Department of Biological Sciences).

REFERENCES

1. Ashley-Ross MA, Hsieh ST, Gibb AC, and Blob RW. 2013 Vertebrate land invasions - past, present, and future: an introduction to the symposium. *Integr. Comp. Biol*. **53**, 192-196.

2. Fish, FE. 1996 Transitions from drag-based to lift-based propulsion in mammalian swimming. *Am. Zool.* **36**, 628-641.

3. Zimmer, C. 1999 *At the water's edge: fish with fingers, whales with legs, and how life came ashore but then went back to sea*. New York: Touchstone.

4. Renous, S, de Lapparent de Broin, F, Depecker, M, Davenport, J, Bels, V. 2008 Evolution of locomotion in aquatic turtles. In *Biology of turtles* (ed. J. Wyneken, M.H. Godfrey, and V. Bels), pp. 97-133. Boca Raton: CRC Press.

5. Carroll, RL. 1988 *Vertebrate paleontology and evolution.* New York: WH Freeman.

6. Walker, JA. 2002 Functional morphology and virtual models: physical constraints on the design of oscillating wings, fins, legs, and feet at intermediate Reynolds numbers. *Integr. Comp. Biol.* **42**, 232-242.

7. Lanyon, LE, Goodship, AE, Pye C, McFie H. 1982 Mechanically adaptive bone remodeling: a quantitative study on functional adaptation in the radius following ulna osteotomy in sheep. *J. Biomech.* **12**, 141-154.

8. Carter DR, Beaupré GS. 2001 *Skeletal function and form.* Cambridge: Cambridge University Press.

9. Bertram JEA, Biewener AA. 1990 Differential scaling of the long bones in the terrestrial Carnivora and other mammals. *J. Morphol.* **204**, 157-169.

10. Vogel, S. 2013 *Comparative biomechanics: life's physical world*. Princeton: Princeton University Press.

11. Gillis GB, Blob RW. 2001 How muscles accommodate movement in different physical environments: aquatic versus terrestrial locomotion in vertebrates. *Comp. Biochem. Physiol*. A **131**, 61-75.

12. Blob RW, Biewener AA. 1999 *In vivo* locomotor strain in the hindlimb bones of *Alligator mississippiensis* and *Iguana iguana*: implications for the evolution of limb bone safety factor and non-sprawling limb posture. *J. Exp. Biol*. **202**, 1023-1046.

13. Butcher MB, Espinoza NR, Cirilo SR, Blob RW. 2008 *In vivo* strains in the femur of river cooter turtles (*Pseudemys concinna*) during terrestrial locomotion: tests of force-platform models of loading mechanics. *J. Exp. Biol.* **211**, 2397-2407.

14. Gosnell JS, Rivera G, Blob RW. 2009 A phylogenetic analysis of sexual size dimorphism in turtles. *Herpetologica* **65**, 70-81.

15. Joyce WG, Gauthier JA. 2004 Palaeoecology of Triassic stem turtles sheds new light on turtle origins. *Proc. Roy. Soc. B* **271**, 1–5.

16. Blob, RW, Rivera, ARV, Westneat MW. 2008 Hindlimb function in turtle locomotion: limb movements and muscular activation across taxa, environment, and ontogeny. In *Biology of turtle*s (eds J Wyneken, MH Godfrey, V Bels), pp. 139-162. Boca Raton: CRC Press.

17. Aiello BR, Blob RW, Butcher MT. 2013 Correlation of muscle function and bone strain in the hindlimb of the river cooter turtle (*Pseudemys concinna*). *J. Morphol.* **274**, 1060-1069.

18. Biewener AA, Dial KP. 1995 *In vivo* strain in the humerus of pigeons (*Columba livia*) during flight. *J. Morphol*. **225**, 61-75.

Table 2.1. Mann-Whitney *U* results for comparisons of peak femoral strains during thrust versus recovery phases of swimming by *T. scripta*. Values are mean ± standard error. pT, principal tensile strain; pC, principal compressive strain; φ_T, angle of principal tensile strain to femoral long axis.

Animal	Gauge Location	Strain Type	N	Thrust (με)	Recovery (με)	|*Z*|	*p*
TS01	Anterior	Longitudinal	52	-169.8 ±100.2	-119.6 ±84.7	2.75	0.0060*
	Ventral	Longitudinal	11	-176.6 ±72.9	-128.9 ±60.9	2.63	0.0086*
	Posterior	Longitudinal	52	-118.5 ±55.3	-126.4 ±83.6	0.17	0.8670
TS03	Anterior	Longitudinal	129	98.2 ±74.6	48.2 ±32.6	5.69	<0.0001*
	Posterior	Longitudinal	129	102.9 ±53.5	48.8 ±36.0	8.83	<0.0001*
TS04	Anterior	Longitudinal	71	124.7 ±120.6	51.2 ±45.3	4.90	<0.0001*
	Posterior	Longitudinal	71	135.7 ±85.8	76.5 ±42.8	8.83	<0.0001*
TS05	Anterior	Longitudinal	47	-22.7 ±9.4	-13.9 ±10.7	0.45	0.6528
	Ventral	Longitudinal	47	-105.2 ±39.0	-83.9 ±39.7	2.19	0.0280*
	Posterior	Longitudinal	47	84.1 ±15.4	33.1 ±11.3	3.10	0.0019*
	Posterior	pT	47	136.1 ±19.9	76.9 ±5.9	3.87	0.0001*
	Posterior	pC	47	-84.4 ±7.3	-60.4 ±4.1	2.61	0.0091*
	Posterior	φ_T[a]	47	-3.1 ±1.2	-1.7 ±0.8	0.94	0.3484
	Posterior	Shear	47	53.7 ±8.4	25.7 ±4.4	2.58	0.0099*
TS07	Anterior	Longitudinal	54	-101.5 ±32.75	-21.9 ±35.0	1.34	0.1794
	Ventral	Longitudinal	54	-49.3 ±15.2	2.52 ±19.1	2.02	0.0429*

Posterior	Longitudinal	54	58.5 ±4.6	15.13 ±6.1	5.51	<0.0001*
Posterior	pT	54	71.4 ±3.7	46.8 ±3.1	4.97	<0.0001*
Posterior	pC	54	-38.9 ±2.9	-36.5 ±2.2	0.49	0.6252
Posterior	φ_T[a]	54	-9.1 ±1.9	-3.2 ±1.9	2.64	0.0083*
Posterior	Shear	54	50.5 ±4.7	26.9 ±3.6	3.91	0.0001*

[a]Units for φ_T in degrees (°).

*$p \leq 0.05$.

Table 2.2. Mann-Whitney *U* results for comparisons of peak femoral strains during swimming versus walking for the thrust/stance phase of limb cycle by *T. scripta*. Values are mean ± standard error. Abbreviations follow Table 1.

ID	Location	N (swim;walk)	Swim (με)	Walk (με)	|*Z*|	*p*
TS03	Anterior	129; 49	98.2 ±74.6	188.4 ±122.8	4.71	<0.0001*
	Posterior	129; 49	102.9 ±53.5	185.1 ±84.7	6.12	<0.0001*
TS05	Anterior	47; 27	-22.7 ±9.4	-	-	-
	Ventral	47; 27	-105.2 ±39.0	-42.2 ±15.5	0.62	0.5323
	Posterior	47; 27	84.1 ±15.4	804.5 ±37.1	7.12	<0.0001*
	pT	47; 27	136.1 ±19.9	1099.6 ±46.1	7.12	<0.0001*
	pC	47; 27	-84.4 ±7.3	-984.4 ±41.5	7.12	<0.0001*
	φ_T[a]	47; 27	-3.1 ±1.2	-22.1 ±0.4	7.03	<0.0001*
	Shear	47; 27	53.7 ±8.4	1446.4 ±63.4	7.12	<0.0001*
TS07	Anterior	54; 29	-101.5 ±32.7	-601.2 ±157.8	3.41	0.0007*
	Ventral	54; 29	-49.3 ±15.2	-83.4 ±12.7	1.19	0.2344
	Posterior	54; 29	58.5 ±4.6	231.5 ±46.2	4.89	<0.0001*
	pT	54; 29	71.5 ±3.7	462.2 ±36.9	7.17	<0.0001*
	pC	54; 29	-38.9 ±2.9	-286.1 ±45.7	7.45	<0.0001*
	φ_T[a]	54; 29	-9.1 ±1.9	-17.6 ±4.4	1.52	0.1277
	Shear	54; 29	-50.5 ±4.7	546.9 ±93.0	6.38	<0.0001*

[a]Units for φ_T in degrees (°).

*$p \leq 0.05$.

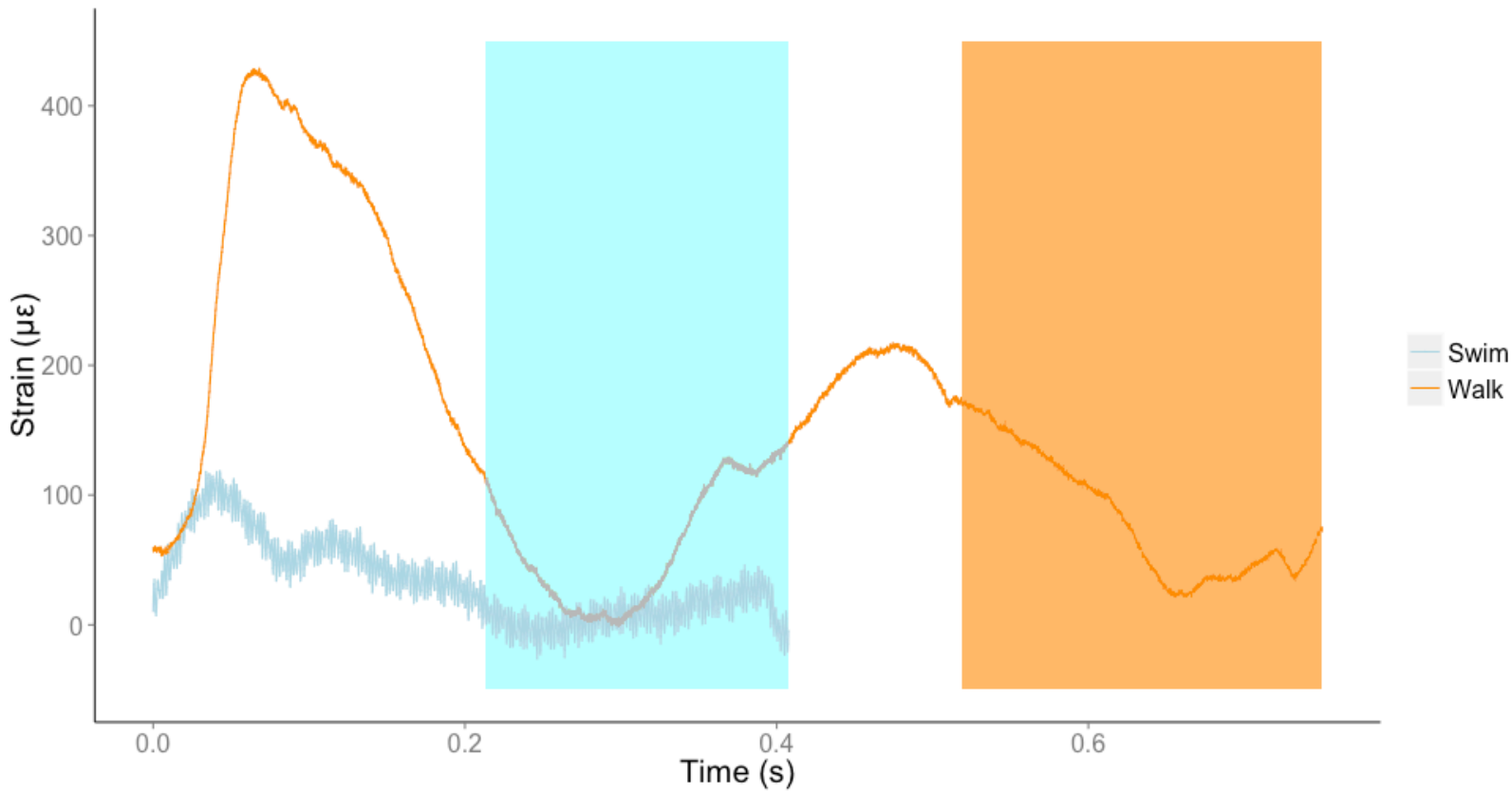
400
300
200
100
0
Strain (με)
0.0
0.2
0.4
0.6
Time (s)
Swim
Walk

Figure 2.1. Femoral strain traces from single, representative limb cycles during swimming and walking in *T. scripta.* Shaded regions indicate recovery phase during swimming (blue) and swing phase during walking (orange).

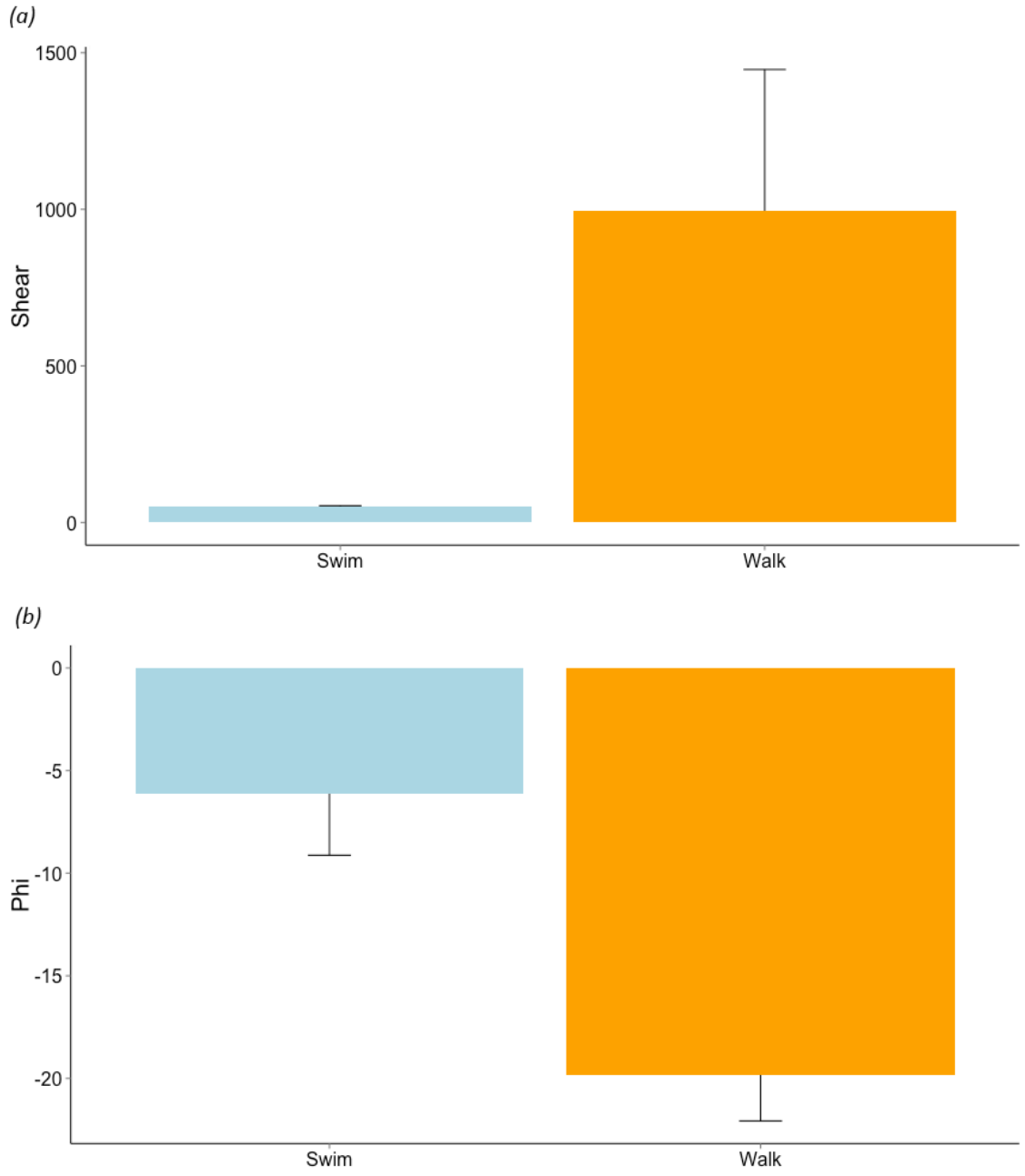

Figure 2.2. Comparison of femoral shear strain (A) magnitudes and (B) orientation (φ_T) between swimming and walking for *T. scripta* (N=2 individuals, 101 swimming limb cycles, 56 walking limb cycles). Shear is significantly lower during swimming, due at least in part to lower φ_T that reflects a decrease in femoral twisting in water.

CHAPTER THREE

HUMERAL LOADS DURING SWIMMING AND WALKING IN TURTLES: IMPLICATIONS FOR MORPHOLOGICAL CHANGE DURING AQUATIC REINVASIONS

ABSTRACT

During evolutionary reinvasions of water by terrestrial vertebrates, ancestrally tubular limbs often flatten to form flippers. Differences in skeletal loading between land and water might have facilitated such changes. In turtles, femoral twisting is significantly lower during swimming than during walking, potentially allowing a release from loads that favor tubular shafts. However, flipper-like morphology in specialized tetrapod swimmers is most accentuated in the forelimbs. To test if the forelimbs of turtles are also released from torsional loading in water, we compared strains on the humerus of river cooters (*Pseudemys concinna*) between swimming and terrestrial walking. Humeral shear strains are also lower during swimming compared to terrestrial walking; however, this appears to relate to reduction in overall strain magnitudes, rather than a specific reduction in twisting. These results indicate that loads show similar changes between swimming and walking for the forelimb and hindlimb, but these changes are produced through different mechanisms.

INTRODUCTION

Habitat transitions have been a prominent driver of evolutionary change in many vertebrate lineages, often leading to specialization for novel environments and radiations of species (Ashley-Ross et al., 2013; Blob et al., 2016). Several ancestrally terrestrial tetrapod lineages (e.g. cetaceans, mosasaurs, manatees, sea turtles) have evolved fully

aquatic lifestyles characterized by changes in body and limb shape (Zimmer, 1999; Caldwell, 2002; Renous et al., 2008; Lindgren et al., 2011; Blob et al., 2016). For example, terrestrial tetrapods have limb bones that are tubular in cross-section, shapes that provide resistance to bending and twisting (Buckwalter et al., 1995; Vogel, 2013; Blob et al., 2014); in contrast, many tetrapods that become secondarily specialized for aquatic environments exhibit flattening of the limbs (Zimmer, 1999; Renous et al., 2008). Such shapes are advantageous for producing both drag- and lift-based thrust during swimming once they are established (Walker, 2002), but the factors that may have promoted evolutionary transitions from tubular to flattened limbs are less clear.

Because the shapes of bones are known to respond to changes in loading environment over both ontogenetic and evolutionary time scales (Lanyon et al., 1982; Bertram and Biewener, 1990), and because the buoyancy conveyed by water should greatly reduce the loads placed on the skeleton to support the body (Zug, 1971), we previously proposed that changes in limb bone loading between land and water might have facilitated the evolution of flattened limb shapes in secondarily aquatic tetrapods (Young and Blob, 2015). Specifically, because torsional loading is high in the limb bones of many tetrapods (Biewener and Dial, 1995; Blob and Biewener, 1999; Butcher et al., 2008; Sheffield et al., 2011), and tubular shapes are well suited to resist torsion (Vogel, 2013), we proposed that a reduction of torsion in particular could have released the limbs from an environment favoring tubular bones and, thereby, facilitated the evolution of flattened shapes (Young and Blob, 2015). To test this proposal, we compared *in vivo* strains between terrestrial walking and swimming for the femur of semi-aquatic slider turtles, *Trachemys scripta* (Young and Blob, 2015). Turtles are advantageous models for

these comparisons because the fusion of the vertebrae to the shell means that propulsion is generated exclusively by the limbs, and comparisons between environments are not confounded by shifts between axial and appendicular propulsion (Gillis and Blob, 2001). Our choice of a semi-aquatic species as a model reflected its use of rowing limb movements (Blob et al., 2008), which were also likely used by species in the initial stages of aquatic reinvasions (Fish, 1996). Moreover, our focus on the femur reflected the dominant propulsive role of the hindlimb in semi-aquatic turtles (Blob et al., 2008). Our results showed that torsional shear strains on turtle femora did, in fact, decrease to a much greater degree than bending strains between terrestrial walking and swimming, with shear declining to nearly negligible levels in water (Young and Blob, 2015). These results were due partly to an overall decrease in load magnitudes in water. However, they also resulted from a substantial change in loading regime, in which principal strains became reoriented to align much more closely with the long axis of the femur during swimming (6.1°) than during walking (19.8°). These patterns indicated sharply reduced twisting of the femur about its long axis during swimming, a conclusion that was verified by subsequent XROMM observations of femoral kinematics in turtles (Mayerl et al., 2016).

Although strain data from turtle femora indicate that reduced torsional loads during aquatic locomotion could have generated a mechanical environment favorable for the evolution of non-tubular limb bones, the restriction of these data to the femur is problematic. In most lineages of tetrapods that became secondarily specialized for aquatic locomotion, including sea turtles, the forelimbs come to dominate appendicular-based propulsion (Wyneken, 1997; Lindgren et al., 2011; Blob et al., 2016). Thus, if changes in

loading are to provide a plausible mechanism that could have contributed to the evolution of flattened limbs during aquatic reinvasions, then a reduction in torsion during swimming should be found in the humerus as well as the femur. However, no loading data are currently available for the forelimbs of any turtle, or any swimming tetrapod. To test whether loading patterns differ between terrestrial walking and swimming for the forelimb, we collected *in vivo* humeral strain data from semi-aquatic river cooter turtles, *Pseudemys concinna* (LeConte 1830), a species that is closely related and ecologically similar to *T. scripta* (Ernst and Lovich, 2009), but which reaches larger body sizes that facilitate successful implantation of strain gauges onto the humerus. If the humerus does not show reduced torsion during swimming in turtles, then the plausibility of limb bone flattening having been facilitated by environmental changes in loading regime would be called into question.

MATERIALS AND METHODS

Animals

Six adult *P. concinna* (3 females, 3 males; carapace length 28.15 ± 2.46 cm; mass 2.65 ± 0.61 kg) were collected from Lake Hartwell, Pickens County, SC, USA in August 2013 and August 2014 (South Carolina Department of Natural Resources Permits 43-2013 and 29-2014). Turtles were housed in a greenhouse in 600 liter cattle tanks half filled with water and exposed to ambient light and temperature. Tanks were equipped with re-circulating filters and basking docks. Animals were fed pellets daily (Young and Blob, 2015).

Surgical procedures

All procedures were approved by the Clemson University IACUC (AUP 2012-056, 2016-011). To induce analgesia and anesthesia, turtles were injected (left forelimb muscles) with initial doses of 1 mg kg^{-1} butorphenol, 100 mg kg^{-1} ketamine, and 1 mg kg^{-1} xylazine, with supplements as needed. Upon achieving anesthesia, a medial incision was made along the proximal aspect of the right forelimb. To access gauge attachment sites, muscles surrounding the humerus were separated and retracted to expose the bone. A window of periosteum was removed, and the exposed bone cortex was swabbed clean with ether and allowed to dry. Single element and rosette strain gauges (FLG-1-11 and FRA-1-11, respectively; Tokyo Sokki Kenkyujo, Japan) were attached using a self-catalyzing adhesive (Duro® Super Glue; Henkel Corporation, Avon, OH, USA). In our largest individual, we implanted two rosette gauges on the humerus, one on the anterior surface and one on the posterior surface. In other large individuals we attached a rosette gauge to either the anterior or ventral surface of the humerus, and single-element gauges to two other surfaces (anterior, ventral, or posterior). For our smallest individuals, in which rosette gauges could not be implanted due to size limitations, three single-element gauges were attached in anterior, ventral, and posterior positions. Once gauges were in place, lead wires were threaded through a second, proximal forelimb incision. Incisions were sutured closed, and wires were soldered to a microconnector and sealed with epoxy. Connectors were secured to the forelimb with self-adhesive bandaging tape (Vetrap®; 3M Animal Care Products, USA), with care taken to avoid restriction of limb movement.

***In vivo* strain data collection and data analysis**

Following 24 hours of recovery, *in vivo* strain data were collected during steady speed swimming in a flow tank and walking on a motorized treadmill (Model DC5; Jog A Dog®; Ottowa Lake, MI, USA). Strain signals were conducted from the gauges to Vishay conditioning bridge amplifiers (model 2120B; Measurements Group, Raleigh, NC, USA) via a shielded cable. To prevent signal disruption by water, the connection between this cable and the connector attached to the turtle was sealed with Plumber's Epoxy Putty (ACE Hardware Corporation, USA). Raw voltages from the strain gauges were sampled through an A/D converter (model PCI-6031E; National Instruments) at 5000 Hz. These data were saved to a computer using data acquisition software written in LabVIEW (v. 6.1; National Instruments) and calibrated to microstrain (με).

Trials were conducted at the maximal speed at which an individual could maintain its position in the flow tank or on the treadmill (0.200-0.495 m s^{-1} in flowtank; 0.103-0.139 m s^{-1} on treadmill). Although these speeds are not strictly dynamically equivalent, they provide comparable levels of exertion that are useful for understanding the selection pressures acting on skeletal design. High-speed videos of each trial were recorded from lateral and ventral (swimming) or dorsal (walking) views (100 Hz; Phantom V5.1, Vision Research Inc., Wayne, NJ, USA). Videos were synchronized with strain recordings using a light box that emitted a visible flash in the video that corresponded with a 1.5V pulse in the strain recording. Upon completion of trials, turtles were euthanized via intraperitoneal injection (Euthasol® pentobarbital sodium solution; Delmarva Laboratories Inc., Midlothian, VA, USA; 200 mg kg^{-1}). Peak strain magnitudes were determined from each gauge location for each stroke (swimming) and step (walking) of the right forelimb, following previously published methods (Blob and Biewener, 1999). Walking and

swimming strains were compared within each individual for each gauge location using Mann-Whitney *U*-tests. Statistical analyses were conducted in SAS® (SAS v. 9.3, SAS Institute Inc. 2010, Cary, NC, USA).

RESULTS AND DISCUSSION

During swimming, longitudinal strains generally maintained the same orientation (i.e. tensile or compressive) during both thrust (retraction) and recovery (protraction) phases of the limb cycle (13 of 16 comparisons: Table 1). Thus, humeral bending did not reverse direction between protraction and retraction, a pattern consistent with femoral swimming strains in slider turtles (Young and Blob, 2015). Single peaks were typically observed during retraction in swimming, whereas strains were more variable during protraction (Fig. 3.1), resembling patterns observed in the femur during both swimming and terrestrial walking (Butcher et al., 2008; Young and Blob, 2015). In contrast to the femur (Young and Blob, 2015), absolute magnitudes of peak humeral strain during swimming (longitudinal, principal, and shear) were not uniformly greater during thrust than during recovery (Table 3.1). These differences between humeral and femoral loading may reflect differences in the size of the paddle formed by the foot in each limb. In both limbs, the foot is rotated perpendicular to oncoming flow during retraction (Pace et al., 2001; Blob et al., 2008), maximizing surface area of the foot against the surrounding medium to produce drag-based thrust. During recovery phase (protraction), the foot is rotated parallel to oncoming flow, reducing drag and minimizing interference to forward motion of the body. Such drag reduction would be expected to minimize the environmental forces acting on the limb, resulting in lower strain magnitudes during recovery (Young

and Blob, 2015). However, the extended surface area of the forefoot paddle is much smaller than the extended surface area of the hindfoot paddle in cooters and sliders (Young et al., 2017), which may lead to greater similarity in the environmental forces applied to the limb between thrust and recovery phases for the forelimb. In a further departure from the loading patterns observed in the femur, the orientation of peak principal tensile strain to the long axis of the humerus (φ_T) was typically near 45° during both thrust and recovery, indicating the significance of twisting as a mechanism through which loads are applied to the forelimb (Table 3.1).

In comparisons between swimming and walking, the orientation of longitudinal strains on the humerus was typically consistent between environments (10 of 12 comparisons: Table 3.2). Peak strain magnitudes also were consistently significantly lower during the thrust phase of swimming than during the stance phase of walking (Table 3.2, Fig. 3.1). For longitudinal strains during retraction, peak magnitudes during swimming are approximately 11% of peak magnitudes during walking. For shear, however, peak swimming strain magnitudes are roughly 40% of walking shear strains (Table 3.2, Fig. 3.1). Though this is a considerable reduction in loads between locomotor environments, it is less of a reduction in shear between environments than was found for the femur, in which shear strains during swimming were only 10% of those during walking (Young and Blob, 2015). In the femur, shear strain reduction during swimming is driven by both an overall reduction in strain magnitudes conveyed by buoyancy in water, and through a reorientation of loading that reduces the high levels of twisting observed in walking to lower levels during swimming (Young and Blob, 2015; Mayerl et al., 2016). In contrast, the reduction of humeral shear strains during swimming appears to

result essentially solely from the overall reduction of strain magnitudes in water compared to land (Table 3.2). Values of φ_T for the humerus (Table 3.2) are near 45° during both terrestrial walking (66.4°±9.7º) and swimming (30.2°±6.1º), indicating that twisting is still likely applied to the humerus in both environments. Therefore, though both shear and torsional loading on the humerus are reduced during swimming compared to walking, this reduction does not appear to result from the substantial reorientation of applied loads that occurs in the femur.

The different mechanisms that reduce aquatic shear strains in the humerus versus the femur of turtles may relate to structural differences between the forelimb and hindlimb, and the kinematic constraints that these impose. The degree of forelimb protraction in turtles is unusually high for tetrapods with sprawling postures (Walker, 1971; Pace et al., 2001; Schmidt et al., 2016). This extent of protraction may be facilitated by humeral morphology, particularly the arched shaft of the humerus and anatomical torsion of distal shaft relative to the humeral head (Ogushi, 1911). However, the range of humeral retraction in turtles is generally limited (Pace et al., 2001; Rivera and Blob, 2010; Schmidt et al., 2016), likely due to restrictions imposed by the anterior edge of the bridge between the carapace and plastron of the shell (Walker, 1971; Zug, 1971). As a potential consequence, in tortoises walking on land, long axis rotation combined with elbow extension accounts for 64% of the range of forelimb motion (Schmidt et al., 2016). Thus, reduction of humeral twisting in water might restrict the forelimb movements of turtles to a much greater degree than the limited impact that reduced femoral twisting appears to have on their hindlimb movements (Mayerl et al., 2016).

Strain patterns of the long bones of the limb indicate a reduction in shear during swimming compared to terrestrial walking in both the forelimb and the hindlimb (Young and Blob, 2015). Despite showing similar patterns of shear reduction, changes in loading between land and water may occur through different mechanisms in the humerus and femur that relate to structural and functional differences between the forelimb and hindlimb in turtles. Nonetheless, the distinctive changes in long bone morphology that characterize most reinvasions of aquatic habitats by tetrapods may likely have been facilitated by release from the demands imposed by torsional loading, allowing greater opportunity for the evolution of novel limb bone shapes.

ACKNOWLEDGEMENTS

We thank C. Mayerl, K. Diamond, J. Pruett, K. Vest, and M. Gregory for assistance with collecting study animals, animal care, and data collection. We also thank C. Mayerl, K. Diamond, and the Clemson Writers Guild for thoughtful feedback on previous versions of this manuscript.

FUNDING

This work was supported by Clemson University Creative Inquiry Grant #479.

REFERENCES

Ashley-Ross, M. A., Hsieh, S. T., Gibb, A. C. and Blob, R. W. (2013). Vertebrate land invasions-past, present, and future: an introduction to the symposium. *Integr. Comp. Biol.* 53, 192-196.

Bertram, J. E. A. and Biewener, A. A. (1990). Differential scaling of the long bones in the terrestrial Carnivora and other mammals. *J. Morphol.* 204, 157-169. (doi: 10.1002/jmor.1052040205).

Biewener, A. A. and Dial, K. P. (1995). *In vivo* strain in the humerus of pigeons (*Columba livia*) during flight. *J. Morphol.* 225, 61-75. (doi: 10.1002/jmor.1052250106).

Blob, R. W. and Biewener, A. A. (1999). *In vivo* locomotor strain in the hindlimb bones of *Alligator mississippiensis* and *Iguana iguana*: implications for the evolution of limb bone safety factor and non-sprawling limb posture. *J. Exp. Biol.* 202, 1023-1046.

Blob, R. W., Espinoza, N. R., Butcher, M. T., Lee, A. H., D'Amico, A. R., Baig, F. and Sheffield, K. M. (2014). Diversity of limb-bone safety factors for locomotion in terrestrial vertebrates: evolution and mixed chains. *Integr. Comp. Biol.* 54, 1058-1071.

Blob, R. W., Mayerl, C. J., Rivera, A. R. V., Rivera, G. and Young, V. K H. (2016). "On the fence" versus "all in": insights from turtles for the evolution of aquatic locomotor specializations and habitat transitions in tetrapod vertebrates. *Integr. Comp. Biol.* 56, 1310-1322. (doi: 10.1093/icb/icw121)

Blob, R. W., Rivera, A. R. V. and Westneat, M. W. (2008). Hindlimb function in turtle locomotion: limb movements and muscular activation across taxa, environment, and ontogeny. In *Biology of Turtles*, pp. 139-162. (ed. J. Wyneken, M. H. Godfrey, V. Bels), pp. 139-162. Boca Raton, FL: CRC Press.

Buckwalter, J. A., Glimcher, M. J., Cooper, R. R. and Recker, R. (1995). Bone biology. Part I: structure, blood supply, cells, matrix, and mineralization. *J. Bone Joint Surg*. 77, 1256 - 1275.

Butcher, M. B., Espinoza, N. R., Cirilo, S. R. and Blob, R. W. (2008). *In vivo* strains in the femur of the river cooter turtles (*Pseudemys concinna*) during terrestrial locomotion: tests of force-platform models of loading mechanics. *J. Exp. Biol*. 211, 2397-2407. (doi: 10.1242/jeb.018986).

Caldwell, M. W. (2002). From fins to limbs to fins: limb evolution in fossil marine reptiles. *Am. J. Med. Gen*. 112, 236-249.

Ernst, C. H. and Lovich, J. E. (2009). *Turtles of the United States and Canada*, 2nd edn.

Baltimore: The Johns Hopkins University Press.

Fish, F. E. (1996). Transitions from drag-based to lift-based propulsion in mammalian swimming. *Am. Zool.* 36, 628-641.

Gillis, G. B. and Blob, R. W. (2001). How muscles accommodate movement in different physical environments: aquatic versus terrestrial locomotion in vertebrates. *Comp. Biochem. Physiol.* 131A, 61–75. (doi: 10.1016/S1095-6433(01)00466-4).

Lanyon, L. E., Goodship, A. E., Pye, C. and McFie, H. (1982). Mechanically adaptive bone remodeling: a quantitative study on functional adaptation in the radius following ulna osteotomy in sheep. *J. Biomech*. 12, 141-154. (doi: 10.1016/0021-9290(82)90246-9).

Lindgren, J., Polcyn, M. J. and Young, B. A. (2011). Landlubbers to leviathans: evolution of swimming in mosasaurine mosasaurs. *Paleobiology* 37, 445-469.

Mayerl, C. J., Brainerd, E. L. and Blob, R. W. (2016). Pelvic girdle mobility of cryptodire and pleurodire turtles during walking and swimming. *J. Exp. Biol.* 219, 2650-2658.

Ogushi, K. (1911). Anatomische studien an der japanichen dreikralligen Lippenschildkrote (*Trionyx japonicus*). I. Das Skeletsystem. *Morpholog. Jahrbuch* 43, 1-106.

Pace, C. M., Blob, R. W. and Westneat, M. W. (2001). Comparative kinematics of the forelimb during swimming in red-eared slider (*Trachemys scripta*) and spiny softshell (*Apalone spinifera*) turtles. *J. Exp. Biol.* 204, 3261-3271.

Renous, S., de Lapparent de Broin, F., Depecker, M., Davenport, J. and Bels, V. (2008). Evolution of locomotion in aquatic turtles. In *Biology of Turtles*, pp. 97-133. (ed. J. Wyneken, M. H. Godfrey, V. Bels), pp. 139-162. Boca Raton, FL: CRC Press.

Rivera, A. R. V. and Blob, R. W. (2010). Forelimb kinematics and motor patterns of the slider turtle (*Trachemys scripta*) during swimming and walking: shared and novel strategies for meeting locomotor demands of water and land. *J. Exp. Biol.* 213, 3515-3526.

Schmidt, M., Mehlhorn, M. and Fischer, M. S. (2016). Shoulder girdle rotation, forelimb movement, and the influence of carapace shape on locomotion in *Testudo hermanni* (Testudinidae). *J. Exp. Biol.* 137059. (doi: 10.1242/jeb.137059).

Sheffield, K. M., Butcher, M. T., Shugart, S. K., Gander, J. C. and Blob, R. W. (2011). Locomotor loading mechanics in the hindlimbs of tegu lizards (*Tupinambis merianae*): comparative and evolutionary implications. *J. Exp. Biol.* 214, 2616-2630. (doi: 10.1242/jeb.048801).

Vogel, S. (2013). *Comparative Biomechanics: Life's Physical World*. Princeton, NJ: Princeton University Press.

Walker, J. A. (2002). Functional morphology and virtual models: physical constraints of the design of oscillating wings, fins, legs, and feet at intermediate Reynolds numbers. *Integr. Comp. Biol.* 42, 232-242. (doi: 10.1093/icb/42.2.232).

Walker, W. F. Jr. (1971). A structural and functional analysis of walking in the turtle, *Chrysemys picta marginata. J. Morphol.* 134, 195-214.

Wyneken, J. (1997). Sea turtle locomotion: mechanisms, behavior, and energetics. In *The Biology of Sea Turtles* (ed. P. L. Lutz and J. A. Musick), pp. 165-198. Boca Raton, FL: CRC Press.

Young, V. K H. and Blob, R. W. (2015). Limb bone loading in swimming turtles: changes in loading facilitate transitions from tubular to flipper-shaped limbs during aquatic invasions. *Biol. Lett.* 11: 20150110. (doi: 10.1098/rsbl.2015.0110).

Young, V. K H., Vest, K. G., Rivera, A. R. V., Espinoza, N. R. and Blob, R. W. (2017). One foot out the door: limb function during swimming in terrestrial versus aquatic turtles. *Biol. Lett.* 13: 1-5.

Zimmer, C. (1999). *At the Water's Edge: Fish with Fingers, Whales with Legs, and How Life Came Ashore but then Went Back to Sea*. New York, NY: Touchstone.

Zug, G. R. (1971). Buoyancy, locomotion, morphology of the pelvic girdle and hind limb, and systematics of cryptodiran turtles. *Misc. Publ. Mus. Zool. Univ. Mich.* 142, 1-98.

Table 3.1. Mann-Whitney *U* results for comparisons of peak humeral strains during thrust versus recovery phases of swimming in *P. concinna*. Values are mean ± s. e.; pT, principal tensile strain; pC, principal compressive strain; φ_T, angle of principal tensile strain to the humeral long axis.

ID	Gauge Location	Strain Type	*N*	Thrust (με)	Recovery (με)	|*Z*|	*p*
PC01	Posterior	Longitudinal	40	58.1 ± 11.9	-60.7 ± 18.8	3.30	0.0010*
PC02	Ventral	Longitudinal	71	-19.6 ± 12.6	-89.4 ± 10.6	3.22	0.0013*
	Posterior	Longitudinal	71	-13.1 ± 18.7	-88.1 ± 16.2	2.75	0.0059*
PC03	Posterior	Longitudinal	22	36.9 ± 24.2	-83.7 ± 27.5	2.27	0.0235*
PC04	Anterior	Longitudinal	34	32.7 ± 13.2	8.7 ± 12.7	1.05	0.2943
	Anterior	pT	34	72.2 ± 7.3	63.7 ± 7.4	0.98	0.3295
	Anterior	pC	34	-70.5 ± 5.8	-73.5 ± 7.0	0.35	0.7267
	Anterior	φ_T[a]	34	51.8 ± 4.1	42.9 ± 4.6	1.21	0.2270
	Anterior	Shear	34	93.8 ± 11.4	90.1 ± 13.8	0.52	0.6022
PC05	Ventral	Longitudinal	12	156.9 ± 35.6	55.2 ± 73.0	0.09	0.9310
	Ventral	pT	12	193.6 ± 26.4	155.9 ± 52.7	2.11	0.0351*
	Ventral	pC	12	-184.2 ± 32.2	-215.2 ± 49.1	0.20	0.8399
	Ventral	φ_T[a]	12	24.1 ± 7.5	48.2 ± 11.7	0.49	0.6236
	Ventral	Shear	12	137.0 ± 24.5	50.4 ± 11.0	2.68	0.0073*
PC06	Ventral	Longitudinal	85	51.6 ± 7.5	-87.3 ± 3.7	2.08	0.0376*
	Ventral	pT	85	156.2 ± 10.9	54.9 ± 6.7	8.46	<0.0001*
	Ventral	pC	85	-124.9 ± 11.5	-117.7 ± 0.1	0.22	0.8273
	Ventral	φ_T[a]	85	36.3 ± 2.0	42.6 ± 3.6	0.24	0.8104
	Ventral	Shear	85	242.4 ± 23.1	93.7 ± 16.7	6.48	<0.0001*

[a]Units for φ_T in deg.

*$p \leq 0.05$.

Table 3.2. Mann-Whitney *U* results for comparisons of peak humeral strains during swimming versus terrestrial walking for the thrust/stance phase of the limb cycle in *P. concinna*. Values are mean ± s. e. pT, principal tensile strain; pC, principal compressive strain; φ_T, angle of principal tensile strain to the humeral long axis.

ID	Gauge Location	Strain Type	*N (swim, walk)*	Swim (με)	Walk (με)	|*Z*|	*p*
PC01	Posterior	Longitudinal	40; 35	58.1 ± 11.9	1398.9 ± 37.6	7.43	<0.0001*
PC02	Ventral	Longitudinal	71; 28	-19.6 ± 12.6	251.9 ± 64.1	7.58	<0.0001*
	Posterior	Longitudinal	71; 28	-13.1 ± 18.7	277.2 ± 58.6	7.28	<0.0001*
PC03	Posterior	Longitudinal	22; 8	36.9 ± 24.2	746.4 ± 95.5	4.10	<0.0001*
PC05	Ventral	Longitudinal	12; 29	156.9 ± 35.6	562.5 ± 93.8	4.97	<0.0001*
	Ventral	pT	12; 29	193.6 ± 26.4	699.3 ± 46.1	3.97	<0.0001*
	Ventral	pC	12; 29	-184.2 ± 32.2	-249.5 ± 32.1	2.22	0.0264*
	Ventral	φ_T[a]	12; 29	24.1 ± 7.5	76.0 ± 3.7	3.65	0.0003*
	Ventral	Shear	12; 29	137.0 ± 24.5	285.5 ± 30.7	2.97	0.0030*
PC06	Ventral	Longitudinal	85; 32	51.6 ± 7.5	274.2 ± 56.1	8.30	<0.0001*
	Ventral	pT	85; 32	156.2 ± 10.9	556.2 ± 31.8	7.88	<0.0001*
	Ventral	pC	85; 32	-124.9 ± 11.5	-362.2 ± 32.4	6.37	<0.0001*
	Ventral	φ_T[a]	85; 32	36.3 ± 2.0	56.7 ± 3.1	4.98	<0.0001*
	Ventral	Shear	85; 32	242.4 ± 23.1	729.2 ± 56.5	6.30	<0.0001*

[a]Units for φ_T in deg.

*$p \leq 0.05$.

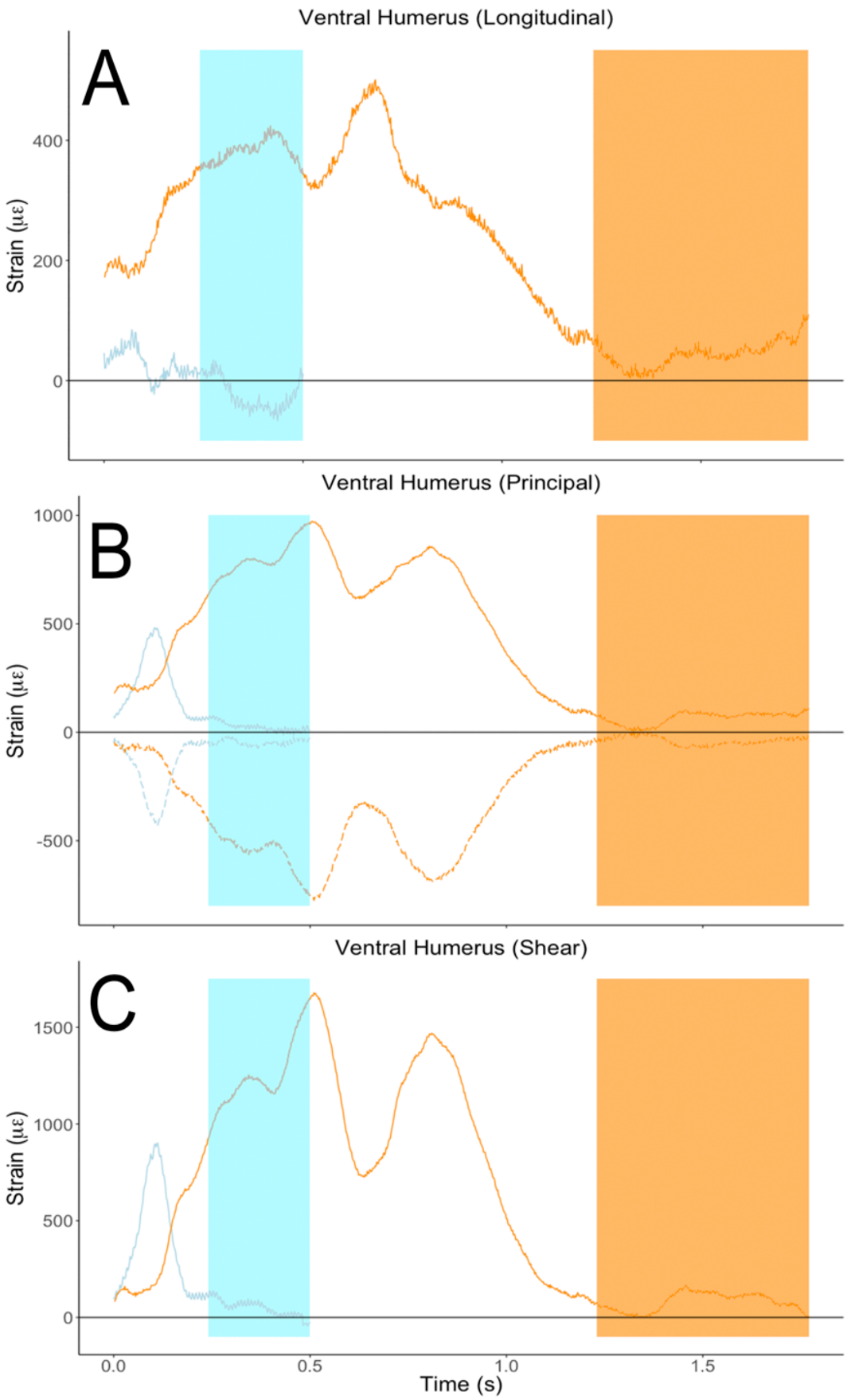
Ventral Humerus (Longitudinal)
A
400
200
0
Strain (με)
Ventral Humerus (Principal)
B
1000
500
0
-500
Strain (με)
Ventral Humerus (Shear)
C
1500
1000
500
0
Strain (με)
0.0
0.5
1.0
1.5
Time (s)

Figure 3.1. Representative strain traces simultaneously recorded from a rosette gauge located on the ventral surface of the humerus during swimming and terrestrial walking in the river cooter turtle, *Pseudemys concinna*. A single limb cycle from the same individual is illustrated for both behaviors. (A) Ventral longitudinal strain. (B) Ventral principal strains. (C) Ventral shear strain. Walking strains are shown in orange and swimming strains are shown in blue. Shaded regions indicate the recovery (protraction) phase of the limb cycle for each locomotor behavior (walking in orange, swimming in blue). Compressive principal strain is represented by a dashed line.

CHAPTER FOUR

ONE FOOT OUT THE DOOR: LIMB FUNCTION DURING SWIMMING IN TERRESTRIAL VERSUS AQUATIC TURTLES

This is a pre-copy-editing, author-produced copy of an article accepted for publication in *Biology Letters* following peer-review. The definitive publisher-authenticated version:

Vanessa K Hilliard Young, Kaitlyn G. Vest, Angela, R. V. Rivera, Nora R. Espinoza, and Richard W. Blob. One foot out the door: limb function during swimming in terrestrial versus aquatic turtles. *Biology Letters* **13**: 20160732. 1 – 5. *doi:10.1098/rsbl.2016.0732*

is available online at: http: http://rsbl.royalsocietypublishing.org/content/13/1/20160732.

ABSTRACT

Specialization for a new habitat often entails a cost to performance in the ancestral habitat. Although aquatic lifestyles are ancestral among extant cryptodiran turtles, multiple lineages, including tortoises (Testudinidae) and emydid box turtles (genus *Terrapene*), independently specialized for terrestrial habitats. To what extent is swimming function retained in such lineages despite terrestrial specialization? Because tortoises diverged from other turtles over 50 million years ago, but box turtles did so only 5 million years ago, we hypothesized that swimming kinematics for box turtles would more closely resemble those of aquatic relatives than those of tortoises. To test this prediction, we compared high-speed video of swimming Russian tortoises (*Testudo horsfieldii*), box turtles (*Terrapene carolina*), and two semi-aquatic emydid species: sliders (*Trachemys scripta*) and painted turtles (*Chrysemys picta*). We identified different

kinematic patterns between limbs. In the forelimb, box turtle strokes most resemble those of tortoises; for the hindlimb, box turtles are more similar to semi-aquatic species. Such patterns indicate functional convergence of the forelimb of terrestrial species, whereas the box turtle hindlimb exhibits greater retention of ancestral swimming motions.

INTRODUCTION

Species that specialize for particular environments often exhibit performance costs in contrasting environments [1, 2]. In some cases, specializations following major habitat transitions become so extreme that a species might rarely, if ever, encounter the contrasting, ancestral habitat [3]. There are few comparative data to evaluate the extent to which ancestral locomotor abilities are retained by such extreme specialists.

Studies of turtles may provide insight into this question. Aquatic lifestyles are ancestral among extant cryptodiran turtles [4]. However, multiple cryptodiran lineages have independently specialized for terrestrial habitats, including tortoises (~50 species, family Testudinidae), and North American box turtles (genus *Terrapene*) [5]. These lineages exhibit several traits reflecting terrestrial specialization. Both groups have highly domed shells, and lose hindfoot webbing that typifies semi-aquatic taxa. Tortoises also show reduced carpals and tarsals, restricting wrist and ankle mobility [6]. Although fossils indicate that tortoises became terrestrial ~50 million years ago, terrestrialization occurred more recently in *Terrapene,* which diverged from aquatic emydids ~5 million years ago [7]. The longer duration of terrestrial specialization in tortoises, and their novel wrist and ankle structure, might lead to distinctive swimming movements compared to semi-aquatic taxa.

To test how swimming capabilities may change with the length of time that a lineage has been a terrestrial specialist, we collected high-speed video of swimming Russian tortoises (*Testudo horsfieldii*) and three-toed box turtles (*Terrapene carolina triunguis*), and compared limb kinematics for these species to those from two semi-aquatic emydids: sliders (*Trachemys scripta*) and painted turtles (*Chrysemys picta*). Given the derivation of box turtles from the emydid lineage [5] and the shorter amount of time for their terrestrial specialization, we predicted that box turtle kinematics would be more similar to those of semi-aquatic emydids than to those of tortoises and, therefore, more closely resemble ancestral patterns of cryptodiran swimming [3].

MATERIALS AND METHODS

High-speed digital video (Appendix A – Fig. A-1) was collected from 3 adults of each species (average carapace lengths ± S.D. = 132 ± 10 mm for *C. picta*, 206 ± 14 mm for *T. scripta*, 113 ± 2 mm for *T. carolina*, 137 ± 18 mm for *T. horsfieldii*). *T. carolina* (Apet, Chicago, IL) and *T. horsfieldii* (LLLReptile, Oceanside, CA) were purchased from suppliers; *T. scripta* and *C. picta* were collected (Union and Alexander Counties, Illinois, permit A99.0550). Animals were housed in 900mm x 600mm x 200mm plastic tubs. Terrestrial enclosures had peat moss substrate; aquatic enclosures were fitted with recirculating filters and basking areas [8].

Swimming trials were conducted in a recirculating flow tank. Kinematic data were collected in lateral and ventral views using two synchronized, high-speed digital video cameras (100Hz). The ventral view was derived from a mirror angled 45° to the tank bottom [8]. After swimming began, flow speed was adjusted to keep the individual

in the video field of view for the duration of the trial [8] except for tortoises, which only swam in still water. Five swimming strokes for both forelimb and hindlimb were analyzed for each turtle. Anatomical landmarks were digitized in each view for every other video frame (including shoulder/hip, elbow/knee, wrist/ankle, metacarpo-phalangeal joints, and tips of first, third, and fifth digits) [8]. Custom MATLAB (MathWorks, Natick, MA, USA) code was used to calculate kinematic variables from three-dimensional coordinate data for each trial. Data were smoothed and normalized prior to comparisons using QuickSAND [9].

Means and standard errors were compared across species for 10 kinematic variables for each limb that reflected maxima and minima of joint motion (Appendix A - Tables S1, S2). Two-way, mixed-model nested ANOVAs were conducted to determine whether swimming kinematics differed overall among the four species. *Post-hoc* Tukey's pair-wise mean comparisons were conducted for each significant ANOVA to determine which species pairs differed. Kinematic differences among species for these variables also were evaluated using principal components analysis (PCA) and Euclidean distance calculations [8]. Statistical analyses were conducted in R (version 3.2.4, R Foundation for Statistical Computing, Vienna, Austria). We did not perform formal phylogenetic corrections to these analyses due to the small number of species in our comparisons, but we did specifically consider phylogenetic relatedness and ecological similarity as bases for predicting kinematic similarities between taxa.

We also compared overall kinematic profiles for each variable across species. After normalizing all trials to the same duration, we calculated average values of each variable for each species for each 1% time increment, from which we generated 100-

dimensional vectors. Using standard equations [8], we then calculated angles between these 100-dimensional vectors for paired combinations of species for each variable, with angles near 0° indicating similarity, and angles near 90° indicating dissimilarity.

RESULTS

Nested MANOVA indicated significant differences in swimming kinematics among the four species in the forelimb and hindlimb (forelimb: Wilks lambda <0.001, F=41.59 , d.f.= 30, 115.15, P<0.001; hindlimb: Wilks lambda <0.001 , F=63.79 , d.f.= 30, 115.15, P<0.001). Overall differences are evident from PCA results (figure 4.1; table 4.1, Appendix A – Tables S3, S4), which show distinct clusters for each species in both limbs, except for overlap between painted turtles (*C. picta*) and box turtles (*T. carolina*) in the hindlimb. Separation for the forelimb is driven by differences in high elbow flexion and extension for box turtles, versus high forefoot feathering for sliders (figure 4.1a, table 4.1). Separation for the hindlimb is driven by low hindfoot feathering for tortoises compared to other species (figure 4.1b, table 4.1).

Differences in swimming kinematics among species were also evident from Euclidian distances (Appendix A – Tables S5, S6). For the forelimb, the smallest differences were between painted turtles (*C. picta*) and the other three species, with the surprising result that the greatest similarity was between distantly related painted turtles and terrestrial tortoises (*T. horsfieldii*), and the greatest difference was between more closely related emydid sliders (*T. scripta*) and terrestrial box turtles (*T. carolina*). For the hindlimb, the greatest similarity was between painted and box turtles, whereas the

greatest differences were between tortoises and the other species (Appendix A – Table S6).

Two-way nested ANOVAs showed differences between species for all 10 kinematic variables (Appendix A – Tables S1, S2). *Post-hoc* Tukey's comparisons indicate that for the forelimb, 4 out of 10 variables for each terrestrial taxon (*T. horsfieldii* and *T. carolina*) are distinct from semi-aquatic emydids (*C. picta* and *T. scripta)*. However, terrestrial taxa do not group together (Appendix A – Table S7). In the hindlimb, *T. horsfieldii* are distinct from the other three taxa for 7 out of 10 variables. In contrast, *T. carolina* are distinct from other taxa for only 2 out of 10 variables (Appendix A – Table S8).

Kinematic vector comparisons provide further insight into similarities and differences in overall limb movements across species. In the forelimb, box turtles are more similar to tortoises than to more closely related semi-aquatic species for four out of five variable profiles (figure 4.2, table 4.2). However, in the hindlimb, box turtles more closely resemble semi-aquatic emydid relatives (painted turtles or sliders) for four out of five variable profiles, most closely resembling tortoises only for the angle of hindfoot feathering (figure 4.2, table 4.2).

DISCUSSION

Comparisons of maxima and minima for forelimb and hindlimb variables indicate considerable kinematic differentiation across all of our study taxa (figure 4.1), even between closely related and ecologically similar species like painted turtles and sliders. In fact, painted turtles and sliders were rarely the most similar taxa for any of the variables

we compared (e.g., two out of ten kinematic profile comparisons: table 4.2). These results highlight the potential for unrecognized, functionally relevant kinematic diversity even among closely related and morphologically similar species.

Although maxima and minima for forelimb variables differ between terrestrial tortoises and box turtles (figure 4.1a), comparisons of overall kinematic profiles show that box turtles are more similar to tortoises than they are to either of the more closely related, semi-aquatic emydid species (figure 4.2, table 4.2). In contrast, for the hindlimb, PCA on kinematic maxima and minima shows substantial overlap between box turtles and painted turtles among semi-aquatic taxa (figure 4.1b), and vector analyses of overall kinematic profiles show box turtles as closest to a semi-aquatic emydid taxon for four of five variables (figure 4.2, table 4.2). Based on these comparisons, the forelimb shows greater functional convergence between terrestrial species, whereas the hindlimb of box turtles, in which terrestriality is a recent evolutionary event, shows considerable retention of semi-aquatic kinematics. Thus, box turtles might be viewed as having "one foot out the door," with terrestrial specialization having greater impact on swimming kinematics for their forelimb than their hindlimb.

Similarities in forelimb kinematics are evident between terrestrial tortoises and box turtles, even with the independent specialization of tortoises to use their forelimbs for digging [6]. In this context, the apparent similarity of box turtle hindlimb movements to those of other emydids may largely reflect the more extreme divergence of tortoises. Tortoises are distinct for many more kinematic variables of the hindlimb than box turtles (seven versus two; Appendix A – Table S8). However, for most swimming turtles (except those using forelimb flapping [6]), the hindlimb is the primary source of propulsive thrust

[10]. Box turtles retain the ancestral ability to flex the ankle related to this role, but ankle flexion is negligible in tortoises (figure 4.2b, Appendix A – Fig. A-2). Thus, our results indicate that the independent paths to terrestriality followed by tortoises and box turtles did not proscribe a similar retention of swimming patterns.

Differences in functional change between the forelimbs and hindlimbs have been noted for other taxa spanning evolutionary transitions in habitat [11]. The reduction of propulsive force from the hindlimbs that appears likely with the loss of ankle flexion in tortoises may contribute to their inability to swim into flowing water during our trials. However, even with extreme specialization for terrestrial locomotion, it is striking that tortoises have been frequent colonizers of oceanic islands [12]. Given the limited swimming ability that our trials show for tortoises, it seems that other factors besides locomotor performance must have facilitated their infiltration of island habitats.

ACKNOWLEDGEMENTS

We thank MW Westneat, CM Pace, S Morar, and MS Fralick for contributions to data collection and preliminary analyses.

FUNDING

Work was supported by Clemson University (Creative Inquiry #479) and the Woman's National Farm and Garden Association (Sarah Bradley Tyson Fellowship to VKHY).

REFERENCES

1. Griffin, TM, Kram, R. 2000. Biomechanics: penguin waddling is not wasteful. *Nature* **408**: 929

2. Shine, R, Shetty, S. 2001. Moving in two worlds: aquatic and terrestrial locomotion in sea snakes (*Laticauda colubrine*, Laticaudidae). *J. Evol. Biol.* **14**: 338-346.

3. Blob, RW, Mayerl, CJ, Rivera, ARV, Rivera, G, Young, VKHY. 2016. "On the fence" versus "all in": insights from turtles for the evolution of aquatic locomotor specializations and habitat transitions in vertebrate tetrapods. *Int. Comp. Biol.* 56: pp 1-13, doi:10.1093/icb/icw121.

4. Joyce, WG, Gauthier, JA. 2003. Palaeoecology of Triassic stem turtle sheds new light on turtle origins. *Proc R. Soc. Lond.* B **271**: 1-5.

5. Gosnell, JS, Rivera, G, Blob, RW. 2009. A phylogenetic analysis of sexual size dimorphism in turtles. *Herpetologica* **65**: 70-81.

6. Walker, FW. 1973. The locomotor apparatus of Testudines. In *Biology of the Reptilia* vol. 4 Morphology D (eds C Gans, P Parsons), pp.1-99. London: Academic Press.

7. Dodd, CK. 2002. *North American Box Turtles: A Natural History*. Norman, OK: University of Oklahoma Press.

8. Rivera, ARV, Rivera, G, Blob, RW. 2013. Forelimb kinematics during swimming in the pig-nosed turtle, *Carettochelys insculpta*, compared with other turtle taxa: rowing *versus* flapping, convergence *versus* intermediacy. *J. Exp. Biol*. **216**, 668-680.

9. Walker, JA. 1998. Estimating velocities and accelerations of animal locomotion: a simulation experiment comparing numerically different algorithms. *J. Exp. Biol.* **201**, 981-995.

10. Blob, RW, Willey, JS, Lauder, GV. 2003. Swimming in painted turtles: particle image velocimetry reveals different propulsive roles for the forelimb and hindlimb. *Int. Comp. Biol.* **43**: 985.

11. Kawano, SM, Economy, DR, Kennedy, MS, Dean, D, Blob, RW. 2016. Comparative limb bone loading in the humerus and femur of the tiger salamander: testing the 'mixed-chain' hypothesis for skeletal safety factors. *J. Exp. Biol.* **219**: 341-353.

12. Caccone, A, Gibbs, JP, Ketmaier, V, Suatoni, E, Powell, JR. 1999. Origin and evolutionary relationships of giant Galapagos tortoises. *PNAS* **96**: 13223-13228. doi:10.1073/pnas.96.23.13223.

13. Young, VKH, Vest, KG, Rivera, ARV, Espinoza, NR, Blob, RW. 2016. Data from 'One foot out the door: limb function during swimming in terrestrial versus aquatic turtles'. *Dryad Digital Repository*. (doi:10.5061/dryad.mt28k).

Table 4.1. Loadings from principal components analyses of forelimb and hindlimb kinematics for ten variables in four species of turtle (see figure 4.1).

Kinematic Variable (Forelimb)	PC1 (35.2%)	PC2 (22.4%)
Maximum Humeral Protraction	-0.377	0.253
Maximum Humeral Retraction	-0.142	0.503
Maximum Humeral Elevation	-0.271	-0.215
Maximum Humeral Depression	-0.312	-0.331
Maximum Elbow Extension	0.270	-0.046
Maximum Elbow Flexion	0.246	0.417
Maximum Wrist Extension	-0.241	-0.477
Maximum Wrist Flexion	-0.332	0.037
Maximum Forefoot Feathering	-0.460	0.134
Minimum Forefoot Feathering	-0.392	0.323

Kinematic Variable (Hindlimb)	PC1 (51.6%)	PC2 (22.3%)
Maximum Femoral Protraction	-0.233	0.485
Maximum Femoral Retraction	-0.089	0.620
Maximum Femoral Elevation	-0.266	-0.098
Maximum Femoral Depression	-0.396	-0.162
Maximum Knee Extension	0.226	-0.453
Maximum Knee Flexion	0.377	-0.101
Maximum Ankle Extension	-0.358	-0.224
Maximum Ankle Flexion	-0.287	0.030
Maximum Hindfoot Feathering	0.397	0.125
Minimum Hindfoot Feathering	0.386	0.251

Table 4.2. Pair-wise angles between vectors representing kinematic profiles for ten variables across four turtle species (see figure 4.2); terr, terrestrial species; sem-aq, semi-aquatic species.

Kinematic Trajectory Vector	*Terrapene carolina (terr) vs. Testudo horsfieldii (terr)*	*Terrapene carolina (terr) vs. Chrysemys picta (sem-aq)*	*Terrapene carolina (terr) vs. Trachemys scripta (sem-aq)*	*Testudo horsfieldii (terr) vs. Chrysemys picta (sem-aq)*	*Testudo horsfieldii (terr) vs. Trachemys scripta (sem-aq)*	*Chrysemys picta (sem-aq) vs. Trachemys scripta (sem-aq)*
Humerus Protraction/Retraction	10.09	11.09	14.14	13.22	9.77	12.31
Humerus Elevation/Depression	23.32	38.25	64.21	56.56	81.81	28.98
Elbow	5.49	3.21	5.57	6.21	5.65	6.91
Wrist	39.45	136.71	84.64	157.41	100.23	62.37
Forelimb Paddle	31.17	41.59	34.66	27.72	15.52	13.14
Femur Protraction/Retraction	39.46	38.80	77.94	35.48	43.45	50.58
Femur Elevation/Depression	17.93	14.47	18.80	24.558	8.44	23.31
Knee	8.44	4.36	8.97	10.71	9.36	10.90
Ankle	158.54	15.88	19.88	168.71	169.37	8.96
Hindlimb Paddle	11.30	51.88	37.94	61.95	47.05	19.51

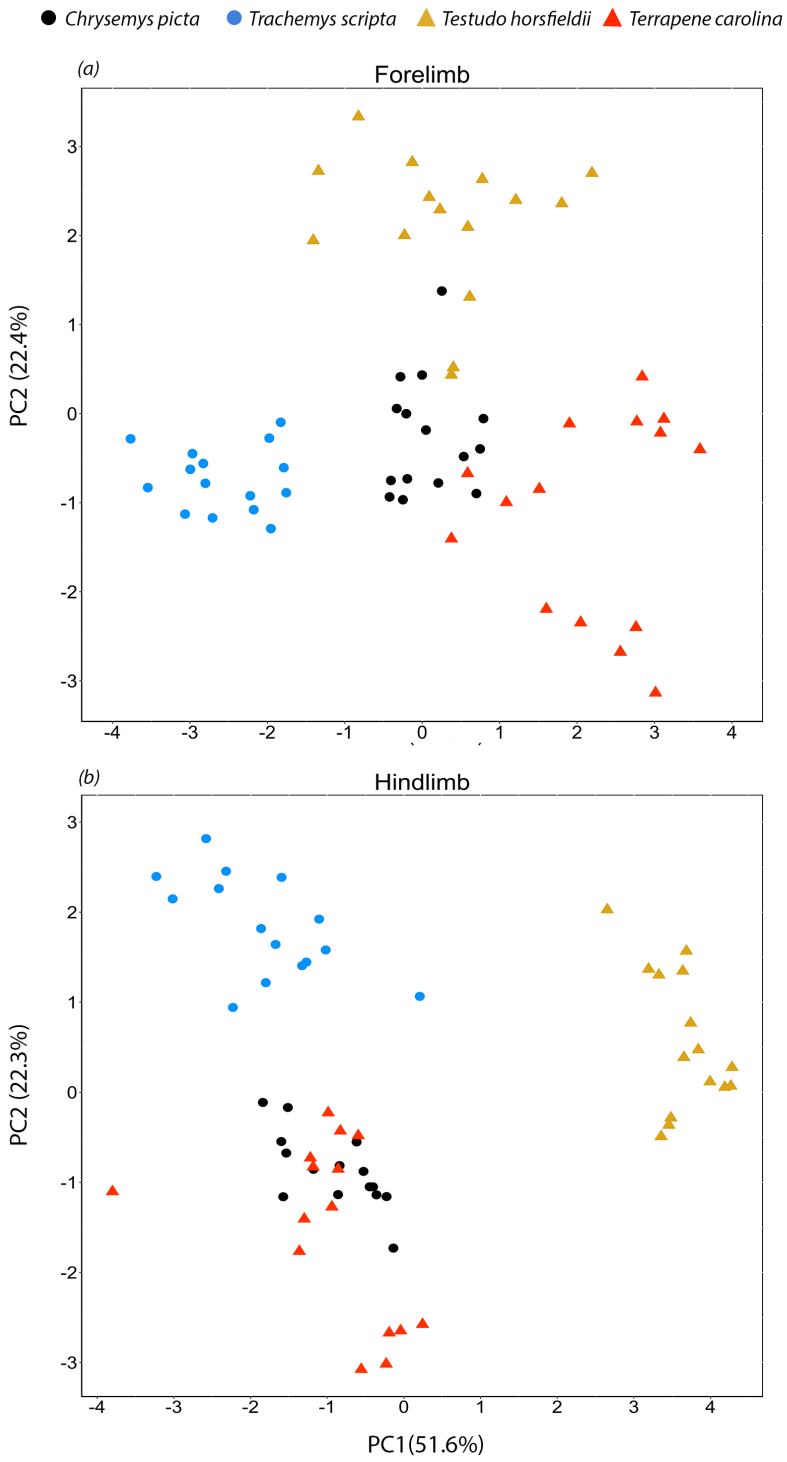

Figure 4.1. Plots of the first two principal components axes (PC1-2) for ten variables from swimming kinematics in the forelimb (a) and hindlimb (b) for four species of turtle:

Chrysemys picta (black circles), *Terrapene carolina* (red triangles), *Testudo horsfieldii* (gold triangles), and *Trachemys scripta* (blue circles). Terrestrial taxa are represented by triangles and semi-aquatic taxa by circles. PC1-2 explain 57.6% of variation in swimming kinematics for the forelimb and 73.9% for the hindlimb.

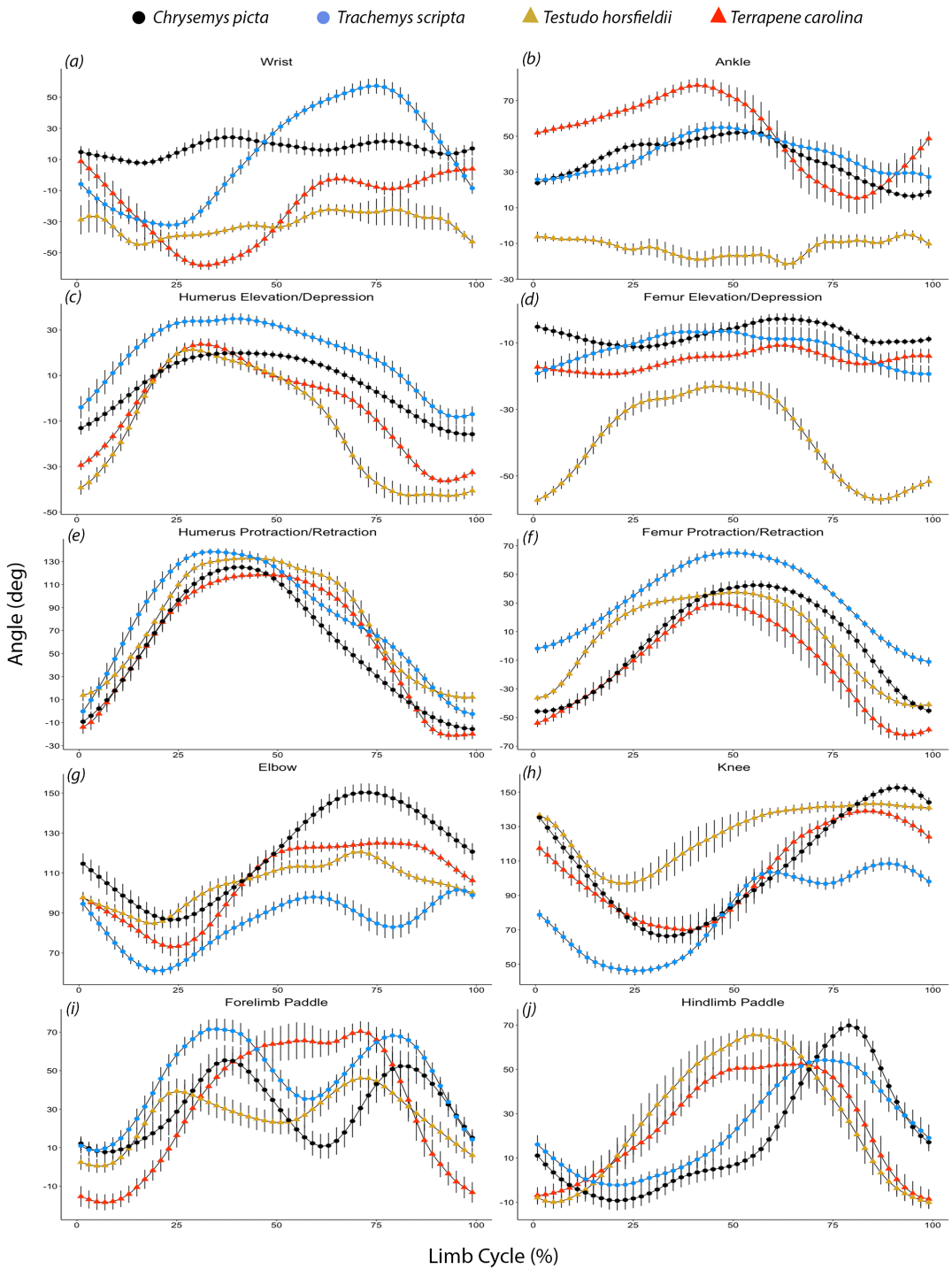

Figure 4.2. Mean kinematic profiles for forelimb and hindlimb variables during swimming in four species of turtle: *Chrysemys picta* (black circles), *Terrapene carolina*

(red triangles), *Testudo horsfieldii* (gold triangles), and *Trachemys scripta* (blue circles). Terrestrial taxa are represented by triangles and semi-aquatic taxa by circles. Plots show mean ± S. E. for every 2% increment of limb cycle duration. (a) Wrist flexion and extension, (b) ankle flexion and extension, (c) humerus elevation and depression, (d) femur elevation and depression, (e) humerus protraction and retraction, (f) femur protraction and retraction, (g) elbow flexion and extension, (h) knee flexion and extension, (i) forefoot orientation, (j) hindfoot orientation.

CHAPTER FIVE

COMPARATIVE LIMB BONE SCALING IN TURTLES: PHYLOGENETIC TRANSITIONS WITH CHANGES IN FUNCTIONAL DEMANDS?

ABSTRACT

Several terrestrial vertebrate lineages include members that have evolved nearly exclusive use of aquatic habitats. Such transitions are often associated with the evolution of flattened limbs used to swim via dorsoventral flapping. Such changes in shape may be facilitated by changes in bone loading during limb use in novel aquatic environments. Recent studies on limb bone loading during walking and swimming in turtles have found that torsion (twisting) is high relative to bending loads on land, but torsion is greatly reduced compared to bending during aquatic rowing (anteroposterior limb cycles). Release from torsion among rowing swimmers could have facilitated the evolution of hydrodynamically advantageous flattened limbs that later emerged among flapping aquatic species. Because aquatic rowing is regarded as an intermediate locomotor stage between walking and flapping, rowing species might show limb bone flattening that is intermediate between the tubular shapes of terrestrial walkers and the highly flattened shapes of marine flappers. To test this hypothesis, morphological measurements of the humerus and femur were collected from museum specimens representing four functionally divergent turtle clades: sea turtles (specialized marine flappers), softshells (specialized freshwater rowers), tortoises (specialized terrestrial walkers), and emydids (generalist semi-aquatic rowers). Patterns of limb bone scaling with respect to estimated

body mass were then compared across lineages using phylogenetic comparative methods. Although rowing taxa did not show clearly intermediate scaling patterns between tortoises and sea turtles, these data provide other functional insights. For example, the flattening of sea turtle limb bones was not associated with negative allometry of the flexion-extension diameter, but rather with positive allometry in the limb bone diameter perpendicular to flexion-extension. Moreover, softshell limb bones exhibit positive allometry of femoral diameters relative to body mass that may provide additional weight to compensate for a reduced shell, helping them maintain their typical benthic position in water. Tortoise limb bones showed positive allometry of their diameters relative to body size, as well as long humeri relative to body size, potentially reflecting specializations for resisting elevated loads associated with digging behaviors. Thus, scaling patterns of some turtle lineages may correlate with their distinctive behaviors or locomotor habits.

INTRODUCTION

Several vertebrate lineages that use terrestrial habitats have members that have evolved nearly exclusive use of aquatic habitats (e.g. sea turtles, mosasaurs, whales). Lineages that have made such transitions typically evolve morphologies reflecting their aquatic habits, such as a streamlined body shape, reduction of the pelvic girdle, and modification of limbs into flippers (Fish 1996). Such evolutionary changes in limb bone shape are often viewed as responses to changes in loading or functional demands (Carter and Beaupré 2001). For example, terrestrial vertebrates often possess tubular limb bone morphologies that reflect the need to resist both torsion (i.e. twisting) and bending loads

(Vogel 2013, Blob et al. 2016). In contrast, many lineages of vertebrates specialized for aquatic locomotion have evolved flattened, flipper-shaped limbs that facilitate swimming with flapping propulsion (Figure 5.1; Fish 1996, Wyneken 2001). However, the extent to which changes in loading regime might be responsible for limb shape changes during aquatic invasions is unclear, due to a lack of comparative morphological data that could reflect stages in such transitions.

Turtles are an excellent system for examining correlations between limb bone shape and function during evolutionary transitions to exclusively aquatic lifestyles. Turtles possess a bony shell that is fused to the dorsal vertebrae, preventing bending of the body axis (Pace et al. 2001). Therefore, all locomotion in turtles, both terrestrial and aquatic, is powered exclusively by the limbs, without axial contributions (Young and Blob 2015; Young 2017). As such, comparisons of limb bone loads during walking and swimming in turtles is not confounded by shifts from limb-powered to body axis-powered locomotion, as is seen in other secondarily aquatic taxa (e.g. mammals; Fish 1996). Furthermore, many semi-aquatic turtle species employ a "rowing" method of swimming, characterized by alternating anteroposterior strokes of fore- and hindlimbs. Because rowing resembles some aspects of terrestrial walking, it is considered an intermediate locomotor stage between walking and aquatic flight (Fish 1996). Therefore, data on limb bone morphology and loading from turtles could provide useful insight to the relationship between structural and functional transitions of the locomotor system during secondary invasions of aquatic habitats.

Previous comparisons of fore- and hind limb bone strains during swimming and walking for semi-aquatic, rowing turtles show that twisting loads are greatly reduced during aquatic rowing (Young and Blob 2015, Young 2017). This pattern of loading could help explain how flat limb bones evolved in aquatic specialists. Tubular bone shapes are optimal for resisting torsion, but bones are released from torsion in rowing. In addition, flapping typically evolves through a transition from rowing (Fish 1996). Thus, the release from torsion in rowing could have facilitated the evolution of hydrodynamically advantageous flat limbs in flappers (Young and Blob 2015; Young 2017). However, whether this mechanism contributed to changes in limb bone morphology in turtles is difficult to evaluate without morphological data from taxa spanning a complete range of locomotor habits, from terrestrial walking through aquatic rowing to aquatic flapping.

This study uses comparisons of allometry of proximal limb bone shapes (i.e. humerus and femur) to test whether there are differences in limb bone morphology across functionally diverse clades of turtles that reflect changes in limb bone loading and may have contributed to adaptive evolution in highly aquatic swimmers. I hypothesized that taxa living in habitats that impose high torsional loads on the limbs (i.e. terrestrial habitats) would exhibit more robust limb bone dimensions, with diameters showing positive allometry relative to body size. In contrast, taxa specializing for an aquatic environment, one less likely to impose high loading demands on the limbs, should show allometric patterns indicating flattening of the limb bones or negative allometry of one diameter relative to other limb bone proportions. Although one previous study of turtle

limb bone scaling has been conducted, measurements permitting functional analyses of limb bone proportions across taxa cannot be extracted from the results in that report (Llorente et al. 2008). Taxa sampled in this study include members of the Testudinidae (tortoises), which are highly specialized terrestrial walkers; Emydidae (pond turtles), which are primarily semi-aquatic freshwater rowers; Trionychia (softshells), which are typically highly specialized freshwater rowers; and Cheloniidae (sea turtles), which are flapping marine specialists. If the loading regime imposed by a locomotor method is a primary driver of limb bone morphology, then species using different modes of aquatic locomotion could show distinct limb bone proportions that correlate with differences in how their limbs are loaded. Because rowing is an intermediate locomotor method between walking and flapping, rowing taxa (e.g. emydids and trionychids) might show morphological patterns that are intermediate between those of terrestrial and flapping lineages. In addition, flattening of the long bones in cheloniids (sea turtles) could be achieved through negative allometry of the medial bone diameter relative to bone length and body mass, rather than positive allometry of the perpendicular diameter that would require maintenance of additional bone mass.

MATERIALS AND METHODS

Morphological Data Collection

I collected morphological data using Mituyoto digital calipers sensitive to 0.01mm from 100 turtle species (Appendix B – Table S1) representing four functionally divergent turtle taxa. Samples were measured between July 2015-June 2016 from five

collections: American Museum of Natural History, New York, NY (AMNH); Carnegie Museum of Natural History, Pittsburgh, PA (CMNH); Chelonian Research Institute, Oviedo, FL (CRI); Florida Museum of Natural History, Gainesville, FL (UF); and Smithsonian National Museum of Natural History, Washington D.C (USNM). Measurements included lengths of the carapace, plastron, humerus, and femur. I measured humeral and femoral lengths from the midpoints of the articular surfaces. Additionally, two diameters were measured from each humerus and femur at mid-shaft: flexion-extension diameter (FED), the diameter in the same plane as flexion and extension of the elbow or knee, and perpendicular diameter (PD), the diameter orthogonal to FED. I measured the largest representative of each species in each collection in order to avoid confounding factors of ontogeny. Only the single largest individual for each species across the five collections was included in the analyses. Estimated body mass of each specimen was derived from straight carapace length (CL) using the following equation (Pough 1980):

$$M = 3.9 \times 10^{-1} CL^{2.69}.$$

All anatomical data were log (base 10) transformed prior to analyses.

Assembly of Phylogenies for Comparative Analyses

I retrieved molecular data for nine genes from GenBank in Summer 2016 (Appendix B – Table S2). The genes included in this study consist of five mitochondrial genes (12S, 16S, COI, ND4, and cytB) and four nuclear genes (R35, c-mos, RAG1, and RAG2). I selected these genes because they are the genes for which the greatest number

of sequences are available (Guillon et al. 2012). Additionally, these genes have been used previously in inferring turtle evolutionary relationships (Guillon et al. 2012).

I aligned gene sequences using MUSCLE (Multiple Sequence Comparison by Log-Expectation; Edgar 2004) in MEGA version 7 (Kumar et al. 2015). Alignments for 12S, 16S, cytB, ND4, and R35 contained many indels; positions that were poorly aligned in these sequences were identified and omitted using default settings in Gblocks v0.91b (Castresana 2000, Talavera and Castresana 2007).

I first analyzed sequence alignments using jModelTest2 (Guindon and Gascuel 2003, Darriba et al. 2012) to select best-fit models of nucleotide substitution (Appendix B – Table S3). I identified optimal models using the corrected Akaike Information Criterion in jModelTest2. These models were implemented for Bayesian Inference analysis in MrBayes (Huelsenbeck and Ronquist 2001). The analysis was performed with 6,000,000 generations with a 10,000-sample burn-in. Every 100^{th} tree was sampled from the Markov Chain Monte Carlo analysis. The 50% majority-rule consensus tree containing branch lengths was calculated from the last 59,000 sampled trees (Figure 5.2). I imported the majority-rule tree into Mesquite for calculation of phylogenetic independent contrasts (Maddison and Maddison 2017). Tree polytomies were resolved in Mesquite using previously published phylogenies (Garland and Dickerman et al. 1993, Guillon et al. 2012, Stephens and Wiens 2003, Le et al. 2006). I calculated phylogenetic independent contrasts within each of the four clades (Cheloniidae, Emydidae, Testudinidae, Trionychia) using the PDTREE program in Mesquite (Figures 5.3-5.6; Midford et al. 2005, Maddison and Maddison 2017).

Scaling Analysis

Within-clade independent contrasts calculated in Mesquite (Midford et al. 2005, Maddison and Maddison 2017) were used to compute reduced major axis (RMA) regressions (Blob 2000) through the origin (Garland et al. 1992) for length of bone on FED and PD, length of bone on estimated body mass, and FED and PD on estimated body mass for each clade (40 total regressions). Values expected for isometry were 1.0 for length-diameter relationships and 0.33 for length-mass and diameter-mass relationships (Blob 2000). I compared allometric patterns among the four clades by evaluating overlap of 95% confidence intervals for regression slopes (Blob 2000), which I calculated following published methods (Jolicoeur and Mosimann 1968).

RESULTS

Analyses of independent contrasts indicate differences in proximal limb bone scaling patterns among the four functionally divergent clades of turtles examined (Table 5.1). However, rowing taxa do not show patterns that are clearly intermediate between those of terrestrial tortoises or flapping sea turtles.

Emydids show negative allometry of humeral length relative to mid-shaft humeral diameter of the flexion-extension plane (FED; Figure 5.7A). Humeral length for this clade scales isometrically with perpendicular humeral mid-shaft diameter (PD; Figure 5.7B). Furthermore, emydid humeral length, FED, and PD show positive allometry relative to estimated body mass (Figure 5.7C-E). Testudinids (tortoises) show similar

scaling patterns to emydids, exhibiting negative allometry of humeral length relative to FED and positive allometry of humeral length, FED, and PD relative to mass (Figure 5.7A, C-E). However, tortoises also show positive allometry of humeral length relative to PD (Figure 5.7B). Trionychids (softshells) show isometric scaling patterns for humeral length relative to FED and PD (Figure 5.7A-B). Humeral length, FED, and PD also scale isometrically relative to mass for this group (Figure 5.7C-E). Cheloniids (sea turtles) exhibit isometric scaling of humeral length to FED and PD, as well as of humeral length and FED relative to mass (Figure 5.7A-D), although it is possible that the small sample of available cheloniid taxa available for measurement impedes the recognition of non-isometric scaling. However, even with only five species available for measurement, sea turtles exhibited positive allometry of humeral PD relative to mass (Figure 5.7E).

For the femur, emydids show isometric scaling of length relative to FED and PD (Figure 5.8A-B). This clade also exhibits positive allometry of femoral length, FED, and PD relative to estimated body mass (Figure 5.7C-E). Tortoises show negative allometry of femur length relative to FED and PD; however, similar to emydids, this group also exhibits positive allometry of femoral length, FED, and PD relative to body mass (Figure 5.8A-E). Trionychids show negative allometry of femoral length relative to FED and PD (Figure 5.8A-B). Softshells also scale isometrically for femoral length and FED relative to body mass, but exhibit positive allometry for PD relative to mass (Figure 5.8C-E). Sea turtles show isometric scaling for femoral length relative to both FED and PD, as well as for length, FED, and PD relative to body mass (Figure 5.8A-E). However, like evaluations for the humerus, the large confidence intervals on regression slopes that lead

to their overlap with predictions for isometry likely relate to the small number of sea turtle taxa available for measurement.

DISCUSSION

If differences in limb bone loading across environments are a strong driver of morphological change in the appendicular skeleton, then taxa inhabiting different habitats could show distinct limb bone proportions relative to body size. I predicted that terrestrial taxa (testudinids) would show positive allometry of humeral and femoral diameters relative to body size, in order to resist high torsional loads on land. In contrast, specialized aquatic taxa (cheloniids) should exhibit limb bone proportions that show negative allometry of flexion-extension diameter relative to body size, in order to achieve a flattened, hydrodynamically advantageous flipper. Rowing taxa (emydids and trionychids), which represent functional intermediates between terrestrial walkers and aquatic flappers, should show intermediate levels of flattening between tortoises and sea turtles.

Emydid turtles exhibited relatively robust humeral diameters (FED and PD) compared to humeral length, and are relatively long for estimated body mass, compared to predictions for isometry. Similarly, emydid femora are robust (FED and PD) and long relative to body mass. Such scaling patterns may be related to strain magnitudes and orientations experienced by the bones of emydid turtles during locomotion, particularly those experienced during walking on land. Previous work (Young and Blob 2015, Young 2017) has indicated that torsion (i.e. twisting) loads are substantially greater on both the

humerus and femur during terrestrial walking compared to aquatic swimming in two species of emydid turtle (*Trachemys scripta* and *Pseudemys concinna*). Shear strains produced by torsional loads can be some of the most likely to cause limb bone failure (Vogel 2013). The likelihood of such a structural failure may be reduced among larger taxa by adding bone material that can help resist such loads (Blob 2000). Therefore, high levels of shear stress in the humerus and femur of semi-aquatic emydids during terrestrial locomotion may have promoted growth of additional bone mass at the mid-shaft of the limb bones among larger members of these lineages.

An additional factor potentially influencing the scaling patterns observed in the emydid humerus is the inclusion of terrestrially specialized emydid taxa in this analysis. Four emydid species have evolved into terrestrial specialists from semi-aquatic ancestors (e.g. box turtles; Dodd 2002, Young et al. 2017). This terrestrial clade of emydids possesses several morphological features suited for terrestriality, such as reduction of foot webbing. One species of box turtle (*Terrapene carolina*) also exhibits reduced swimming function of the forelimb, based on kinematic analyses (Young et al. 2017), further suggesting terrestrial specialization for the limbs in this group. In our phylogenetic independent contrasts analyses, terrestrial taxa within the emydid clade were not analyzed separately from semi-aquatic emydid taxa. Therefore, the inclusion of terrestrial specialists in this grouping may have influenced the contrasts for emydid humeri disproportionately toward a terrestrially specialized scaling pattern. Additional analyses of humeral scaling patterns that separate terrestrial from semi-aquatic emydid taxa could help resolve this possibility.

Testudinids (tortoises) show scaling patterns that indicate that the humeri of these taxa are robust, with large FED and PD, relative to length. Additionally, tortoise humeri are long and robust relative to estimated body mass. Tortoise femora also exhibit relatively robust mid-shaft diameters (FED and PD) for femur length and body mass. However, the femur does not show the same length-body mass relationship as the humerus, instead scaling isometrically to body mass. As terrestrial specialists, the limb bones of tortoises must bear their body weight during all locomotor activities. In addition, several taxa within this clade grow to large sizes (e.g., members of the genera *Aldabrachelys, Chelonoides,* and *Geochelone*: Pritchard 1979), which could increase the forces that their limb bones must resist during locomotion (Blob 2000). Such load increases may be further exacerbated by the robust, heavily ossified shells characteristic of this group (Pritchard 1979). Many tortoise taxa are also known to exhibit digging behaviors, using their forelimbs to remove substrate from burrows (Pritchard 1979, Ernst and Lovitch 2009). Previous studies have shown that humeri of taxa that use their forelimbs for digging exhibit characteristics associated with withstanding high mechanical stress (Biknevicius 1993; Woodman and Gaffney 2014; Henrici 2016). By extension, the robust scaling patterns observed for humeral diameters and length relative to mass in tortoises may reflect adaptations for resisting increased loads experienced during digging.

Trionychids (softshells) scale isometrically for humeral FED and PD relative to humeral length and body mass. Likewise, this clade also shows isometric humeral scaling for length relative to body mass. However, scaling patterns for the femur indicate that

FED and PD are relatively large for femur length, and PD is robust relative to body mass as well. Unlike many other freshwater taxa, which employ the hindlimb as the primary force generator during swimming, both the forelimb and hindlimb contribute substantially to swimming propulsion in softshell turtles (Pace et al. 2001; Blob et al. 2008). As such, increased strains on the limb during the power-generating stroke of swimming are unlikely to explain the differences in humeral and femoral scaling in this lineage. However, softshell turtles are characterized by shells with reduced bone mass, particularly in the posterior region of the carapace (dorsal shell; Pritchard 1979). Members of this clade are highly specialized freshwater species that rarely make terrestrial excursions (Pace et al. 2001). Furthermore, softshells spend much of their time on the bottom of streams and ponds (Ernst and Lovitch 2009). As such, the additional bone mass in the femur may be a compensatory mechanism to provide weight that helps individuals maintain their typical benthic positions, thus offsetting the consequences of posterior shell reduction.

Cheloniid (sea turtle) proximal limb bones show isometric scaling patterns for most of the relationships investigated in this study. Such patterns may, in part, be related to the small number of sea turtle taxa available for comparison (n=5). However, despite the limited taxonomic diversity of this lineage and its influence on confidence intervals for scaling slopes, sea turtle humeri still exhibit positive allometry for PD relative to mass. Additionally, FED fails to show negative allometry relative to body mass. Taken together, these results indicate that sea turtles achieve their extensive flattening of the forelimb through the addition of bone mass along the perpendicular plane of the humerus,

rather than through reducing bone mass in the flexion-extension plane. In contrast, the weak allometric patterns found for the hindlimbs of sea turtles may correspond to the fact that sea turtles generate propulsive force for locomotion primarily with the forelimbs, whereas the propulsive role of the hindlimbs is negligible (Davenport et al. 1984, Renous and Bels 1993).

Results from this study do not clearly support a gradient of limb bone scaling patterns that relate to changes in limb bone loading associated with shifts to aquatic habitats. However, the proximal limb bones of both the forelimb and hindlimb exhibit scaling patterns that reflect functional and life history differences among the turtle clades examined. Thus, limb bone shapes of turtles may relate to a combination of factors, including multiple functional roles, body size, and phylogenetic ancestry.

ACKNOWLEDGMENTS

Collection of morphological data for this research would not have been possible without the access to specimens and the generous assistance provided by Kenneth Tighe and Addison Wynn (Smithsonian National Museum of Natural History); David Kizirian and Lauren Vonnahme (American Museum of Natural History); Max Alan Nickerson (Florida Museum of Natural History); Steve Rogers (Carnegie Museum of Natural History), and Peter and Sybille Pritchard (Chelonian Research Institute). I also thank Nicole Mazouchova for her introduction to Peter and Sybille, whose collection at the Chelonian Research Institute provided access to several rare specimens not found in other

collections. I also wish to thank Antonio Baeza for his indispensable council on the molecular phylogenetics aspect of this study.

FUNDING

This research was funded by generous support from: Society for Integrative and Comparative Biology Grants-In-Aid of Research, American Museum of Natural History Theodore Roosevelt Memorial Grant, Women's National Farm & Garden Association Sarah Bradley Tyson Fellowship, Clemson University Professional Enrichment Grants, and Clemson University Biological Sciences Graduate Student Association Travel Grants.

REFERENCES

Biknevicius, A. R. 1993. Biomechanical scaling of limb bones and differential limb use in caviomorph rodents. *Journal of Mammalogy* 74: 95-107.

Blob, R. W., A. R. V. Rivera, M. W. Westneat. 2008. Hindlimb function in turtle locomotion: limb movements and muscular activation across taxa, environment, and ontogeny. In *Biology of turtles* (Eds. J. Wyneken, M. H. Godfrey, and V. Bels), pp. 139-162. Boca Raton, FL: CRC Press.

Blob, R. W. 2000. Interspecific scaling of the hindlimb skeleton in lizards, crocodilians, felids, and canids: does limb bone shape correlate with limb posture? *Journal of Zoology* 250: 507-531.

Blob, R. W., C. J. Mayerl, A. R. V. Rivera, G. Rivera, and V. K H. Young. 2016. "On the fence" versus "all in": insights from turtles for the evolution of aquatic locomotor specializations and habitat transitions in tetrapod vertebrates. *Integrative and Comparative Biology* 56: 1310-1322.

Carter, D. R. & G. S. Beaupré. 2001. *Skeletal function and form*. Cambridge: Cambridge University Press.

Castresana, J. 2000. Selection of conserved bocks from multiple alignments for their use in phylogenetic analysis. *Molecular Biology and Evolution* 17: 540-552.

Darriba, D., G. L. Taboada, R. Doallo, and D. Posada. 2012. jModelTest 2: more models, new heuristics and parallel computing. *Nature Methods* 9: 772.

Davenport, J., S. A. Munks, and P. J. Oxford. 1984. A comparison of the swimming of marine and freshwater turtles. *Proceedings of the Royal Society B* 220: 447-475.

Dodd, C. K. 2002. *North American box turtles: a natural history*. Norman, OK: University of Oklahoma Press.

Edgar, R. C. 2004. MUSCLE: multiple sequence alignment with high accuracy and high throughput. *Nucleic Acids Research* 32: 1792-1797.

Ernst, C. H. and J. E. Lovitch. 2009. *Turtles of the United States and Canada*. Baltimore, MD: Johns Hopkins University Press.

Fish, F. E. 1996. Transitions from drag-based to lift-based propulsion in mammalian swimming. *American Zoologist* 36: 628-641.

Garland, T., P. H. Harvey, and A. R. Ives. 1992. Procedures for the analysis of comparative data using phylogenetically independent contrasts. *Systematic Biology* 41: 18-32.

Garland, T., A. W. Dickerman, C. M. Janis, and J. A. Jones. 1993. Phylogenetic analysis of covariance by computer simulation. *Systematic Biology* 42: 265-292.

Guindon, S. and O. Gascuel. 2003. A simple, fast and accurate method to estimate large phylogenies by maximum-likelihood. *Systematic Biology* 52: 696-704.

Guillon, J-M., G. Lorelei, V. Hulin, and M. Girondot. 2012. A large phylogeny of turtles (Testudines) using molecular data. *Contributions to Zoology* 81: 147-158.

Henrici, A. C. 2016. Digging through the past: the evolutionary history of burrowing and underground feeding in rhinophrynid anurans. *Paleobiodiversity and Paleoenvironments* 96: 97-109.

Huelsenbeck, J. P. and F. Ronquist. 2001. MrBayes: Bayesian inference of phylogenetic trees. *Bioinformatics* 17: 754-755.

Jolicoeur, P. and J. E. Mosimann. 1968. Intervalles de confiance pour la pente de l'axe majeur d'une distribution normale bidimensionelle. *Biometrie-praximetrie* 9: 121-140.

Kumar, S., G. Stecher, and K. Tamura. 2015. MEGA7: Molecular Evolutionary Genetics Analysis version 7.0 for bigger datasets. *Molecular Biology and Evolution* 33: 1870-1874.

Le, M., C. J, Raxworthy, W. P. McCord, and L. Mertz. 2006. A molecular phylogeny of tortoises (Testudines: Testudinidae) based on mitochondrial and nuclear genes. *Molecular Phylogenetics and Evolution* 40: 517-531.

Llorente, G. A., X. Ruiz, A. Casinos, I. Barandalla, and C. Viladiu. 2008. Long bone allometry in tortoises and turtles. In *Biology of turtles* (Eds. J. Wyneken, M. H. Godfrey, and V. Bels), pp. 85-96. Boca Raton, FL: CRC Press.

Maddison, W. P. and D. R. Maddison. 2017. Mesquite: a modular system for evolutionary analysis. Version 3.04. http://mesquiteproject.org.

Midford, P. E., T. Garland Jr., and W. P. Maddison. 2005. PDAP Package of Mesquite. Version 1.07.

Pace, C. M., R. W. Blob, and M. W. Westneat. 2001. Comparative kinematics of the forelimb during swimming in red-eared slider (*Trachemys scripta*) and spiny softshell (*Apalone spinifera*) turtles. *Journal of Experimental Biology* 204: 3261-3271.

Pough, F. H. 1980. The advantages of ectothermy for tetrapods. *The American Naturalist* 115: 92-112.

Pritchard, P. C. H. 1979. *Encyclopedia of turtles*. Neptune, NJ: T.F.H. Publications.

Renous, S. and V. Bels. 1993. Comparison between aquatic and terrestrial locomotion of the leatherback sea turtle (*Dermochelys coriacea*). *Journal of Zoology* 230: 357-378.

Stephens, P. R. & J. J. Wiens. 2003. Ecological diversification and phylogeny of emydid turtles. *Biological Journal of the Linnean Society* 79: 577-610.

Talavera, G. and J. Castresana. 2007. Improvement of phylogenies after removing divergent and ambiguously aligned blocks from protein sequence alignments. *Systematic Biology* 56: 564-577.

Vogel, S. 2013. *Comparative biomechanics: life's physical world*. Princeton, NJ: Princeton University Press.

Woodman, N. and S. A. Gaffney. 2014. Can they dig it? Functional morphology and semifossoriality among small-eared shrews, genus *Cryptotis* (Mammalia, Sorcicdae). *Journal of Morphology* 275: 745-759.

Wyneken, J. 2001. The anatomy of sea turtles. U.S. Department of Commerce NOAA Technical Memorandum NMFS-SEFSC-470, p. 172.

Young, V. K H. & R. W. Blob. 2015. Limb bone loading in swimming turtles: changes in loading facilitate transitions from tubular to flipper-shaped limbs during aquatic invasions. *Biology Letters* 11: 20150110.

Young, V. K H., K. G. Vest, A. R. V. Rivera, N. R. Espinoza, and R. W. Blob. 2017. One foot out the door: limb function during swimming in terrestrial versus aquatic turtles. *Biology Letters* 13: 20160732.

Young, V. K H. 2017. Humeral loads during swimming and walking in turtles: implications for morphological change during aquatic reinvasions. In *Secondary land to water transitions: turtles as models for understanding morphological evolution* (Doctoral dissertation), pp. 28-44. Clemson, SC.

Table 5.1. Estimates of allometric scaling exponents for the humerus and femur of turtles based on RMA regressions of phylogenetic independent contrasts. Number of contrasts used in the analysis are denoted by n_c; number of taxa are listed elsewhere (see Appendix B – Table S1).

x	*y*	Clade	n_c	r^2	RMA slope	95% CI	Allometry
Humerus FED	Humerus Length	Emydidae	35	0.885	0.850	0.756-0.957	-
		Testudinidae	34	0.925	0.855	0.776-0.942	-
		Trionychia	23	0.878	0.920	0.789-1.072	0
		Cheloniidae	4	0.901	0.863	0.498-1.945	0
Humerus PD	Humerus Length	Emydidae	35	0.894	0.925	0.826-1.036	0
		Testudinidae	34	0.925	0.872	0.791-0.961	-
		Trionychia	23	0.867	0.909	0.774-1.066	0
		Cheloniidae	4	0.994	0.880	0.763-1.014	0
Mass	Humerus Length	Emydidae	35	0.935	0.372	0.341-0.407	+
		Testudinidae	34	0.937	0.378	0.346-0.413	+
		Trionychia	23	0.805	0.338	0.279-0.411	0
		Cheloniidae	4	0.972	0.380	0.281-0.515	0
Mass	Humerus FED	Emydidae	35	0.827	0.439	0.380-0.507	+
		Testudinidae	34	0.906	0.442	0.397-0.493	+
		Trionychia	23	0.718	0.368	0.292-0.464	0
		Cheloniidae	4	0.965	0.441	0.315-0.618	0
Mass	Humerus PD	Emydidae	35	0.94	0.403	0.370-0.439	+

		Testudinidae	34	0.877	0.434	0.383-0.491	+
		Trionychia	23	0.75	0.373	0.300-0.464	0
		Cheloniidae	4	0.991	0.433	0.364-0.515	+
Femur FED	Femur Length	Emydidae	35	0.935	0.995	0.910-1.087	0
		Testudinidae	34	0.934	0.832	0.760-0.911	-
		Trionychia	23	0.945	0.804	0.726-0.892	-
		Cheloniidae	4	0.976	0.836	0.631-1.107	0
Femur PD	Femur Length	Emydidae	35	0.932	0.920	0.840-1.007	0
		Testudinidae	34	0.925	0.817	0.742-0.900	-
		Trionychia	23	0.948	0.808	0.731-0.893	-
		Cheloniidae	4	0.839	0.992	0.501-1.964	0
Mass	Femur Length	Emydidae	35	0.955	0.388	0.360-0.418	+
		Testudinidae	34	0.921	0.355	0.322-0.392	0
		Trionychia	23	0.802	0.320	0.264-0.389	0
		Cheloniidae	4	0.945	0.390	0.257-0.592	0
Mass	Femur FED	Emydidae	35	0.963	0.390	0.365-0.417	+
		Testudinidae	34	0.891	0.427	0.380-0.480	+
		Trionychia	23	0.778	0.398	0.324-0.489	0
		Cheloniidae	4	0.951	0.467	0.314-0.693	0
Mass	Femur PD	Emydidae	35	0.907	0.422	0.380-0.469	+
		Testudinidae	34	0.864	0.435	0.382-	+

Trionychia	23	0.826	0.396	0.495 0.330-0.475	+
Cheloniidae	4	0.916	0.393	0.236-0.654	0

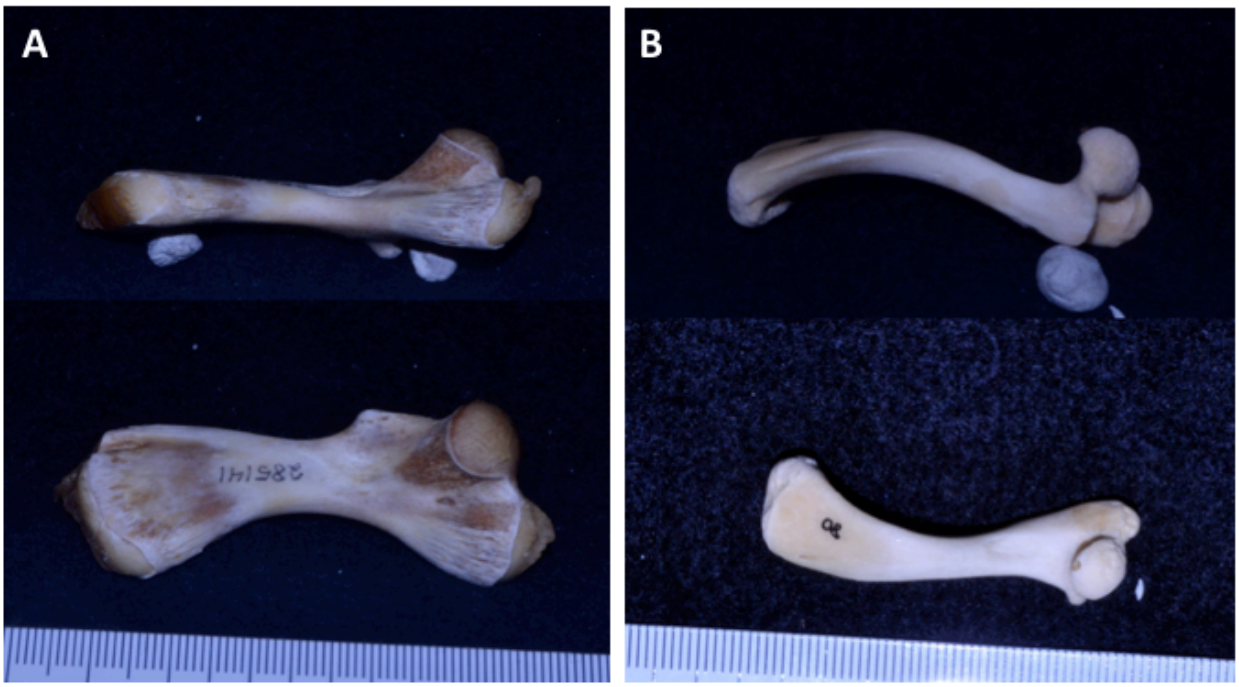

Figure 5.1. Views of medial (top) and flexor (bottom) surface of humeri of sea turtle (A; *Lepidochelys kempii*) and tortoise (B; *Geochelone elegans*). Scale units = 1 mm. Note the extensive flattening of the sea turtle humerus compared to the tubular shape of the tortoise humerus.

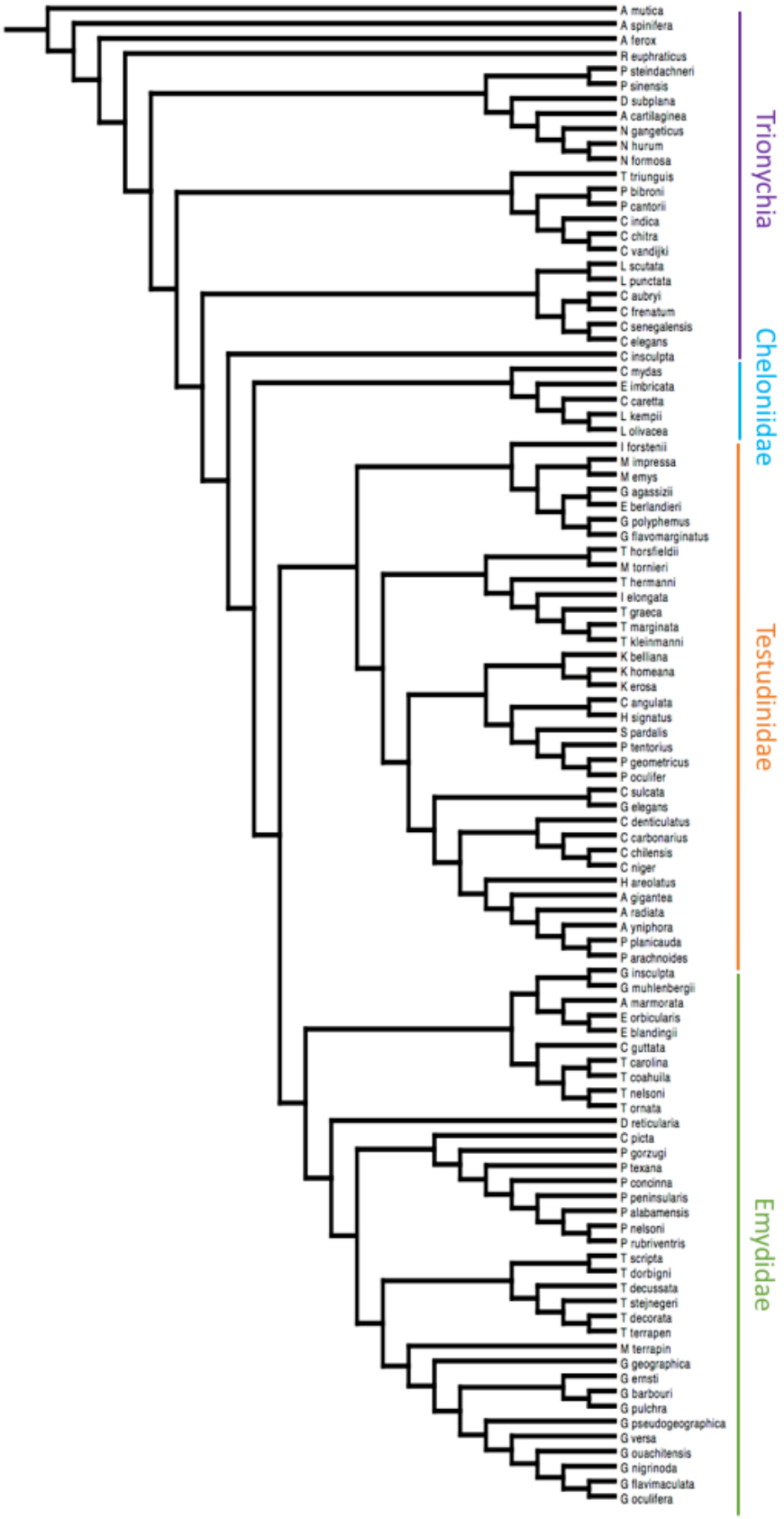
A mutica
A spinifera
A ferox
R euphraticus
P steindachneri
P sinensis
D subplana
A cartilaginea
N gangeticus
N hurum
N formosa
T triunguis
P bibroni
P cantorii
C indica
C chitra
C vandijki
L scutata
L punctata
C aubryi
C frenatum
C senegalensis
C elegans
C insculpta
C mydas
E imbricata
C caretta
L kempii
L olivacea
I forstenii
M impressa
M emys
G agassizii
E berlandieri
G polyphemus
G flavomarginatus
T horsfieldii
M tornieri
T hermanni
I elongata
T graeca
T marginata
T kleinmanni
K belliana
K homeana
K erosa
C angulata
H signatus
S pardalis
P tentorius
P geometricus
P oculifer
C sulcata
G elegans
C denticulatus
C carbonarius
C chilensis
C niger
H areolatus
A gigantea
A radiata
A yniphora
P planicauda
P arachnoides
G insculpta
G muhlenbergii
A marmorata
E orbicularis
E blandingii
C guttata
T carolina
T coahuila
T nelsoni
T ornata
D reticularia
C picta
P gorzugi
P texana
P concinna
P peninsularis
P alabamensis
P nelsoni
P rubriventris
T scripta
T dorbigni
T decussata
T stejnegeri
T decorata
T terrapen
M terrapin
G geographica
G ernsti
G barbouri
G pulchra
G pseudogeographica
G versa
G ouachitensis
G nigrinoda
G flavimaculata
G oculifera
Trionychia
Cheloniidae
Testudinidae
Emydidae

Figure 5.2. Bayesian inference phylogenetic tree representing 4 functionally divergent turtle clades: Trionychia (mostly freshwater rowers; purple), Cheloniidae (marine flappers; blue), Testudinidae (terrestrial specialists; orange), and Emydidae (generalist, mostly semi-aquatic species; green).

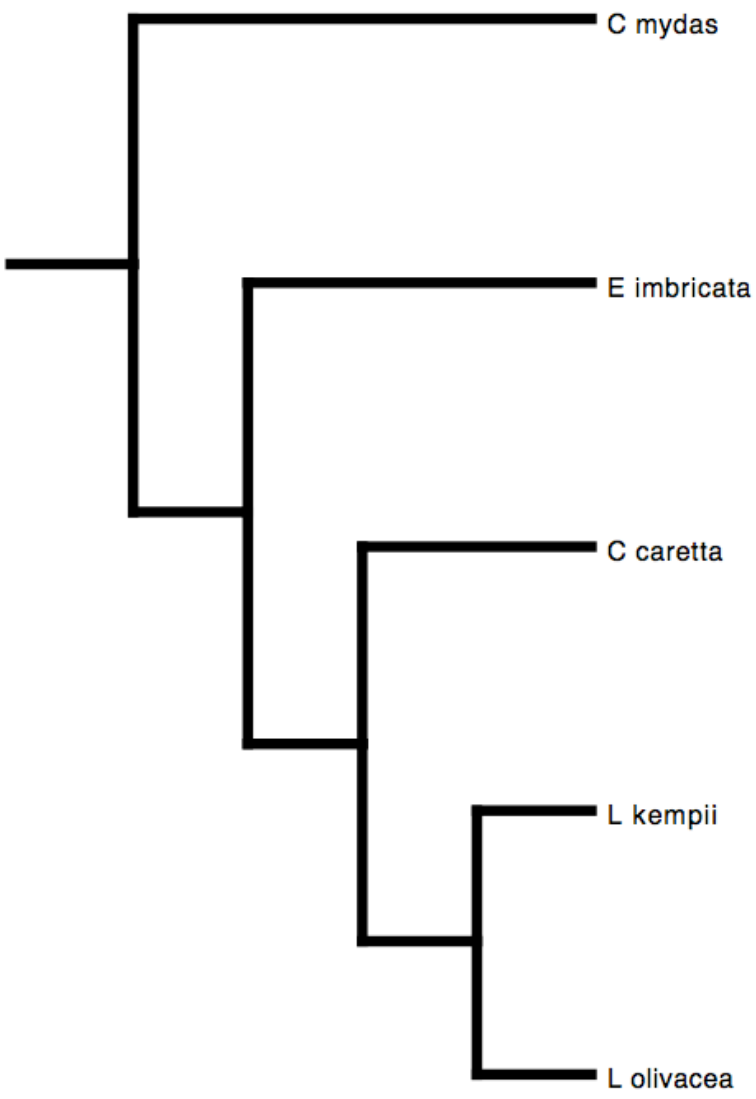

Figure 5.3. Phylogeny for cheloniids (sea turtles) used in analysis of independent contrasts.

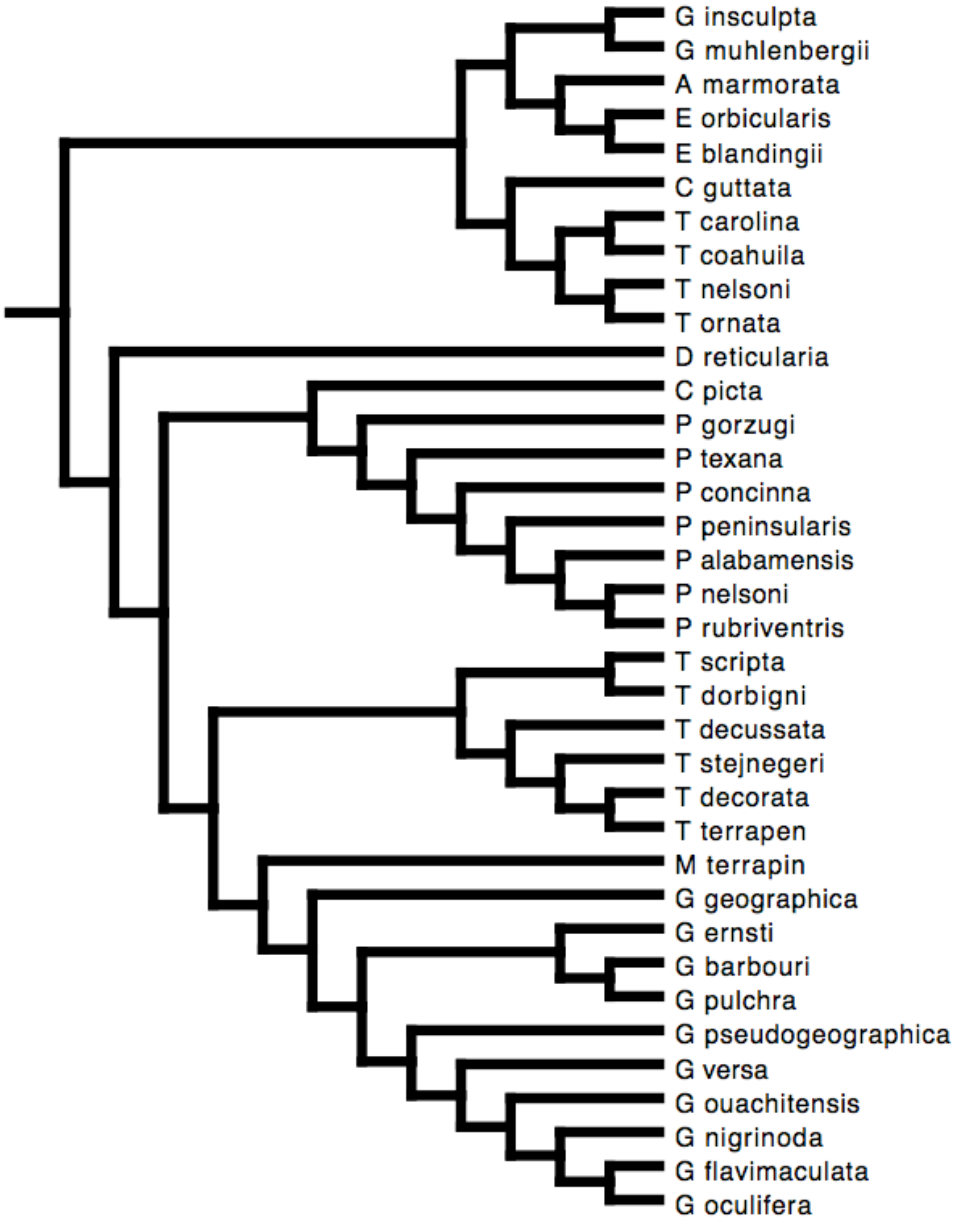

Figure 5.4. Phylogeny for emydids (generally semi-aquatic pond turtles) used in analyses of independent contrasts.

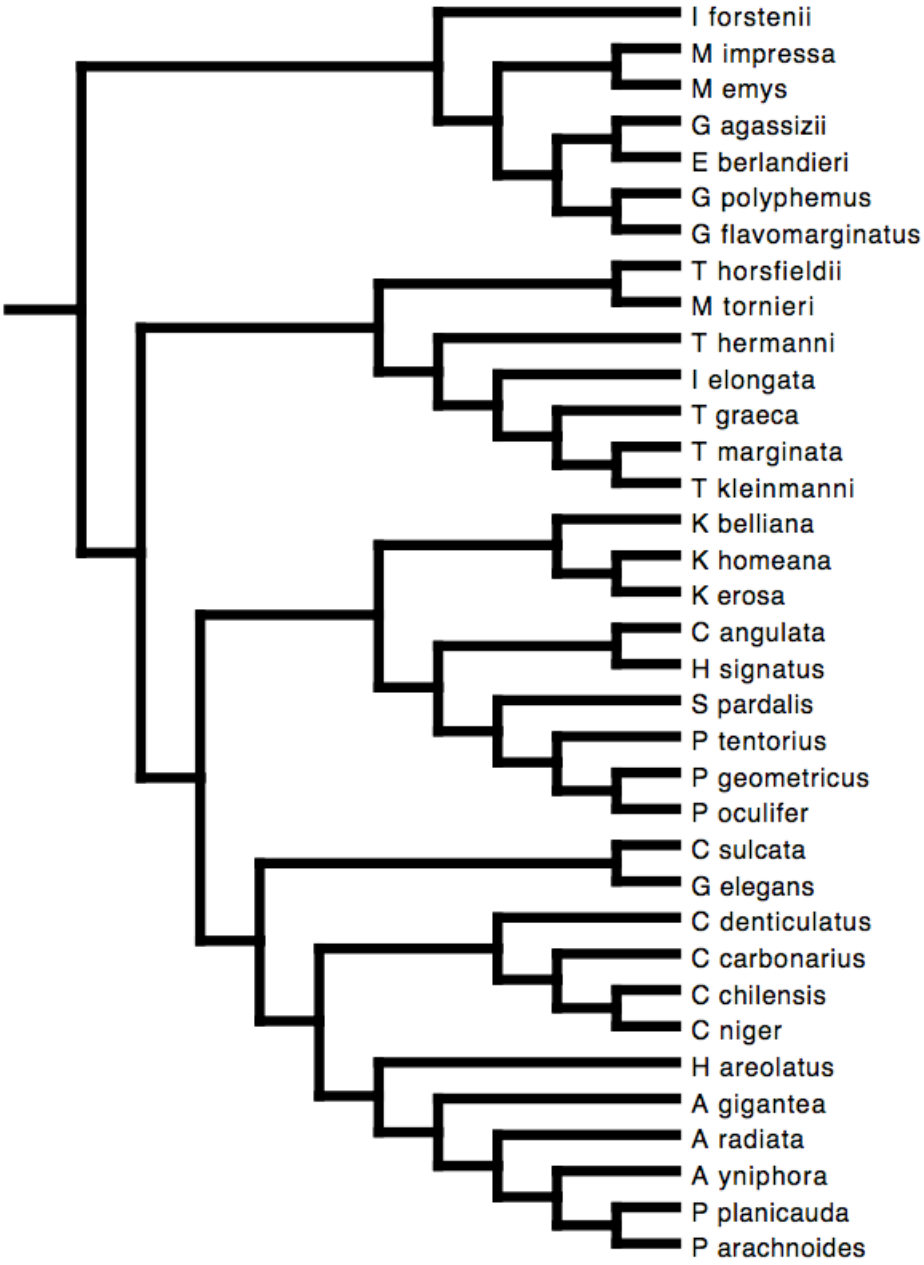

Figure 5.5. Phylogeny for Testudinids (tortoises) used in analysis of independent contrasts.

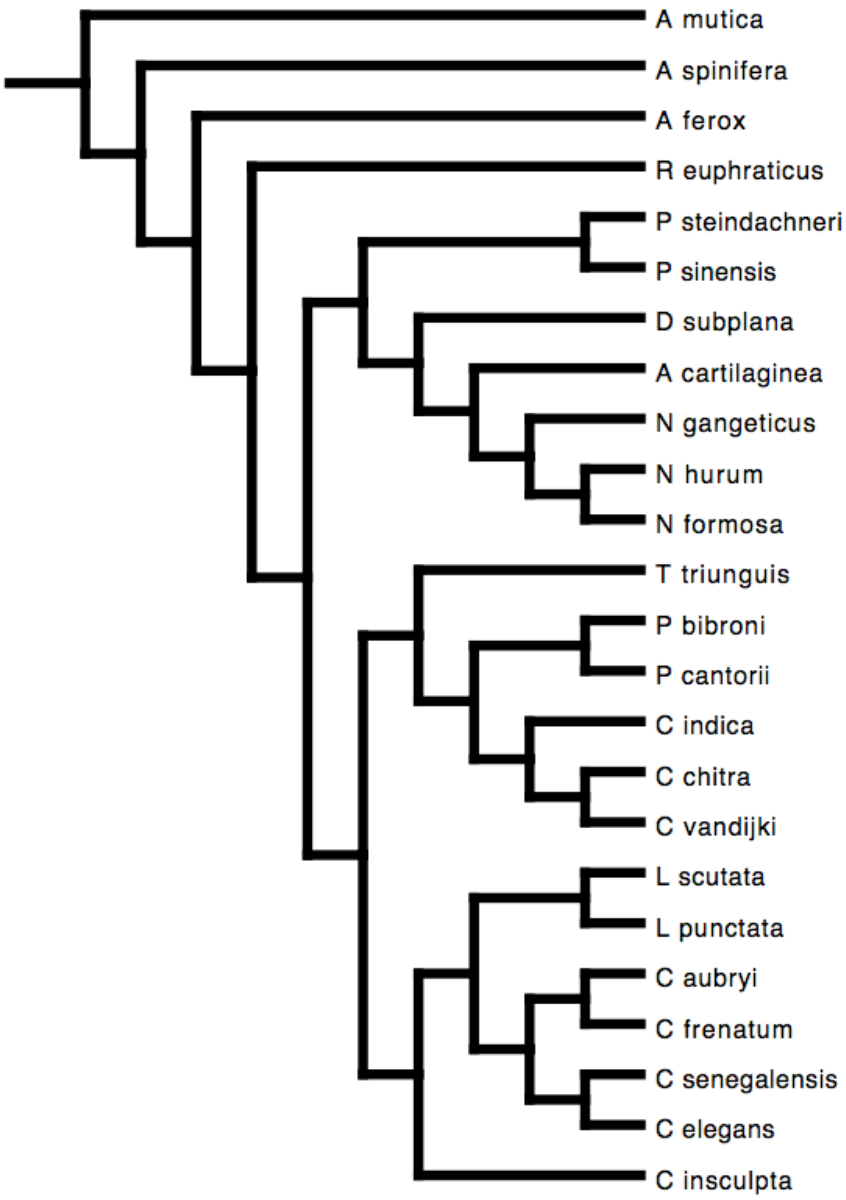

Figure 5.6. Phylogeny of trionychids (softshells) used in analysis of independent contrasts.

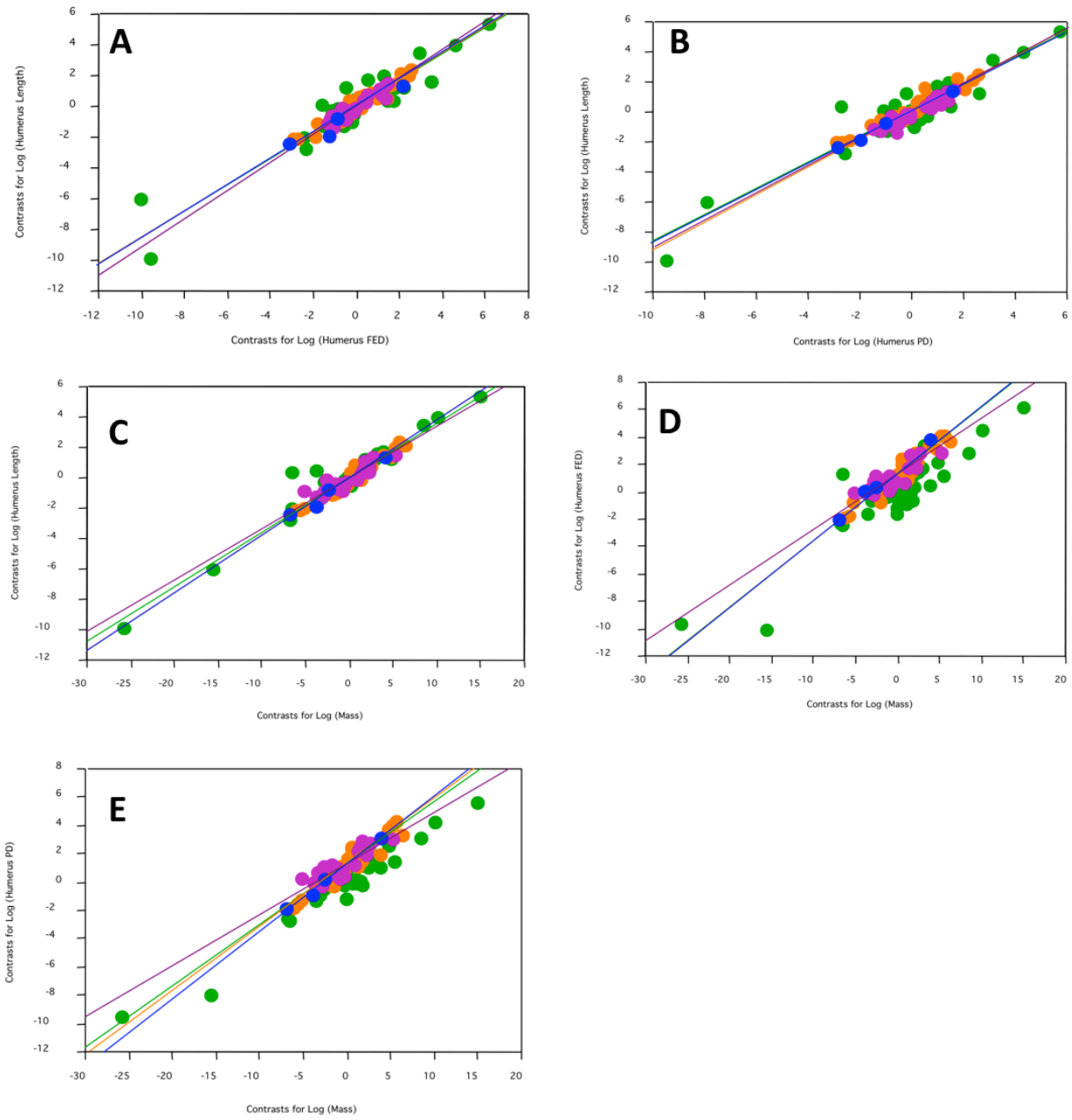

Figure 5.7. Plots of log-log reduced major axis regressions of independent contrasts comparing humeral scaling of four turtle clades. In all plots, contrasts for emydids are green, testudinids are orange, trionychids are purple, and cheloniids are blue. Regression line colors also correspond to the above color designations. (A) Standardized contrasts

for humerus length versus standardized contrasts for humerus flexion-extension diameter (FED); (B) standardized contrasts for humerus length versus standardized contrasts for humerus perpendicular diameter (PD); (C) standardized contrasts for humerus length versus standardized contrasts for estimated body mass; (D) standardized contrasts for humerus flexion-extension diameter (FED) versus standardized contrasts for estimated body mass; (E) standardized contrasts for humerus perpendicular diameter (PD) versus standardized contrasts for estimated body mass.

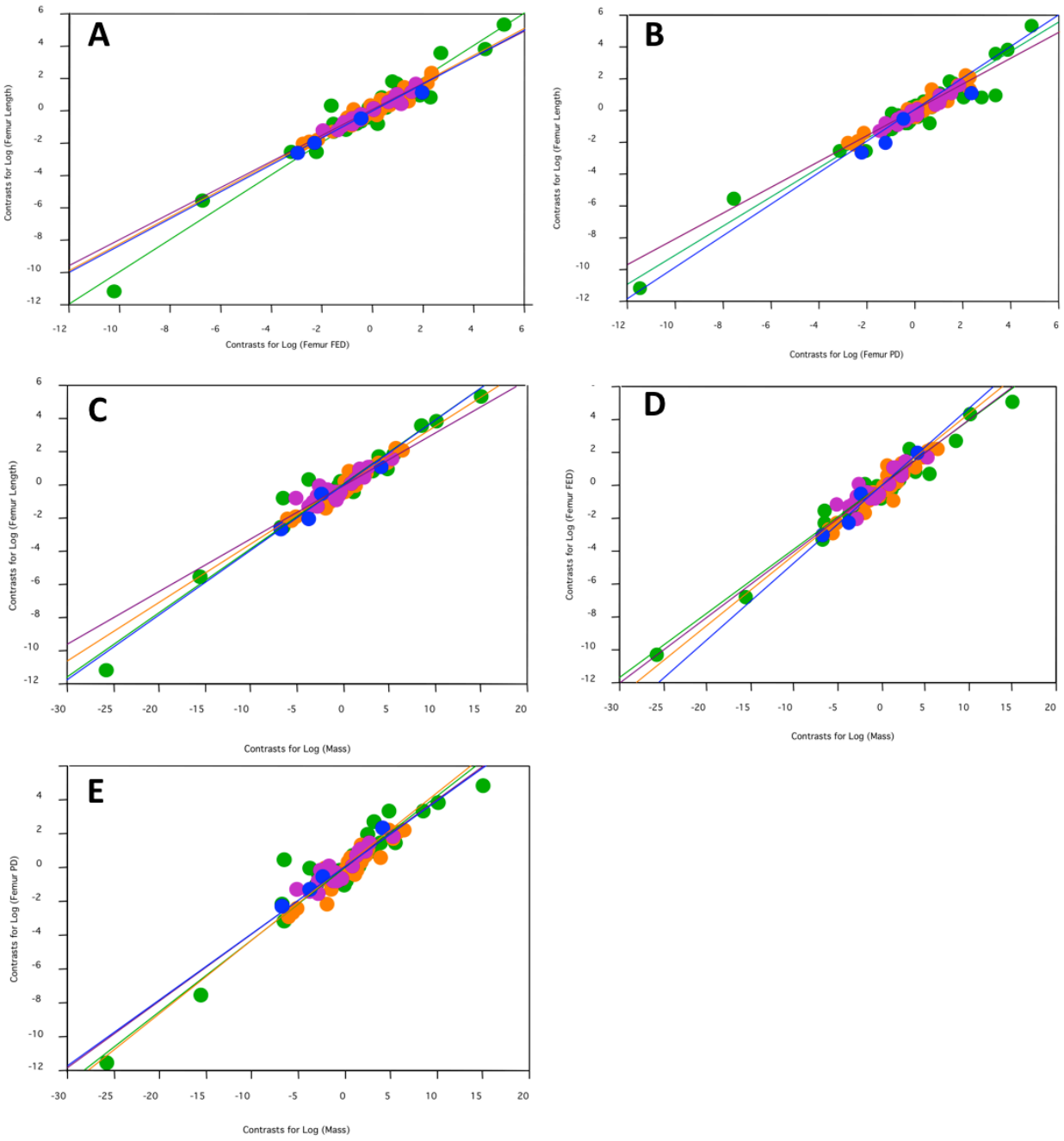

Figure 5.8. Plots of log-log reduced major axis regressions of independent contrasts comparing femoral scaling of four turtle clades. In all plots, contrasts for emydids are green, testudinids are orange, trionychids are purple, and cheloniids are blue. Regression

line colors also correspond to the above color designations. (A) Standardized contrasts for femur length versus standardized contrasts for femur flexion-extension diameter (FED); (B) standardized contrasts for femur length versus standardized contrasts for femur perpendicular diameter (PD); (C) standardized contrasts for femur length versus standardized contrasts for estimated body mass; (D) standardized contrasts for femur flexion-extension diameter (FED) versus standardized contrasts for estimated body mass; (E) standardized contrasts for femur perpendicular diameter (PD) versus standardized contrasts for estimated body mass.

APPENDICES

Appendix A

SUPPLEMENTARY MATERIAL - CHAPTER 4

One foot out the door: limb function during swimming in terrestrial versus aquatic turtles

Table S1. Mean values and standard errors of forelimb kinematic variables among four turtle species. *F*-values for the main effect of species from two-factor mixed-model nested ANOVAs, performed separately for variable. Kinematic variables are angles measured in degrees.

Variable	*Chrysemys picta*	*Trachemys scripta*	*Terrapene carolina*	*Testudo horsfieldii*	*F*-value (d.f. 3, 51)
Maximum Humeral Protraction	127.29±2.4	143.46±2.15	121.42±2.97	137.24±2.92	10.89**
Maximum Humeral Retraction	-21.26±2.45	-11.62±4.19	-23.01±4.08	9.40±4.21	21.84**
Maximum Humeral Elevation	34.34±3.84	38.39±2.22	25.75±2.53	24.24±2.69	4.20*
Maximum Humeral Depression	-18.44±3.09	-13.16±3.54	-38.34±1.39	-47.61±2.15	24.87**
Maximum Elbow Extension	154.05±4.27	114.12±3.17	137.50±1.99	125.82±2.42	30.48**
Maximum Elbow Flexion	76.28±3.01	56.53±1.24	66.41±3.54	83.42±3.19	16.49**
Maximum Wrist Extension	24.45±3.13	62.38±3.57	29.68±3.24	-2.17±8.84	23.50**
Maximum Wrist Flexion	-55.25±3.27	-38.51±2.07	-62.46±2.90	-52.45±3.68	8.46**
Maximum Forefoot Feathering	158.19±4.96	180.08±2.46	87.09±5.07	145.35±5.00	77.59**
Minimum Forefoot Feathering	81.03±5.99	91.28±2.41	-24.15±3.93	85.67±3.43	184.79**

*$P \leq 0.001$; **$P \leq 0.0001$

Table S2. Mean values and standard errors of hindlimb kinematic variables among four turtle species. *F*-values for the main effect of species from two-factor mixed-model nested ANOVAs, performed separately for variable. Kinematic variables are angles measured in degrees.

Variable	*Chrysemys picta*	*Trachemys scripta*	*Terrapene carolina*	*Testudo horsfieldii*	*F*-value (d.f. 3, 51)
Maximum Femoral Protraction	49.79±2.72	66.16±3.04	40.78±3.13	41.90±1.69	19.74**
Maximum Femoral Retraction	-49.81±1.76	-12.36±2.94	-69.49±3.12	-43.61±1.95	81.99**
Maximum Femoral Elevation	1.76±1.17	-2.79±2.69	-7.30±2.15	-16.45±2.12	13.61**
Maximum Femoral Depression	-14.90±0.89	-23.02±2.67	-24.69±1.00	-61.59±1.15	168.20**
Maximum Knee Extension	154.67±2.18	115.33±2.81	146.78±1.61	155.12±3.04	44.41**
Maximum Knee Flexion	59.75±3.26	44.07±2.58	50.10±3.42	88.60±5.29	26.88**
Maximum Ankle Extension	60.14±3.72	63.76±3.80	87.31±3.19	13.09±3.49	76.32**
Maximum Ankle Flexion	13.16±1.82	14.08±3.94	16.72±18.21	-35.26±2.65	7.74*
Maximum Hindfoot Feathering	80.43±2.93	69.89±3.71	78.03±5.86	168.94 2.47±	145.32**
Minimum Hindfoot Feathering	-17.40±3.25	-6.82±3.48	-22.08±5.07	70.88±3.06	135.51**

*$P \leq 0.001$; **$P \leq 0.0001$

Table S3. PC loadings from a principal components analysis of forelimb swimming kinematics for ten variables in four species of turtle.

	PC1 (35.2%)	PC2 (22.4%)
Maximum Humeral Protraction	-0.377	0.253
Maximum Humeral Retraction	-0.142	0.503
Maximum Humeral Elevation	-0.271	-0.215
Maximum Humeral Depression	-0.312	-0.331
Elbow Extension	0.270	-0.045
Elbow Flexion	0.246	0.417
Wrist Extension	-0.241	-0.477
Wrist Flexion	-0.332	0.037
Maximum Forefoot Feathering	-0.460	0.134
Maximum Forefoot Feathering	-0.392	0.323

Table S4. PC loadings from a principal components analysis of hindlimb swimming kinematics for ten variables in four species of turtle.

	PC1 (51.6%)	PC2 (22.3%)
Maximum Femoral Protraction	-0.233	0.484
Maximum Femoral Retraction	-0.089	0.619
Maximum Femoral Elevation	-0.266	-0.097
Maximum Femoral Depression	-0.396	-0.162
Knee Extension	0.226	-0.453
Knee Flexion	0.377	-0.101
Ankle Extension	-0.358	-0.224
Ankle Flexion	-0.287	0.029
Maximum Hindfoot Feathering	0.397	0.125
Maximum Hindfoot Feathering	0.386	0.251

Table S5. Euclidian distance matrix comparing swimming kinematics of the forelimb in four turtle species.

	Chrysemys picta	*Terrapene carolina*	*Testudo horsfieldii*
Terrapene carolina	3.34	-	-
Testudo horsfieldii	3.15	3.84	-
Trachemys scripta	3.38	4.81	4.06

Table S6. Euclidian distance matrix comparing swimming kinematics of the hindlimb in four turtle species.

	Chrysemys picta	*Terrapene carolina*	*Testudo horsfieldii*
Terrapene carolina	1.83	-	-
Testudo horsfieldii	4.86	5.11	-
Trachemys scripta	3.05	3.63	5.65

Table S7. *P*-values from Tukey's pair-wise comparisons of forelimb kinematic variables in four turtle species.

Variable		*C. picta*	*T.carolina*	*T. scripta*
Humeral Protraction	*T. carolina*	0.2334	-	-
	T. scripta	**0.0123**	**<0.001**	-
	T. horsfieldii	0.0928	**<0.001**	0.7465
Humeral Retraction	*T. carolina*	0.683	-	-
	T. scripta	0.994	0.639	-
	T. horsfieldii	**<0.0001**	**<0.0001**	**<0.0001**
Humeral Elevation	*T. carolina*	0.233253	-	-
	T. scripta	0.71097	**0.02744**	-
	T. horsfieldii	0.11112	0.98015	**0.00961**
Humeral Depression	*T. carolina*	**<0.001**	-	-
	T. scripta	0.9756	**<0.001**	-
	T. horsfieldii	**<0.001**	**0.0251**	**<0.001**
Elbow Extension	*T. carolina*	**<0.001**	-	-
	T. scripta	**<0.001**	**<0.001**	-
	T. horsfieldii	**<0.001**	**0.0381**	**0.0371**
Elbow Flexion	*T. carolina*	0.0734	-	-
	T. scripta	**<0.001**	0.0733	-
	T. horsfieldii	0.2978	**<0.001**	**<0.001**
Wrist Extension	*T. carolina*	0.93144	-	-
	T. scripta	**<0.001**	**<0.001**	-
	T. horsfieldii	**0.00144**	**<0.001**	**<0.001**
Wrist Flexion	*T. carolina*	0.32355	-	-
	T. scripta	**0.00409**	**<0.001**	-
	T. horsfieldii	0.93402	0.06742	**0.02287**
Maximum Forefoot Feathering	*T. carolina*	**<0.001**	-	-
	T. scripta	**0.00337**	**<0.001**	-
	T. horsfieldii	0.18323	**<0.001**	**<0.001**
Minimum Forefoot Feathering	*T. carolina*	**<0.0001**	-	-
	T. scripta	0.667	**<0.0001**	-
	T. horsfieldii	1.000	**<0.0001**	0.672

Table S8. *P*-values from Tukey's pair-wise comparisons of hindlimb kinematic variables in four turtle species.

Variable		*C. picta*	*T.carolina*	*T. scripta*
Femoral Protraction	*T. carolina*	0.322	-	-
	T. scripta	**<0.001**	**<0.001**	-
	T. horsfieldii	0.495	0.986	**<0.001**
Femoral Retraction	*T. carolina*	**<0.0001**	-	-
	T. scripta	**<0.0001**	**<0.0001**	-
	T. horsfieldii	0.625	**<0.0001**	**<0.0001**
Femoral Elevation	*T. carolina*	**0.0125**	-	-
	T. scripta	0.4203	0.4289	-
	T. horsfieldii	**<0.001**	**0.0113**	**<0.001**
Femoral Depression	*T. carolina*	**<0.001**	-	-
	T. scripta	**0.00188**	0.88385	-
	T. horsfieldii	**<0.001**	**<0.001**	**<0.001**
Knee Extension	*T. carolina*	0.1098	-	-
	T. scripta	**<0.001**	**<0.001**	-
	T. horsfieldii	0.9998	0.0662	**<0.001**
Knee Flexion	*T. carolina*	0.08564	-	-
	T. scripta	**0.00757**	0.68961	-
	T. horsfieldii	**<0.001**	**<0.001**	**<0.001**
Ankle Extension	*T. carolina*	**<0.0001**	-	-
	T. scripta	0.89	**<0.0001**	-
	T. horsfieldii	**<0.0001**	**<0.0001**	**<0.0001**
Ankle Flexion	*T. carolina*	0.99914	-	-
	T. scripta	0.98116	0.99422	-
	T. horsfieldii	**0.00111**	**<0.001**	**<0.001**
Maximum Hindfoot Feathering	*T. carolina*	0.5828	-	-
	T. scripta	**0.0216**	0.2681	-
	T. horsfieldii	**<0.001**	**<0.001**	**<0.001**
Minimum Hindfoot Feathering	*T. carolina*	0.636	-	-
	T. scripta	0.578	0.083	-
	T. horsfieldii	**<0.001**	**<0.001**	**<0.001**

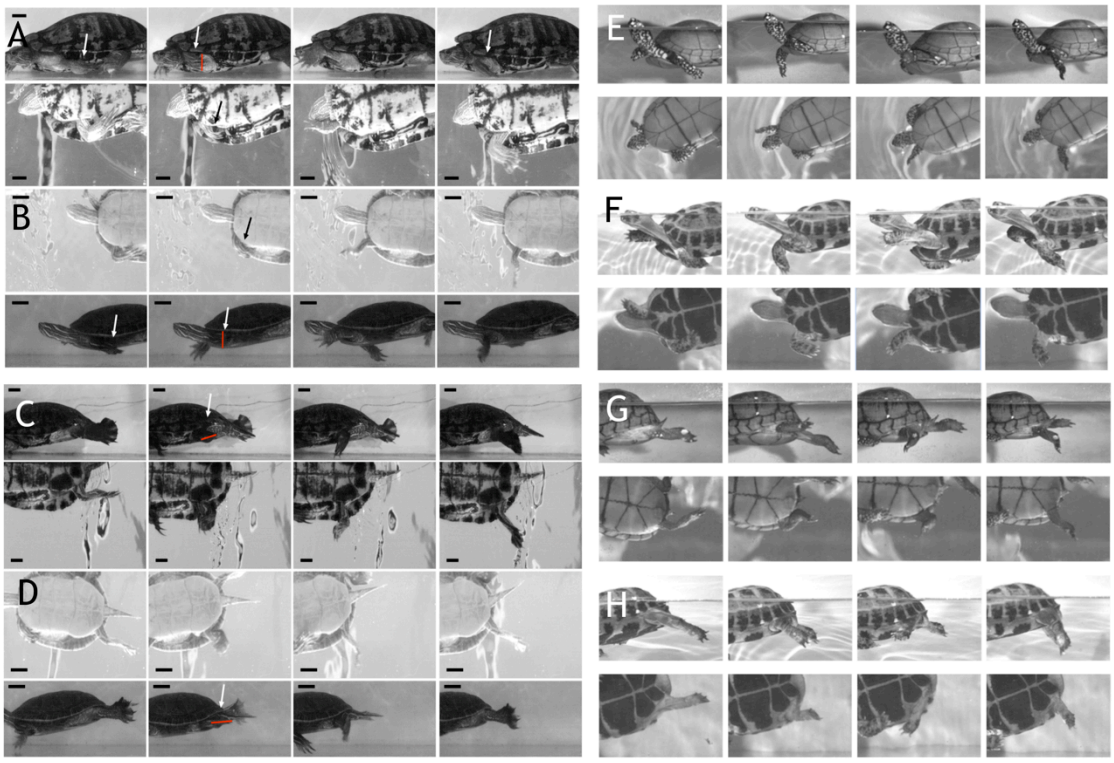

Figure A-1. Ventral and lateral views of limb kinematics. Four columns illustrate early recovery phase (protraction), mid-recovery phase, early thrust phase (retraction), and late thrust phase. (A) *T. scripta*, forelimb. (B) *C. picta*, forelimb (C) *T. scripta*, hindlimb. (D) *C. picta*, hindlimb. (E) *T. carolina*, forelimb. (F) *T. horsfieldii*, forelimb. (G) *T. carolina*, hindlimb. (H) *T. horsfieldii*, hindlimb.

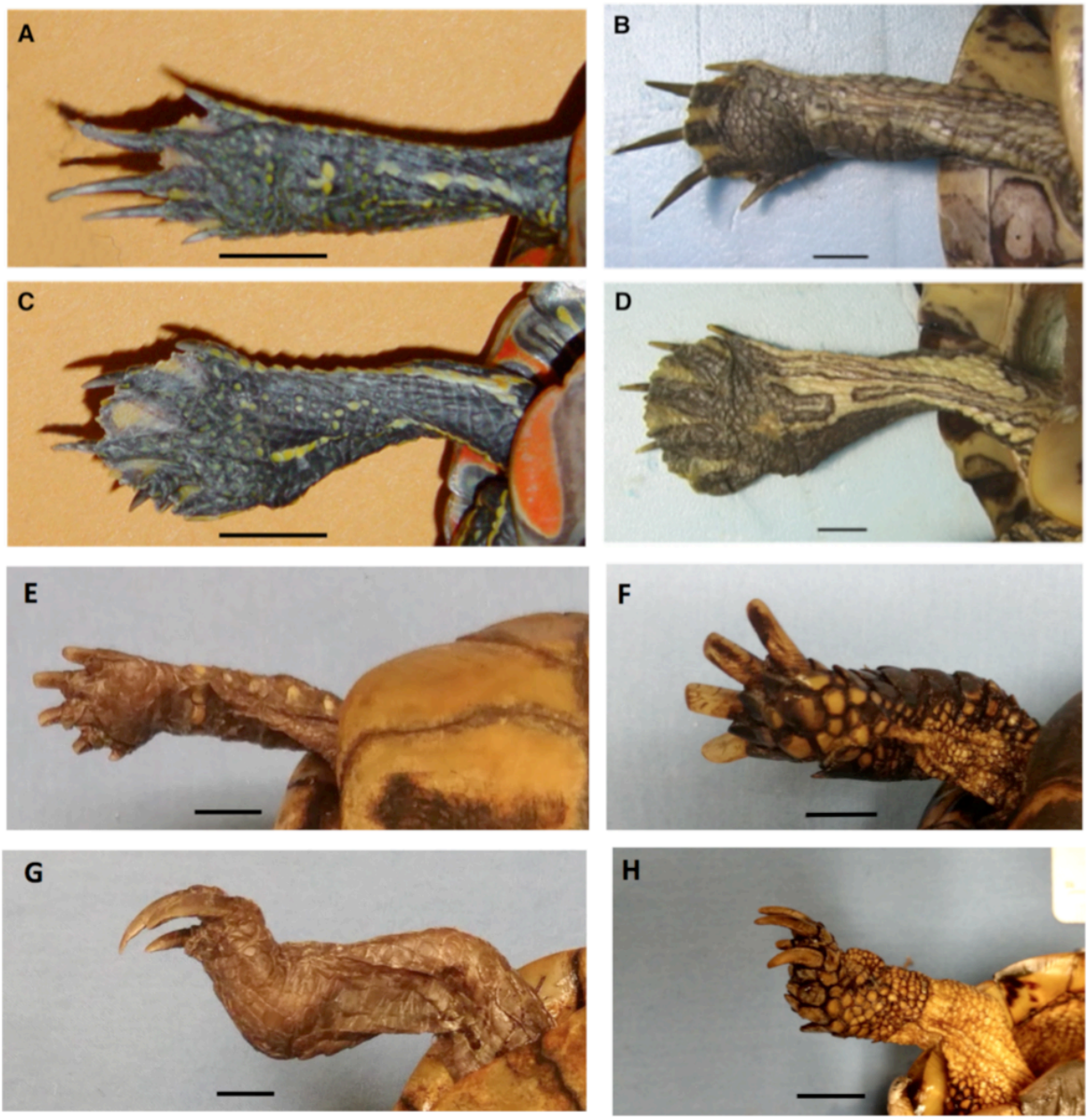

Figure A-2. Limb morphology. (A) *C. picta*, forelimb. (B) *T. scripta*, forelimb (C) *C. picta*, hindlimb. (D) *T. scripta*, hindlimb. (E) *T. carolina*, forelimb. (F) *T. horsfieldii*, forelimb. (G) *T. carolina*, hindlimb. (H) *T. horsfieldii*, hindlimb. Scale bar = 1 cm.

Appendix B

SUPPLEMENTARY MATERIAL - CHAPTER 5

Comparative limb bone scaling in turtles: relationships with functional demands

Table S1. Length and diameter measurements used to calculate scaling relationships of the femur and humerus in four clades of turtles (n = 100 species). Bone lengths, flexion-extension diameter (FED), perpendicular diameter (PD), and straight carapace length (CL) are reported in mm. Mass for each specimen was calculated based on straight carapace length, as described by Pough (1980). Institutional abbreviations for specimens are those used by the respective institutions in their accession numbers and are as follows: American Museum of Natural History (AMNH), Carnegie Museum of Natural History (CMNH), Chelonian Research Institute (CRI), Florida Museum of Natural History (UF), and Smithsonian National Museum of Natural History (USNM).

Species	Specimen	CL (mm)	Mass (g)	Humerus			Femur		
				Length (mm)	FED (mm)	PD (mm)	Length (mm)	FED (mm)	PD (mm)
Cheloniidae									
Caretta caretta	USNM 214140	735	40867.5	148.37	15.36	28.58	136.14	15.55	16.4
Chelonia mydas	USNM 220773	1068	111666.1	201	22.28	40.83	146.47	17.74	22.89
Eretmochelys imbricata	AMNH R58562	779	47785.9	155.6	18.86	30.5	131.03	18.01	23.16
Lepidochelys kempii	AMNH R131151	320	4364.3	64.57	5.94	10.92	55.11	5.62	7.75
olivacea	AMNH R74825	404	8170.2	89.01	7.22	15.08	77.13	8.18	9.6
Emydidae									
Actinemys marmorata	AMNH R68856	156	631.8	35.71	3.97	4.14	38.69	3.41	3.36
Chrysemys picta	CMNH 96156	191	1089.0	37.02	3.68	3.51	41.03	3.73	3.41
Clemmys guttata	AMNH R75269	115	278.2	26.66	2.73	2.2	24.82	2.68	2.28
Deirochelys reticularia	UF37555	190	1073.8	33.58	3.98	4.08	37.13	3.79	3.68
Emydoidea blandingii	AMNH R140774	220	1592.9	51.63	4.59	4.94	54.75	5.25	4.47
Emys orbicularis	UF57716	134	419.7	31.16	3.61	3.36	34.11	3.32	2.92
Glyptemys insculpta	CMNH 113079	241	2035.6	56.08	5.44	5.7	58.14	4.93	5.02

Species	Specimen	CL (mm)	Mass (g)	Humerus Length (mm)	Humerus FED (mm)	Humerus PD (mm)	Femur Length (mm)	Femur FED (mm)	Femur PD (mm)
muhlenbergii	CMNH 122521	99	185.9	20.73	2.42	2.38	20.79	2.3	1.95
Graptemys barbouri	UF3356	263	2574.8	51.8	5.74	5.19	59.01	5.73	4.75
ernsti	UF6819	96	171.1	19.11	1.96	1.91	22.11	2.22	2.00
flavimaculata	CMNH 118575	114	271.7	21.32	2.21	2.38	23.57	2.36	1.99
geographica	CMNH 36963	235	1902.1	46.82	4.45	4.21	52.32	4.39	4.08
nigrinoda	CMNH 67407	159	665.0	29.32	2.76	3.19	35.45	3.21	2.78
oculifera	USNM 015510	207	1352.1	39.28	4.01	4.29	46.92	4.45	4.06
ouachitensis	CMNH 61656	217	1535.1	40.64	4.83	4.9	47.46	4.66	4.24
pseudogeographica	UF4274	221	1612.4	42.3	4.26	4.68	48.87	4.92	3.99
pulchra	USNM 266204	239	1990.5	43.13	6.22	5.36	53.64	4.89	4.52
versa	USNM 290956	179	914.6	34.28	3.58	3.71	40.29	3.74	3.46
Malaclemys terrapin	AMNH R142307	200	1232.6	40.62	4.58	4.04	45.84	4.27	3.92
Pseudemys alabamensis	CMNH 113078	315	4183.3	55.45	6.48	5.46	60.88	6.88	5.36
concinna	CMNH 95987	331	4779.7	57.4	6.2	6.08	65.64	6.83	5.38
gorzugi	USNM 026438	165	734.7	29.76	2.97	2.73	33.38	3.11	2.82
nelsoni	USNM 335598	282	3106.2	57.43	6.43	5.24	61.94	6.07	5.35
peninsularis	USNM 222391	374	6638.8	70.23	8.31	6.91	79.81	7.87	7.38
rubriventris	AMNH R99145	302	3734.9	58.52	6.54	5.03	64.88	6.35	5.46
texana	AMNH R111960	273	2846.7	52.48	5.47	4.7	60.01	5.74	4.25
Terrapene carolina	UF151564	179	914.6	39.74	5.21	4.16	42.8	4.5	4.4
coahuila	AMNH R140861	136	436.8	31.37	3.42	3.07	33.51	3.25	2.46
nelsoni	UF27138	143	499.9	30.97	3.81	3.52	31.91	3.67	3.36
ornata	USNM 020989	128	371.0	32.7	5.01	3.59	35.53	3.89	3.28
Trachemys decorata	USNM 063096	271	2790.9	53.95	5.78	5.21	59.34	5.68	5.21
decussata	UF21747	228	1753.5	43.01	6.25	5.44	47.04	5.09	4.71
dorbigni	CMNH 96002	156	631.8	30.56	3.2	3.04	32.57	3.66	2.86
scripta	CMNH 58088	264	2601.2	52.04	4.43	4.41	53.81	4.49	4.2
stejnegeri	UF150285	206	1334.7	38.24	4.25	3.87	43.17	4.36	3.96

Species	Specimen	CL (mm)	Mass (g)	Humerus Length (mm)	Humerus FED (mm)	Humerus PD (mm)	Femur Length (mm)	Femur FED (mm)	Femur PD (mm)
terrapen	AMNH R160180	209	1387.6	38.78	5.27	4.34	42.74	4.82	3.91
			Testudinidae						
Aldabrachelys gigantea	USNM 269964	775	47128.8	184.58	23.71	28.44	147.92	24.49	21.12
Astrochelys radiata	UF67621	343	5260.2	74.16	11.61	11.26	64.05	8.75	7.28
yniphora	AMNH R119971	403	8115.9	91.29	12.79	11.94	76.76	13.23	9.47
Centrochelys sulcata	CMNH 155273	333	4857.8	91.57	10.63	11.95	76.92	10.14	9.15
Chelonoidis carbonarius	AMNH R62590	454	11182.7	94.41	13.3	12.04	75.49	11.35	8.51
chilensis	UF33621	199	1216.1	46.91	5.44	5.95	42.55	5.52	4.7
denticulatus	CMNH 108720	484	13283.1	103.84	12.01	12.72	90.5	11.33	14.3
niger	AMNH R63415	609	24642.5	130.02	21.78	23.6	110.91	19.06	18.73
Chersina angulata	AMNH R147509	209	1387.6	47.17	6.17	3.97	40.6	4.81	3.53
Geochelone elegans	CMNH 145707	298	3603.3	66.25	7.6	7.38	65.82	7.48	8.32
Gopherus agassizii	USNM 222096	258	2445.2	61.87	6.72	7.52	54.46	6.75	7.37
berlandieri	UF62107	214	1478.7	56.33	6.53	6.51	48.67	5.74	5.3
flavomarginatus	USNM 051357	334	4897.1	93.55	10.74	10.64	71.83	11.5	9.23
polyphemus	UF151910	318	4291.3	78.25	9.03	8.46	59.35	9.44	7.51
Homopus areolatus	UF43420	99	185.9	21.05	2.06	2.27	23.72	2.45	2.54
signatus	AMNH R175220	102	201.5	22.21	2.38	3.08	20.2	2.69	2.52
Indotestudo elongata	AMNH R110183	276	2931.6	53.98	7.04	5.8	51.6	5.9	5.67
forstenii	CRI7129	218	1554.2	47.93	6.56	5.64	45.69	5.37	4.96
Kinixys belliana	USNM 222517	191	1089.0	45.77	6.38	4.45	42.88	5.35	3.78
erosa	CMNH 114617	191	1089.0	51.6	5.64	4.76	46.71	5.31	3.94
homeana	AMNH R43306	197	1183.5	50.45	5.75	4.75	44.01	4.86	3.73
Malacochersus tornieri	CMNH 124251	151	578.8	31.89	3.26	3.34	30.43	2.56	3.11
Manouria emys	CRI4642	304	3801.8	87.26	9.32	8.67	78.76	8.97	8.5
impressa	CRI2900	251	2270.8	72.87	6.98	6.26	66.77	7.51	6.93
Psammobates geometricus	AMNH R147542	124	340.7	28.64	3.78	2.75	24.46	3.18	2.22
oculifer	AMNH R160186	95	166.4	20.48	1.97	2.24	23.13	2.73	2.76

Species	Specimen	CL (mm)	Mass (g)	Humerus Length (mm)	Humerus FED (mm)	Humerus PD (mm)	Femur Length (mm)	Femur FED (mm)	Femur PD (mm)
tentorius	AMNH R139337	129	378.9	32.43	3.23	3.66	27.44	3.16	3.2
Pyxis arachnoides	CRI6403	123	333.4	31.62	2.95	3.04	26.04	3.03	2.57
planicauda	CRI7065	145	518.9	29.99	3.26	3.02	26.29	3.08	2.39
Stigmochelys pardalis	USNM 222502	292	3411.5	79.03	9.01	9.6	67.97	8.05	7.03
Testudo graeca	AMNH R96936	244	2104.5	56.78	9.28	6.99	56.28	6.47	7.35
hermanni	AMNH R6467	202	1266.1	50.47	7.53	6.05	46.69	6.81	5.48
horsfieldii	CMNH 114626	169	783.6	46.84	5.00	4.86	45.91	4.43	4.23
kleinmanni	AMNH R153833	123	333.4	25.25	3.3	3.1	23.73	2.4	2.25
marginata	CMNH 114628	285	3195.9	54.26	6.92	5.88	49.68	5.3	5.02
			Trionychia						
Carettochelys insculpta	AMNH R84212	493	13957.9	76.24	9.39	9.99	89.1	11.93	15.03
Amyda cartilaginea	USNM 222522	295	3506.6	92	11.49	12.83	101.21	14.55	12.41
Apalone ferox	USNM 222548	377	6783.0	76.05	9.44	10.13	76.92	8.4	9.49
mutica	CMNH 39816	177	887.4	50.31	6.56	6.07	56.61	5.9	6.14
spinifera	USNM 562752	198	1199.8	59.67	6.71	7.4	62.37	6.35	6.63
Chitra chitra	CRI11756	331	4779.7	88.9	10.19	10.76	93.5	10.41	10.52
indica	CRI7044	294	3474.7	82.86	10.71	8.64	85.06	9.3	9.72
vandijki	CRI5050	353	5683.0	103.34	12.51	12.58	111.43	12.25	12.88
Cyclanorbis elegans	CRI8225	414	8725.6	114.49	13.89	11.17	106.31	12.79	12.58
senegalensis	CRI3665	218	1554.2	53.71	8.05	7.93	61.02	7.04	6.43
Cycloderma aubryi	AMNH R108909	166	746.7	42.59	4.95	4.4	39.97	4.97	4.76
frenatum	AMNH R110180	367	6309.8	89.17	10.04	8.86	80.04	10.31	10.38
Dogania subplana	USNM 222523	180	928.4	69.21	10.83	8.62	64.11	7.78	7.64
Lissemys punctata	USNM 293690	222	1632.1	44.55	5.82	5.42	49.81	5.72	4.85
scutata	CRI5036	170	796.1	39.36	5.04	5.11	44.41	4.88	4.99
Nilssonia formosa	CRI7512	206	1334.7	65.87	9.82	8.86	66.12	7.96	8.6
gangeticus	CRI4391	151	578.8	47.54	4.46	4.69	47.31	4.37	4.78
hurum	CRI4959	172	821.6	49.29	5.59	5.77	51.42	5.75	5.88

Species	Specimen	CL (mm)	Mass (g)	Humerus			Femur		
				Length (mm)	FED (mm)	PD (mm)	Length (mm)	FED (mm)	PD (mm)
Palea steindachneri	CRI11894	159	665.0	45.92	6.33	5.67	48.67	5.04	5.21
Pelochelys bibroni	CMNH 118595	448	10789.5	121.11	13.99	15.83	133.7	18.77	16.19
cantorii	CRI4974	369	6402.7	109.97	11.65	11.55	112.42	11.23	11.29
sinensis	USNM 539335	104	212.3	30.82	3.63	4.02	34.28	3.25	3.16
Rafetus euphraticus	AMNH R80026	295	3506.6	100.65	11.46	11.31	95.3	11.78	11.97
Trionyx triunguis	USNM 337920	384	7127.1	117.13	16.11	19.47	129.11	15.64	16.91

Table S2. Species names and GenBank accession numbers for the sequences used in this study.

Species	*Mitochondrial genome*					*Nuclear genome*			
	12S	16S	COI	ND4	cytB	R35	Cmos	RAG1	RAG2
				Cheloniidae					
Caretta caretta		AY770545.1	GQ152889.1	AY673559.1	AF385671.1	FJ009031.1	FJ009023.1	FJ009032.1	FJ009033.1
Chelonia mydas	FJ039948.1	HQ377551.1	GQ152882.1	JN632503.1	EU918368.1	AY339635.1	FJ039951.1	FJ039953.1	FJ039954.1
Eretmochelys imbricata	FJ039970.1	FJ039971.1	JX751768.1		JN10005.1	FJ039974.1	FJ039973.1	FJ039975.1	FJ039976.1
Lepidochelys kempii	FJ039991.1	FJ039992.1	GQ152891.1	AY673520.1	AF385668.1	FJ039995.1	FJ039994.1	FJ039996.1	FJ039997.1
olivacea	FJ039984.1	AY390777.1	GQ152890.1			FJ039988.1	FJ039987.1	FJ039982.1	FJ039990.1
				Emydidae					
Actinemys marmorata	U81321.1			AF258855.1	AF258867.1	AY339631.1		AY687917.1	
Chrysemys picta	HE590227.1			KC688173.1	FJ770588.1	FJ770671.1	HE590439.1	FJ770717.1	HE590556.1
Clemmys guttata			KC750819.1	AF258858.1	AF258870.1	DQ649461.1		FJ770719.1	
Deirochelys reticularia	DQ497266.1	DQ497289.1		AF258865.1	AF258877.1	FJ770675.1	DQ497358.1	FJ770721.1	DQ497394.1
Emydoidea blandingii			HQ329642.1	AF258857.1	AF258869.1	AY905211.2			
Emys orbicularis	AB090021.1	AB090049.1	FJ402875.1	AF258856.1	AF258868.1	EU277643.1			
Glyptemys insculpta	DQ497265.1	DQ497288.1	HQ329644.1	AF258864.1	AF258876.1	DQ661020.1	DQ497357.1	EU930786.1	DQ497393.1
muhlenbergii			HQ329645.1	AF258863.1	AF258875.1	FJ770682.1		FJ770727.1	
Graptemys barbouri	HE590229.1		HQ329646.1	EU909370.1	HE590300.1	HE590498.1	HE590441.1	HE590528.1	HE590558.1
ernsti			HQ329648.1						
flavimaculata			HQ329649.1	EU909371.1	GQ395734.1				
geographica				EU909372.1	FJ770598.1	FJ770685.1		FJ770731.1	
nigrinoda	HE590231.1		HQ329651.1	DQ646420.1	GQ896195.1	DQ649456.1	HE590443.1	HE590530.1	HE590560.1
oculifera			HQ329652.1	EU909374.1	GQ896196.1				
ouachitensis				EU909375.1	FJ770599.1	DQ649457.1		FJ770732.1	
pseudogeographica	U81322.1			HE590374.1	FJ770600.1	AY742457.1	HE590444.1	AY687916.1	590561.1
pulchra				EU909377.1	GQ896199.1				
versa			HQ329653.1	DQ646422.1	GQ896200.1				
Malaclemys terrapin	HE590234.1		HQ329654.1	DQ646423.1	FJ770602.1	EU169877.1	HE590446.1	FJ770735.1	HE590563.1
Pseudemys alabamensis			HQ329655.1	KC688180.1	GQ395716.1				
concinna	HE590235.1			DQ646424.1	FJ770604.1	FJ770691.1	HE590447.1	FJ770736.1	HE590564.1
gorzugi			HQ329656.1	JN707420.1	GQ395700.1	JN707530.1			
nelsoni	HE590237.1			EU909379.1	EU909384.1	FJ770694.1		FJ770739.1	
peninsularis				EU909378.1	FJ770606.1	FJ770695.1		FJ770740.1	
rubriventris	HE590238.1		KT075338.1	EU909380.1	GQ395708.1	GQ896248.1			

Species	*Mitochondrial genome*					*Nuclear genome*			
	12S	16S	COI	ND4	cytB	R35	Cmos	RAG1	RAG2
texana				DQ338475.1					
Terrapene carolina	EU930737.1	EU930758.1	HQ329658.1	AF258859.1	AF258871.1	FJ770703.1	EU930779.1	EU930812.1	
coahuila			KC059161.1	AF258860.1	AF258872.1	FJ770699.1		FJ770745.1	
nelsoni			KF059167.1	AF258861.1	AF258873.1	KC181180.1		HQ266660.1	
ornata			HQ329660.1	AF258862.1	AF258874.1	DQ649464.1		FJ770749.1	
Trachemys decorata			HQ329661.1	DQ338515.1		JN707509.1			
decussata	HE590263.2			DQ338521.1	HE590334.1	JN707517.1	HE590455.1	HE590542.1	HE590572.1
dorbigni	HE590269.1			DQ338513.1	HE590341.1	HE590513.1	HE590456.1	HE590543.1	HE590573.1
scripta	HE590290.1	L28077.1	JF700194.1	DQ338479.1	GQ395731.1	AY742458.1	HE590462.1	AY687915.1	HQ260654.1
stejnegeri			HQ329666.1	DQ338527.1	FJ770621.1	FJ770709.1		FJ770754.1	
terrapen			HQ329668.1	DQ338523.1		JN707495.1			
				Testudinidae					
Aldabrachelys gigantea		AY081782.1		AF351625.1	AY081790.1				
Astrochelys radiata		AF020890.1	HQ329747.1	AY673595.1	DQ497304.1		DQ497337.1		DQ497373.1
yniphora		AF020889.1	HQ329748.1	AY673541.1	DQ497306.1		DQ497339.1		DQ497375.1
Centrochelys sulcata	AF175334.1	AY081788.1	HQ329754.1	AY673478.1	DQ497305.1		DQ497338.1		DQ497374.1
Chelonoidis carbonarius	AB090019.1	AF192926.1		AF351692.1	DQ497296.1		DQ497329.1	EU930790.1	DQ497365.1
chilensis	HQ289809.1	AF192924.1	HQ329749.1	AF351674.1			DQ497330.1	EU930791.1	DQ497366.1
denticulatus	AF175336.1	AF192927.1	HQ329749.1	AF351693.1	DQ497298.1		DQ497331.1	EU930792.1	DQ497367.1
niger	AY097636.1	AY097785.1	HQ329751.1	AY673457.1	DQ497300.1		DQ497333.1		DQ497369.1
Chersina angulata	DQ497248.1	DQ497269.1		AY673443.1	DQ497292.1		DQ497325.1		DQ497361.1
Geochelone elegans		AY081786.1	HQ329752.1	AY673465.1	DQ497299.1		DQ497332.1		DQ497368.1
Gopherus agassizii	AY434630.1		HQ329756.1	AY673591.1	AY434562.1				
berlandieri			HQ329757.1	AY673482.1	AY678350.1	KM411538.1			
flavomarginatus			HQ329758.1	AY673473.1	AY678348.1				
polyphemus		AF020886.1	HQ329759.1	AY673485.1	DQ497307.1		DQ497340.1	EU930793.1	DQ497376.1
Homopus areolatus				AY673587.1	AY678323.1				
signatus	DQ497255.1	DQ497275.1	HQ329760.1	AY673429.1	DQ497309.1		DQ497342.1		DQ497378.1
Indotestudo elongata	GU477777.1	HQ123500.1	KP268858.1	AY673560.1	AY434643.1	HQ260650.1	DQ497343.1	EU930795.1	DQ497379.1
forstenii			KF894793.1	AY673565.1	EF491693.1				
Kinixys belliana	DQ497258.1	DQ497278.1		AY673583.1	DQ497312.1	HE662478.1	DQ497345.1		DQ497381.1
erosa	HE662202.1			AY673553.1	AY678414.1	HE662490.1	HE662423.1		
homeana	DQ497259.1	DQ497279.1	HQ329762.1	AY673562.1	DQ497313.1	HE662492.1	DQ497346.1		DQ497382.1
Malacochersus tornieri				AY673530.1	AY678387.1		DQ497347.1		DQ497383.1
Manouria emys			KP268846.1	AY673497.1	AY434563.1		DQ497348.1		DQ497384.1
impressa		HQ123499.1	GQ867670.1	AY673501.1	AY678409.1		DQ497350.1		DQ497386.1
Psammobates geometricus			HQ329765.1	AY673580.1	AY678376				
oculifer				AY673576.1	AY678378.1				
tentorius	DQ497264.1	DQ497284.1		AY673571.1	DQ497318.1		DQ497351.1		DQ497387.1

Species	*Mitochondrial genome*					*Nuclear genome*			
	12S	16S	COI	ND4	cytB	R35	Cmos	RAG1	RAG2
Pyxis arachnoides		AF020887.1	JQ909571.1	AY673507.1	DQ497319.1		DQ497352.1		DQ497388.1
planicauda		AF020888.1	HQ329767.1	AY673547.1	DQ497320.1		DQ497353.1		DQ497389.1
Stigmochelys pardalis	AF175335	AF020891.1		AY73462.1	AY678367.1	AY742459.1	DQ497334.1	AY687912.1	DQ497370.1
Testudo graeca	AY775180.1			HE585807.1	HE588138.1	GU085692.1	DQ497354.1		DQ497390.1
hermanni	AF067503.1	AM491034.1	NC_007696.1	AY673514.1	AY678389.1	DQ386652.1	AM491036.1		AM491038.1
horsfieldii	AB090020.1	AB090048.1		AY673551.1	FM883692.1		DQ497355.1		DQ497391.1
kleinmanni	DQ991958.1			AY673567.1	AM398197.1		DQ497356.1		DQ497392.1
marginata	AF175333.1	AM491033.1		SY673519.1	AY678405.1		AM491035.1		AM491037.1
				Carettochelyidae					
Carettochelys insculpta	U81334.1	HQ123495.1	HQ329586.1	AY673526.1	AY259546.1	AY259571.1		AY687904.1	JQ950719.1
				Trionychidae					
Amyda cartilaginea	LM537461.1		KP268860.1	AY259600.1	AY259550.1	AY259575.1	LM537546.1		
Apalone ferox			JF700189.1	AY259605.1	AY259555.1	AY259580.1	DQ785894.1	DQ785893.1	JQ950717.1
mutica				AY259606.1	AY259556.1	AY259581.1	DQ529206.1	DQ529173.1	
spinifera	U81319.1			AY259607.1	AY259557.1	AY259582.1	DQ529193.1	AY687901.1	JQ950718.1
Chitra chitra			HQ329770.1	AF414366.1	AY259562.1	AY259587.1			
indica			HQ329771.1	AF494491.1	AY259561.1	AY259586.1		JQ950731.1	JQ950720.1
vandijki					AY259563.1	AY259588.1			
Cyclanorbis elegans			HQ329771.1	AY259615.1	AY259570.1	AY259595.1			
senegalensis	FR850553.1		HQ329773.1	AY259614.1	AY259569.1	AY259594.1		AY687903.1	
Cycloderma aubryi	FR850555.1			AY259611.1	AY259566.1	AY259591.1			
frenatum			HQ329774.1	AY259610.1	AY259565.1	AY259590.1			
Dogania subplana				AY259601.1	AY259551.1	AY259576.1			
Lissemys punctata	U81337.1	HM040950.1	KF894768.1	AY259613.1	AY259568.1	AY259593.1		AY687902.1	
scutata	FR850552.2		GQ867673.1	AY259612.1	AY259567.1	AY259592.1		JQ950732.1	JQ950721.1
Nilssonia formosa	HE801638.1		HQ329779.1	AY259597.1	AY259547.1	AY259572.1	HE801763.1		
gangeticus	HE801654.1	GQ398145.1	HQ329780.1	AY259599.1	AY259549.1	AY259574.1	HE801777.1		
hurum	HE801667.1	HM921188.1	JN416996.1	AY259598.1	AY259548.1	AY259573.1	HE801787.1		
Palea steindachneri	AY743419.2	AY743418.1	HQ329783.1	AY259602.1	AY259552.1	AY259577.1	HE801804.1	KC668144.1	JQ950716.1
Pelochelys bibroni			HQ329784.1	AF414361.1	AY259559.1	AY259584.1			
cantorii			HQ329785.1	AF414360.1	AY259560.1	AY259585.1			JQ950713.1
sinensis		AB090045.1	JF700186.1	AY259603.1	AY583692.1	AY259578.1	FJ230869.1	FJ230871.1	AF369089.1
Rafetus euphraticus	FM999033.1		HQ329786.1	AY259604.1	AY259554.1	AY259579.1			
Trionyx triunguis			KP136743.1	AY259609.1	HQ012626.1	AY259589.1			

Table S3. Best fit models selected through corrected Akaike Information Criterion (cAIC) in jModelTest2. Mitochondrial and nuclear genes are shown, including informative sites, base frequencies, rate matrix, kappa, gamma shape parameter, and proportion of invariable sites for appropriate models.

	Gene Fragment								
	12S	16S	COI	ND4	cytB	R35	Cmos	RAG1	RAG2
Total sites	281	386	650	553	212	734	602	2750	668
Informative sites	108	86	136	198	141	134	107	98	105
Model	TIM2+I+G	GTR+I+G	HKY+I+G	TIM1+I+G	K80	TPM2uf+G	TPM3+G	TrN+I	TrN+I+G
Base frequency									
%A	0.3613	0.3234	0.3587	0.4132		0.3069		0.3135	0.3196
%C	0.2426	0.3377	0.3042	0.3217		0.1880		0.2118	0.1858
%G	0.1846	0.2103	0.812	0.0432		0.1945		0.2318	0.2393
%T	0.2116	0.2386	0.2559	0.2220		0.3106		0.2429	0.2553
Rate matrix									
[A-C]	9.0595	15746.1603		0.2984		0.6720	2.0371	1.0000	1.0000
[A-G]	21.3277	40264.1048		10.8519		3.3868	9.4916	5.1119	4.0335
[A-T]	9.0595	4590.6278		0.2984		0.6720	1.0000	1.0000	1.0000
[C-G]	1.0000	1296.2441		1.0000		1.0000	2.0371	1.0000	1.0000
[C-T]	123.8463	104631.9179		5.7352		3.3868	9.4916	9.2431	6.4276
[G-T]]	1.0000	1.0000		1.0000		1.0000	1.0000	1.0000	1.0000
Kappa (ti/tv)			16.3162 (7.0838)		4.0808 (2.0404)				
Shape parameter	0.5590	0.3530	0.9670	0.4120		1.9440	0.4160		0.8120
Invariable sites	0.3560	0.4080	0.5350	0.0500				0.6340	0.4210